



THE 2021 NATIONAL NUCLEAR PHYSICS SUMMER SCHOOL

LATTICE QCD
AND
NUCLEON(US) STRUCTURE

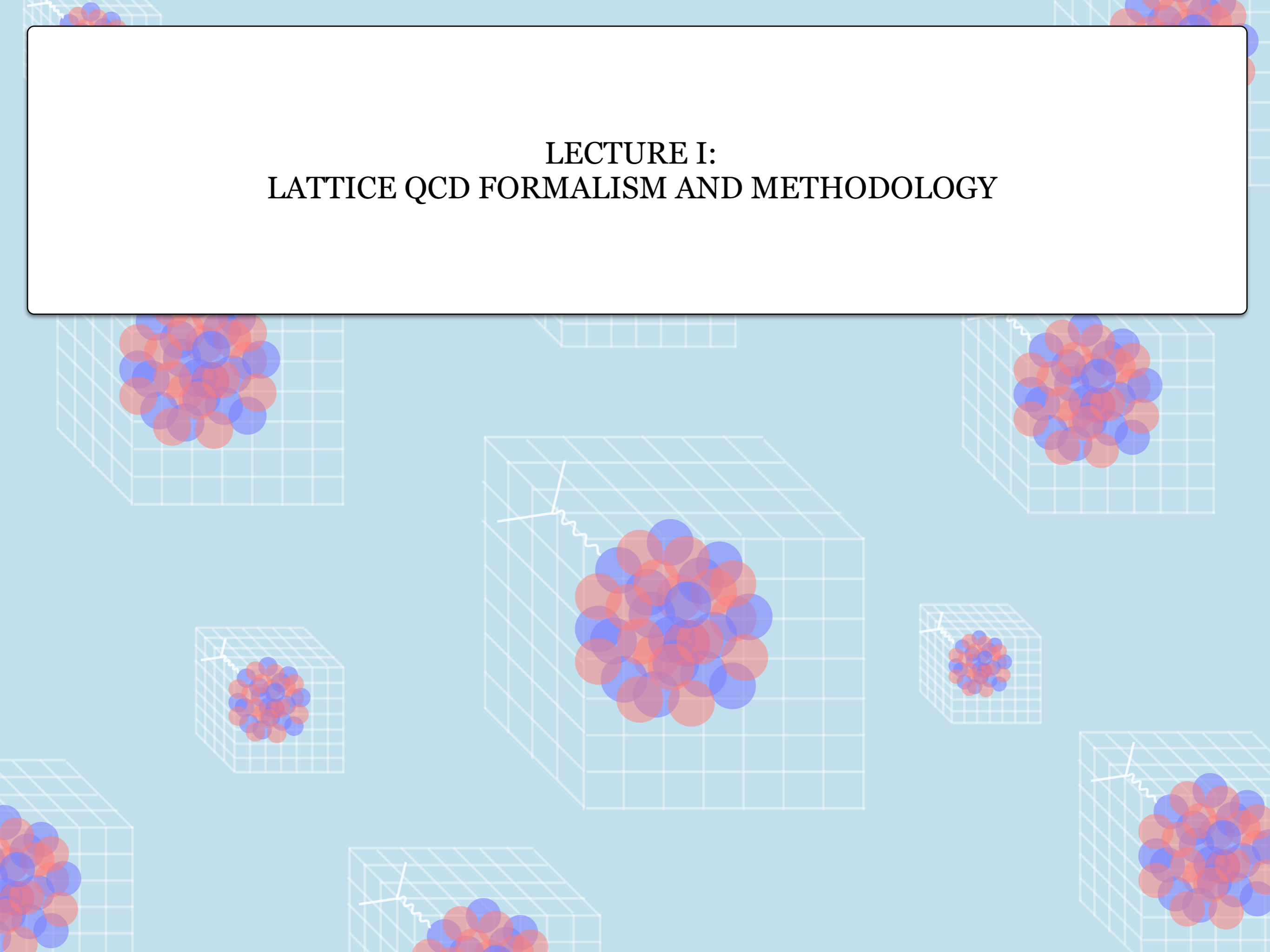
ZOHREH DAVOUDI
UNIVERSITY OF MARYLAND AND RIKEN FELLOW

**LECTURE I:
LATTICE QCD FORMALISM AND METHODOLOGY**

**LECTURE II:
NUCLEON STRUCTURE FROM LATTICE QCD**

**LECTURE III:
TOWARDS NUCLEAR STRUCTURE FROM LATTICE QCD**

LECTURE I: LATTICE QCD FORMALISM AND METHODOLOGY



Quantum chromodynamics (QCD) in continuum:

QCD is a SU(3) Yang-Mills theory augmented with several flavors of massive quarks:

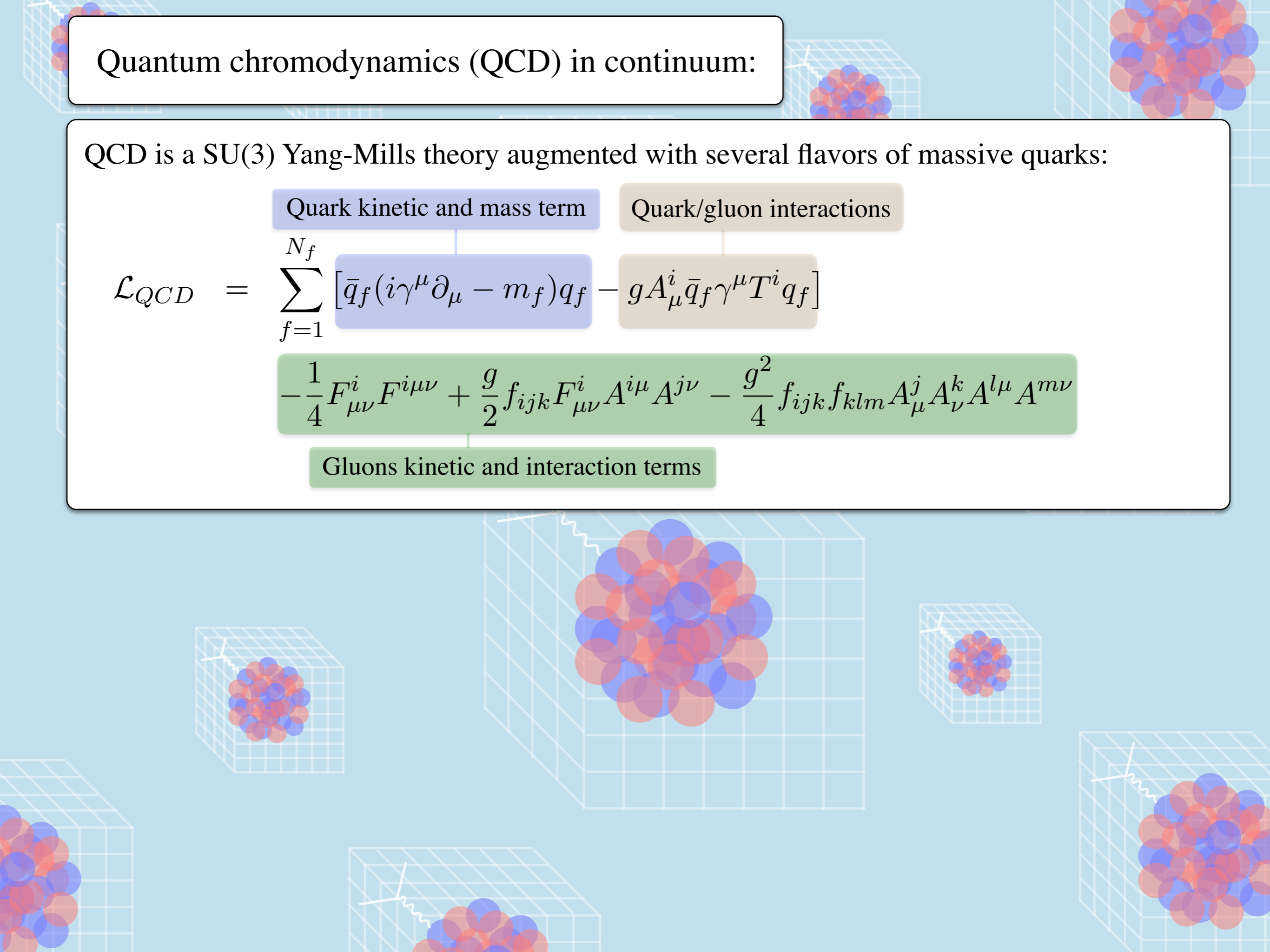
Quark kinetic and mass term

Quark/gluon interactions

$$\mathcal{L}_{QCD} = \sum_{f=1}^{N_f} \left[\bar{q}_f (i\gamma^\mu \partial_\mu - m_f) q_f - g A_\mu^i \bar{q}_f \gamma^\mu T^i q_f \right]$$

$$-\frac{1}{4} F_{\mu\nu}^i F^{i\mu\nu} + \frac{g}{2} f_{ijk} F_{\mu\nu}^i A^{j\mu} A^{k\nu} - \frac{g^2}{4} f_{ijk} f_{klm} A_\mu^j A_\nu^k A^{l\mu} A^{m\nu}$$

Gluons kinetic and interaction terms



Quantum chromodynamics (QCD) in continuum:

QCD is a SU(3) Yang-Mills theory augmented with several flavors of massive quarks:

$$\mathcal{L}_{QCD} = \sum_{f=1}^{N_f} \left[\bar{q}_f (i\gamma^\mu \partial_\mu - m_f) q_f - g A_\mu^i \bar{q}_f \gamma^\mu T^i q_f \right] - \frac{1}{4} F_{\mu\nu}^i F^{i\mu\nu} + \frac{g}{2} f_{ijk} F_{\mu\nu}^i A^{j\mu} A^{k\nu} - \frac{g^2}{4} f_{ijk} f_{klm} A_\mu^j A_\nu^k A^{l\mu} A^{m\nu}$$

Quark kinetic and mass term Quark/gluon interactions

Gluons kinetic and interaction terms

Observe that:

i) There are only $1 + N_f$ input parameters plus QCD coupling. Fix them by a few quantities and all strongly-interacting aspects of nuclear physics is predicted (in principle)!

ii) QCD is asymptotically free such that: $\alpha_s(\mu') = \frac{1}{2b_0 \log \frac{\mu'}{\Lambda_{QCD}}}$

Positive constant for $N_f \leq 16$

Quantum chromodynamics (QCD) in continuum:

QCD is a SU(3) Yang-Mills theory augmented with several flavors of massive quarks:

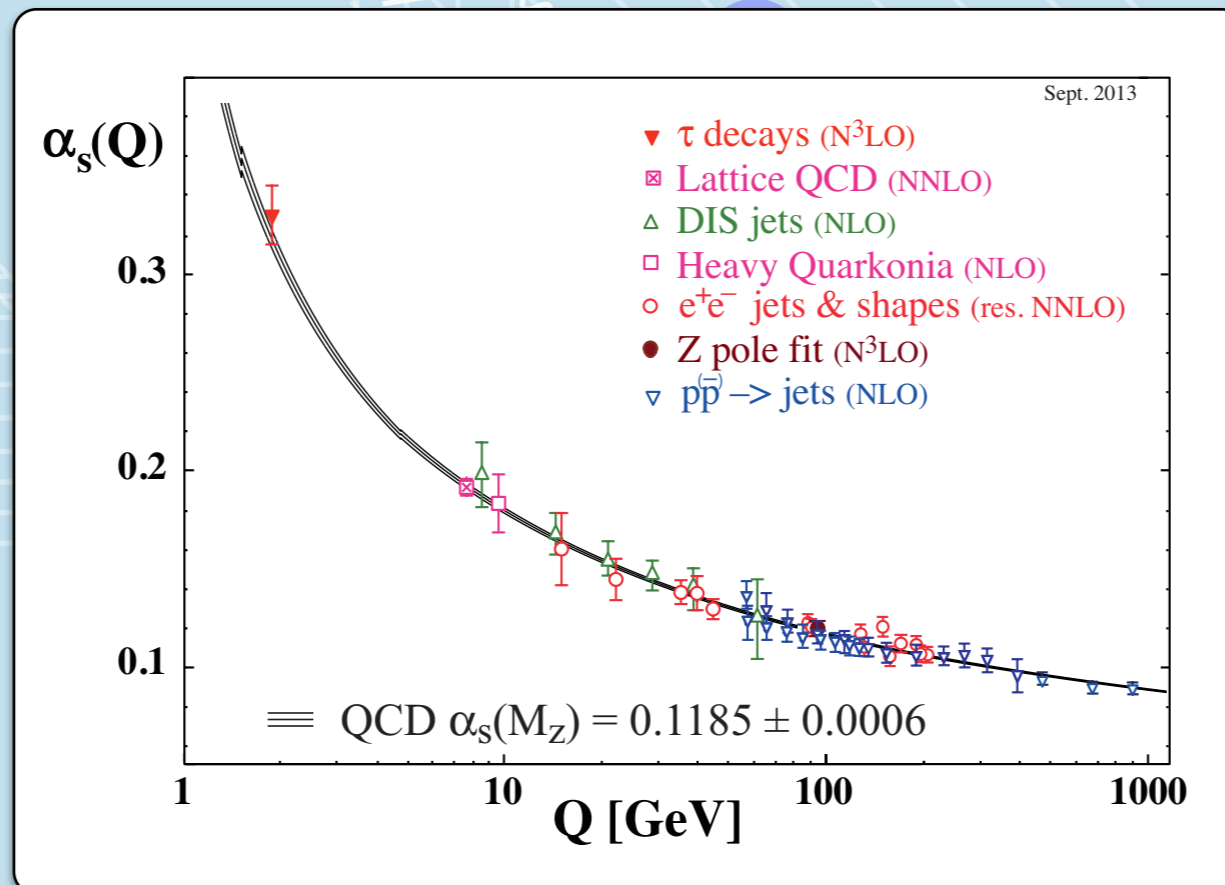
Quark kinetic and mass term

Quark/gluon interactions

$$\mathcal{L}_{QCD} = \sum_{f=1}^{N_f} \left[\bar{q}_f (i\gamma^\mu \partial_\mu - m_f) q_f - g A_\mu^i \bar{q}_f \gamma^\mu T^i q_f \right]$$

$$-\frac{1}{4} F_{\mu\nu}^i F^{i\mu\nu} + \frac{g}{2} f_{ijk} F_{\mu\nu}^i A^{i\mu} A^{j\nu} - \frac{g^2}{4} f_{ijk} f_{klm} A_\mu^j A_\nu^k A^{l\mu} A^{m\nu}$$

Gluons kinetic and interaction terms



Let's enumerate the steps toward numerically simulating this theory nonperturbatively...

Step I: Discretize the QCD action in both space and time. Consider a finite hypercubic lattice. Wick rotate to imaginary times.

Step II: Generate a large sample of thermalized decorrelated vacuum configurations.

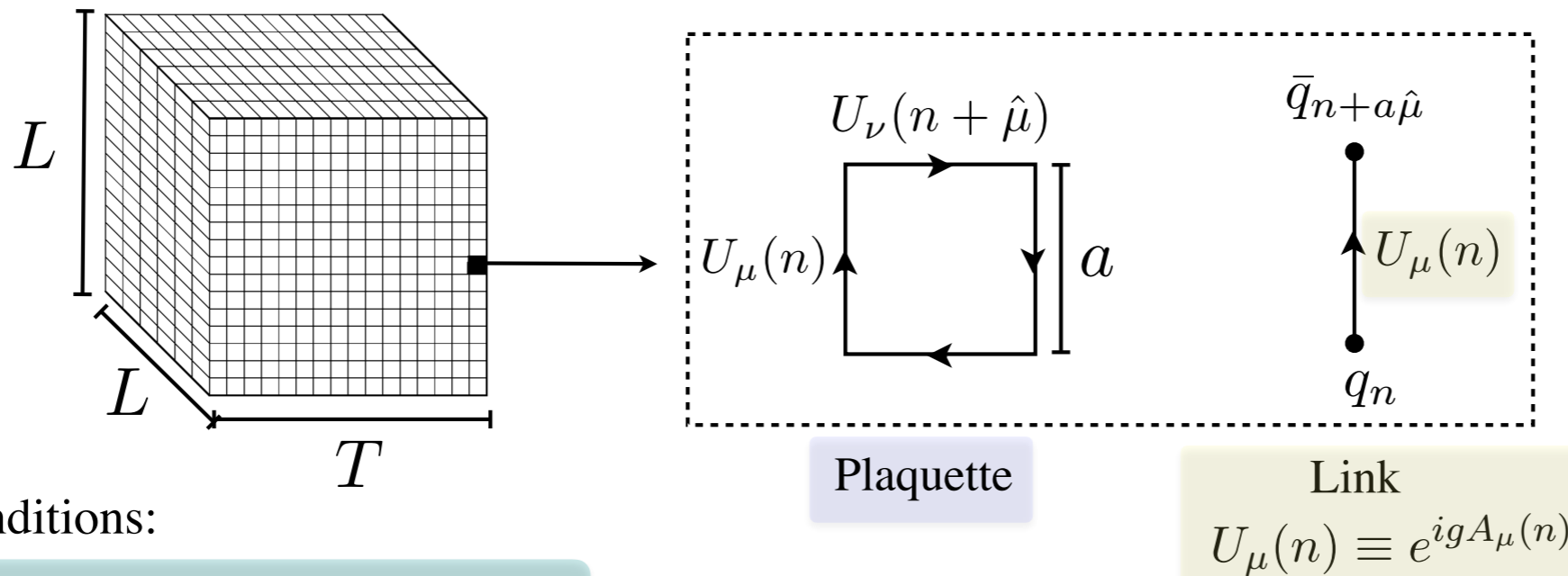
Step III: Form the correlation functions by contracting the quark fields. Need to specify the interpolating operators for the state under study.

Step IV: Extract energies and matrix elements from correlation functions.

Step V: Make the connection to physical observables, such as scattering amplitudes, decay rates, etc.

See e.g., ZD, arXiv:1409.1966 [hep-lat]

Step I: Discretize the QCD action in both space and time. Consider a finite hypercubic lattice. Wick rotate to imaginary times.

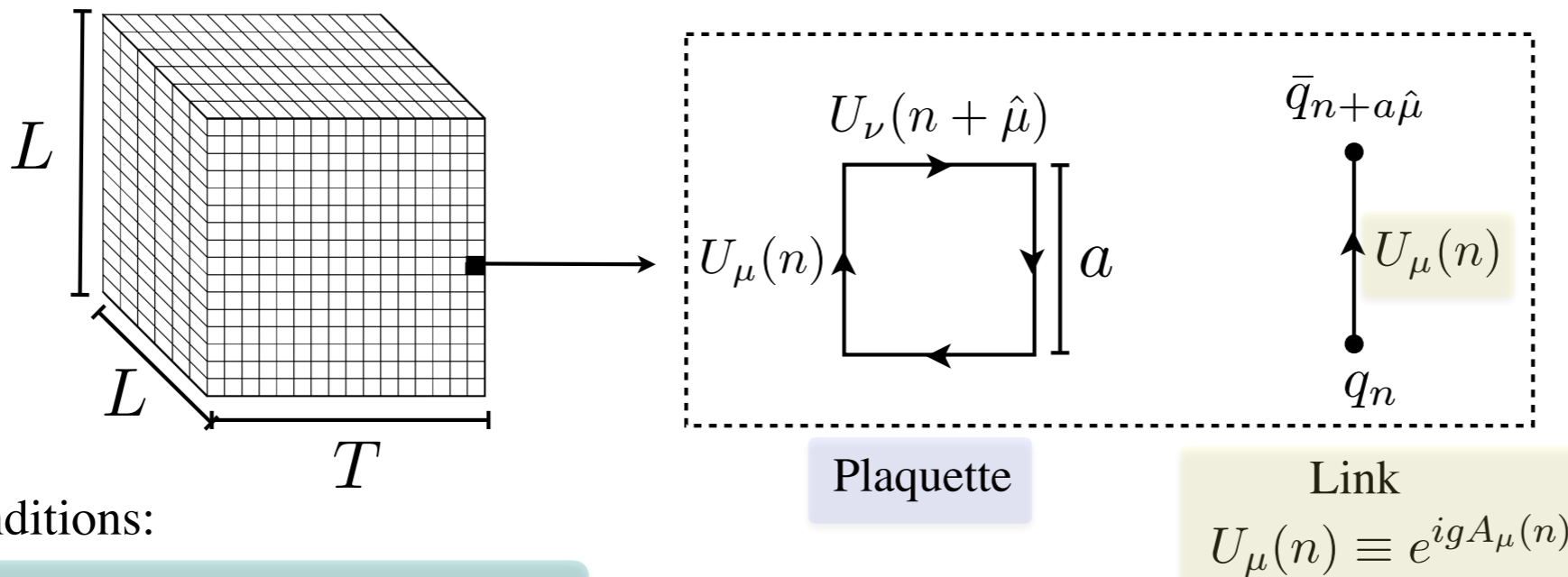


Two conditions:

$$T, L \gg m_\pi^{-1} \quad a \ll \Lambda_{QCD}^{-1}$$

$$U_\mu(n) \equiv e^{igA_\mu(n)}$$

Step I: Discretize the QCD action in both space and time. Consider a finite hypercubic lattice. Wick rotate to imaginary times.



Two conditions:

$$T, L \gg m_\pi^{-1} \quad a \ll \Lambda_{QCD}^{-1}$$

An example of a discretized action by K. Wilson:

$$S_{\text{Wilson}}^{(E)} = \frac{\beta}{N_c} \sum_n \sum_{\mu < \nu} \Re \text{Tr} [\mathbb{1} - P_{\mu\nu;n}] - \sum_n \bar{q}_n [\bar{m}^{(0)} + 4] q_n + \sum_n \sum_\mu \left[\bar{q}_n \frac{r - \gamma_\mu}{2} U_\mu(n) q_{n+\hat{\mu}} + \bar{q}_n \frac{r + \gamma_\mu}{2} U_\mu^\dagger(n - \hat{\mu}) q_{n-\hat{\mu}} \right]$$

Wilson parameter. Gives the naive action if set to zero and has doublers problem.

For discussions of actions consistent with chiral symmetry of continuum see: Kaplan, arXiv:0912.2560 [hep-lat].

Step II: Generate a large sample of thermalized decorrelated vacuum configurations.

$$\langle \hat{O} \rangle = \frac{1}{Z} \int \mathcal{D}U_\mu \mathcal{D}q \mathcal{D}\bar{q} e^{-S_{\text{lattice}}^{(G)}[U] - S_{\text{lattice}}^{(F)}[U, q, \bar{q}]} \hat{O}[U, q, \bar{q}]$$

Step II: Generate a large sample of thermalized decorrelated vacuum configurations.

$$\langle \hat{O} \rangle = \frac{1}{Z} \int \mathcal{D}U_\mu \mathcal{D}q \mathcal{D}\bar{q} e^{-S_{\text{lattice}}^{(G)}[U] - S_{\text{lattice}}^{(F)}[U, q, \bar{q}]} \hat{O}[U, q, \bar{q}]$$

Quark part of expectation values

Step II: Generate a large sample of thermalized decorrelated vacuum configurations.

$$\langle \hat{\mathcal{O}} \rangle = \frac{1}{\mathcal{Z}} \int \mathcal{D}U_\mu \mathcal{D}q \mathcal{D}\bar{q} e^{-S_{\text{lattice}}^{(G)}[U] - S_{\text{lattice}}^{(F)}[U, q, \bar{q}]} \hat{\mathcal{O}}[U, q, \bar{q}]$$

Quark part of expectation values

Define: $\langle \hat{\mathcal{O}} \rangle_F = \frac{1}{\mathcal{Z}_F} \int \mathcal{D}q \mathcal{D}\bar{q} e^{-S_{\text{lattice}}^{(F)}[U, q, \bar{q}]} \mathcal{O}[q, \bar{q}, U]$

$$\mathcal{Z}_F = \int \mathcal{D}q \mathcal{D}\bar{q} e^{-S_{\text{lattice}}^{(F)}[U, q, \bar{q}]} = \prod_f \det D_f \quad \text{Dirac matrix}$$

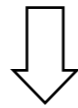
Step II: Generate a large sample of thermalized decorrelated vacuum configurations.

$$\langle \hat{\mathcal{O}} \rangle = \frac{1}{\mathcal{Z}} \int \mathcal{D}U_\mu \mathcal{D}q \mathcal{D}\bar{q} e^{-S_{\text{lattice}}^{(G)}[U] - S_{\text{lattice}}^{(F)}[U, q, \bar{q}]} \hat{\mathcal{O}}[U, q, \bar{q}]$$

Quark part of expectation values

Define: $\langle \hat{\mathcal{O}} \rangle_F = \frac{1}{\mathcal{Z}_F} \int \mathcal{D}q \mathcal{D}\bar{q} e^{-S_{\text{lattice}}^{(F)}[U, q, \bar{q}]} \mathcal{O}[q, \bar{q}, U]$

$$\mathcal{Z}_F = \int \mathcal{D}q \mathcal{D}\bar{q} e^{-S_{\text{lattice}}^{(F)}[U, q, \bar{q}]} = \prod_f \det D_f \quad \text{Dirac matrix}$$



$$\langle \hat{\mathcal{O}} \rangle = \frac{1}{\mathcal{Z}} \int \mathcal{D}U_\mu e^{-S_{\text{lattice}}^{(G)}[U]} \mathcal{Z}_F[U] \langle \hat{\mathcal{O}} \rangle_F$$

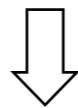
Step II: Generate a large sample of thermalized decorrelated vacuum configurations.

$$\langle \hat{\mathcal{O}} \rangle = \frac{1}{\mathcal{Z}} \int \mathcal{D}U_\mu \mathcal{D}q \mathcal{D}\bar{q} e^{-S_{\text{lattice}}^{(G)}[U] - S_{\text{lattice}}^{(F)}[U, q, \bar{q}]} \hat{\mathcal{O}}[U, q, \bar{q}]$$

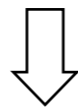
Quark part of expectation values

Define: $\langle \hat{\mathcal{O}} \rangle_F = \frac{1}{\mathcal{Z}_F} \int \mathcal{D}q \mathcal{D}\bar{q} e^{-S_{\text{lattice}}^{(F)}[U, q, \bar{q}]} \mathcal{O}[q, \bar{q}, U]$

$$\mathcal{Z}_F = \int \mathcal{D}q \mathcal{D}\bar{q} e^{-S_{\text{lattice}}^{(F)}[U, q, \bar{q}]} = \prod_f \det D_f \quad \text{Dirac matrix}$$



$$\langle \hat{\mathcal{O}} \rangle = \frac{1}{\mathcal{Z}} \int \mathcal{D}U_\mu e^{-S_{\text{lattice}}^{(G)}[U]} \mathcal{Z}_F[U] \langle \hat{\mathcal{O}} \rangle_F$$



$$\langle \hat{\mathcal{O}} \rangle = \frac{1}{N} \sum_i^N \langle \hat{\mathcal{O}} \rangle_F [U^{(i)}]$$

N number of $U^{(i)}$ sampled from the distribution: $\frac{1}{\mathcal{Z}} e^{-S_{\text{lattice}}^{(G)}[U]} \prod_f \det D_f$

Steps II is computationally costly...

Example: Consider a lattice with: $L/a = 48$, $T/a = 256$

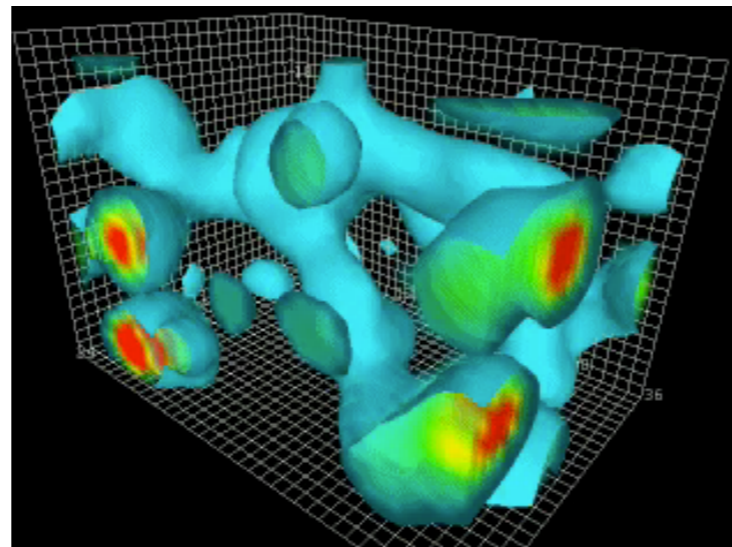
Sampling SU(3) matrices. Already for one sample requires storing

$$8 \times 48^3 \times 256 = 226,492,416$$

c-numbers in the computer!

Requires calculating determinant of a large matrix.

Requires tens of thousands of uncorrelated samples. Molecular-dynamics-inspired hybrid Monte Carlo sampling algorithms often used.

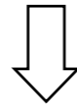


Step III: Form the correlation functions by contracting the quarks. Need to specify the interpolating operators for the state under study.

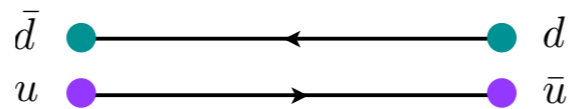
$$\langle \hat{\mathcal{O}} \rangle_F = \frac{1}{\mathcal{Z}_F} \int \mathcal{D}q \mathcal{D}\bar{q} e^{-S_{\text{lattice}}^{(F)}[U, q, \bar{q}]} \mathcal{O}[q, \bar{q}, U]$$

Step III: Form the correlation functions by contracting the quarks. Need to specify the interpolating operators for the state under study.

$$\langle \hat{\mathcal{O}} \rangle_F = \frac{1}{\mathcal{Z}_F} \int \mathcal{D}q \mathcal{D}\bar{q} e^{-S_{\text{lattice}}^{(F)}[U, q, \bar{q}]} \mathcal{O}[q, \bar{q}, U]$$

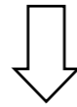


e.g., $\hat{\mathcal{O}} = \bar{u} \gamma_5 d$

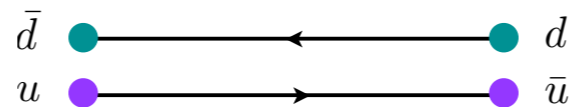


Step III: Form the correlation functions by contracting the quarks. Need to specify the interpolating operators for the state under study.

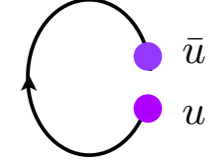
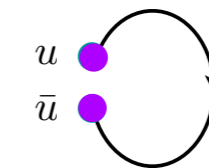
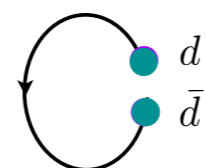
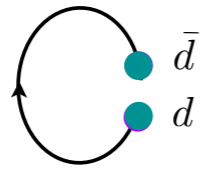
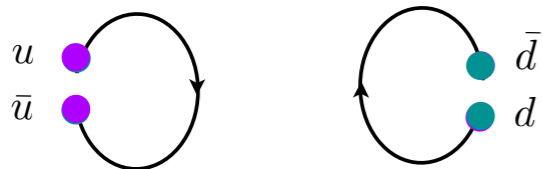
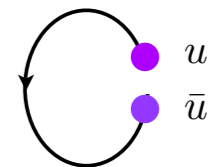
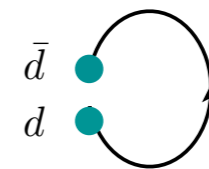
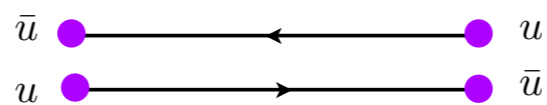
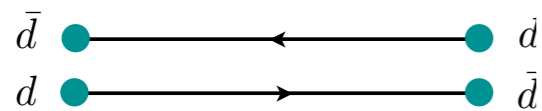
$$\langle \hat{\mathcal{O}} \rangle_F = \frac{1}{\mathcal{Z}_F} \int \mathcal{D}q \mathcal{D}\bar{q} e^{-S_{\text{lattice}}^{(F)}[U, q, \bar{q}]} \mathcal{O}[q, \bar{q}, U]$$



e.g., $\hat{\mathcal{O}} = \bar{u}\gamma_5 d$



e.g., $\hat{\mathcal{O}} = \frac{1}{\sqrt{2}} (\bar{u}\gamma_5 u - \bar{d}\gamma_5 d)$



Quark disconnected diagrams. Require expensive all-to-all propagators.

Steps III is computationally costly...

Example: Consider a lattice with: $L/a = 48$, $T/a = 256$

Solving

$$[D(U)]_{X,Y} [S(U)]_{Y,X_0} = G_{X,X_0}$$

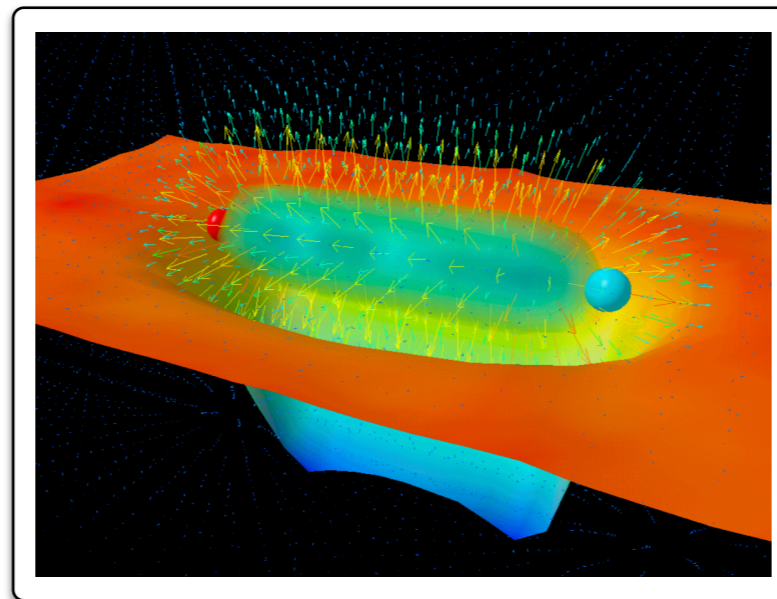
Dirac
matrix

Quark
propagator

Source

Requires taking determinant and inverting
a matrix with dimensions:

$$(4 \times 3 \times 48^3 \times 256)^2 =$$
$$339,738,624 \times 339,738,624$$



EXERCISE 1

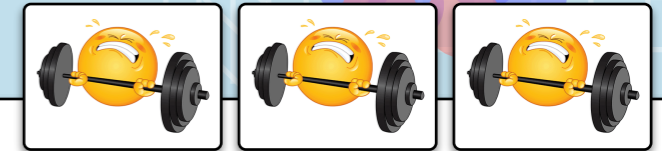


Show that for the correlation function of the charged pion:

$$\langle \hat{O}^{\pi^+}(n) \hat{O}^{\pi^+\dagger}(0) \rangle_F = -\text{Tr} [D_u^{-1}(n, 0) D_d^{-1}(n, 0)]$$

where D_u^{-1} and D_d^{-1} denote the the inverse Dirac matrix (the quark propagator) for the u and d quarks, respectively. Trace is over spin and color degrees of freedom.

BONUS EXERCISE 1



Show that for the correlation function of the neutral pion:

$$\begin{aligned} \langle \hat{O}^{\pi^0}(n) \hat{O}^{\pi^0\dagger}(0) \rangle_F &= -\frac{1}{2} \text{Tr} [\gamma^5 D_u^{-1}(n, 0) \gamma^5 D_u^{-1}(0, n)] \\ &+ \frac{1}{2} \text{Tr} [\gamma^5 D_u^{-1}(n, n)] \text{Tr} [\gamma^5 D_u^{-1}(0, 0)] \\ &- \frac{1}{2} \text{Tr} [\gamma^5 D_u^{-1}(n, n)] \text{Tr} [\gamma^5 D_d^{-1}(0, 0)] + \{u \leftrightarrow d\} \end{aligned}$$

Step IV: Extract energies and matrix elements from correlation functions

$$C_{\hat{O},\hat{O}'}(\tau; \mathbf{d}) = \sum_{\mathbf{x}} e^{2\pi i \mathbf{d} \cdot \mathbf{x} / L} \langle 0 | \hat{O}'(\mathbf{x}, \tau) \hat{O}^\dagger(\mathbf{0}, 0) | 0 \rangle = \mathcal{Z}'_0 \mathcal{Z}_0^\dagger e^{-E^{(0)}\tau} + \mathcal{Z}'_1 \mathcal{Z}_1^\dagger e^{-E^{(1)}\tau} + \dots$$

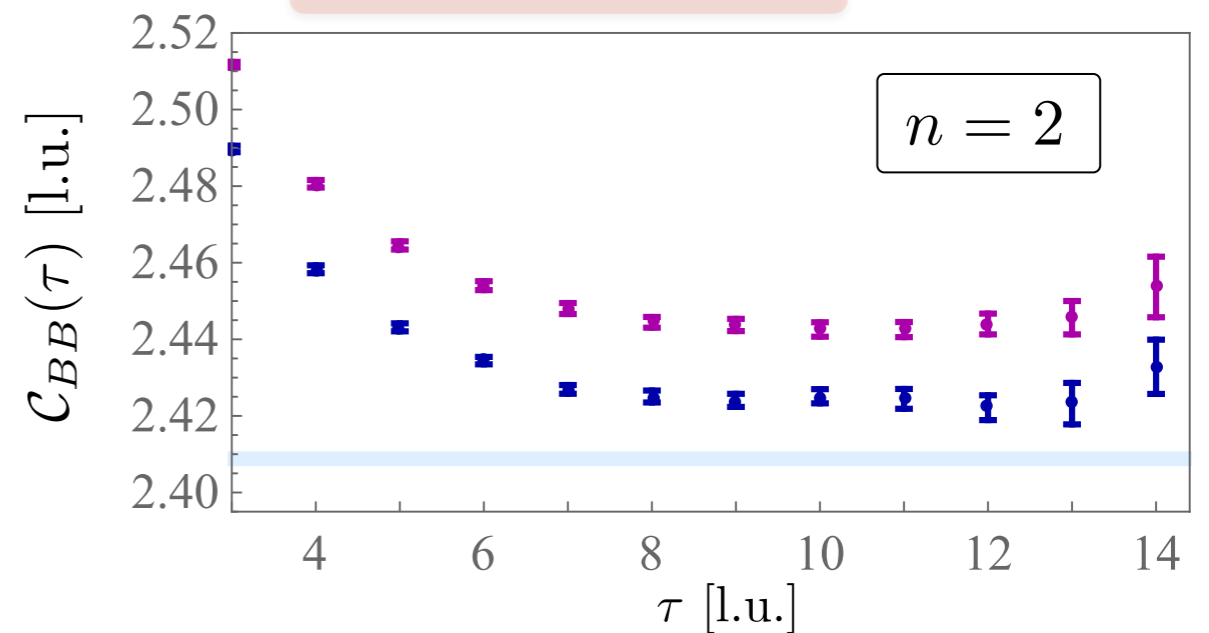
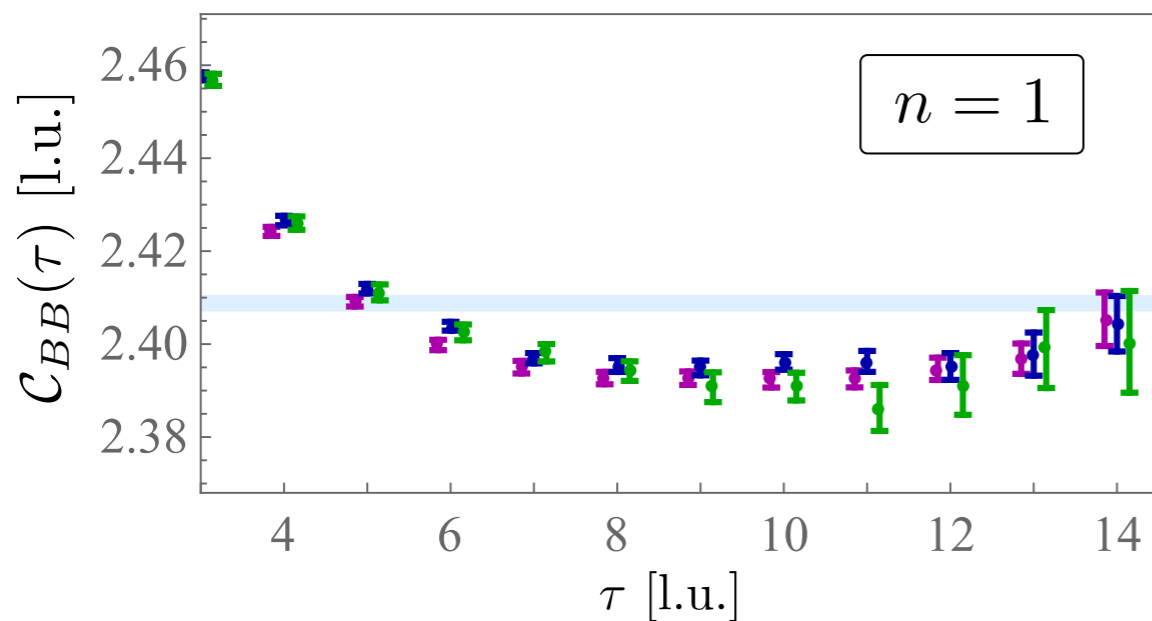
Ground state and a tower of excited states are, in principle, accessible!

Step IV: Extract energies and matrix elements from correlation functions

$$C_{\hat{O},\hat{O}'}(\tau; \mathbf{d}) = \sum_{\mathbf{x}} e^{2\pi i \mathbf{d} \cdot \mathbf{x} / L} \langle 0 | \hat{O}'(\mathbf{x}, \tau) \hat{O}^\dagger(\mathbf{0}, 0) | 0 \rangle = Z'_0 Z_0^\dagger e^{-E^{(0)}\tau} + Z'_1 Z_1^\dagger e^{-E^{(1)}\tau} + \dots$$

Ground state and a tower of excited states are, in principle, accessible!

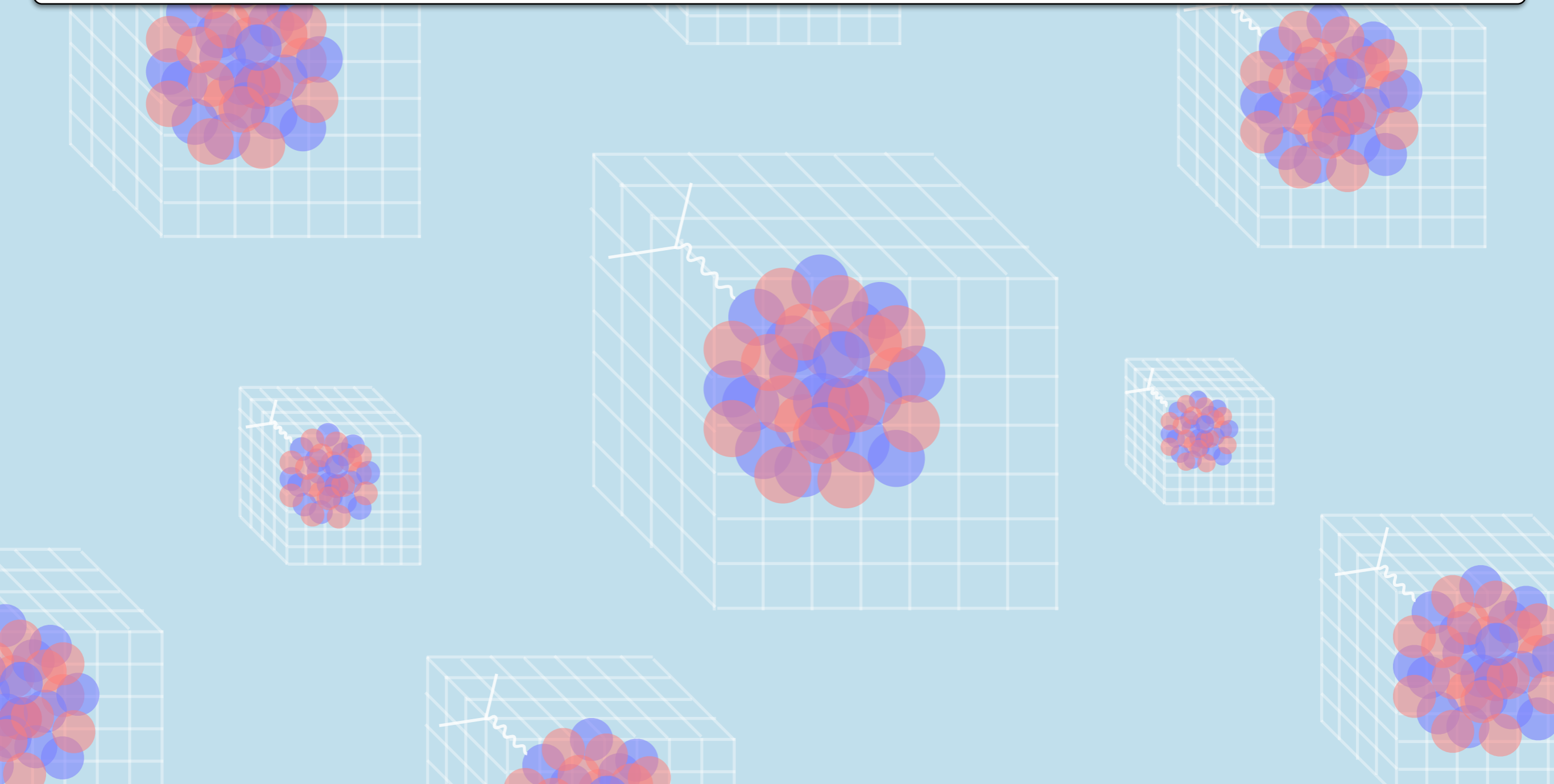
Example: $NN (^1S_0)$



What should we make of the volume dependence?

I $24^3 \times 48$
 I $32^3 \times 48$
 I $48^3 \times 64$
 — $2M_N$

**[STILL CONTINUING ON] LECTURE I:
LATTICE QCD FORMALISM AND METHODOLOGY**



[Recap] Steps involved in any lattice QCD calculation:

Step I: Discretize the QCD action in both space and time. Consider a finite hypercubic lattice. Wick rotate to imaginary times.

Step II: Generate a large sample of thermalized decorrelated vacuum configurations.

Step III: Form the correlation functions by contracting the quark fields. Need to specify the interpolating operators for the state under study.

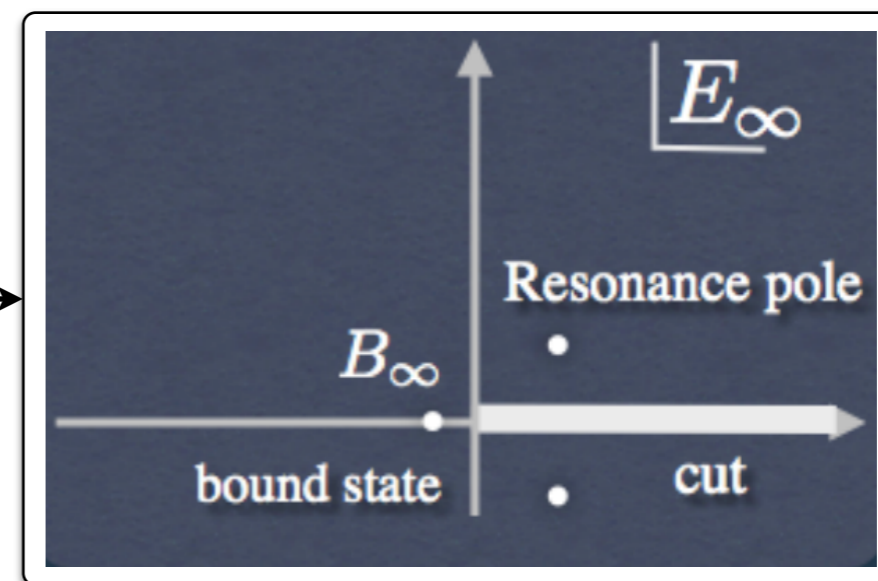
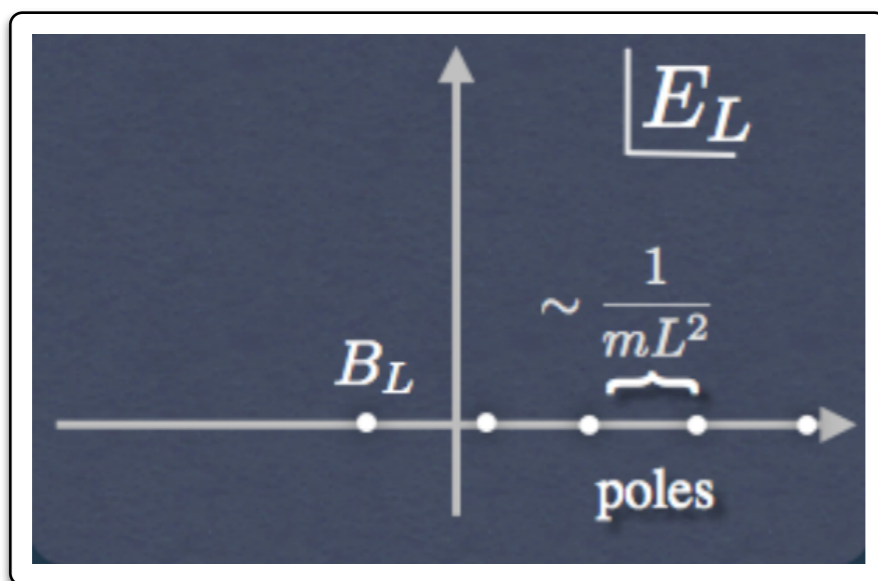
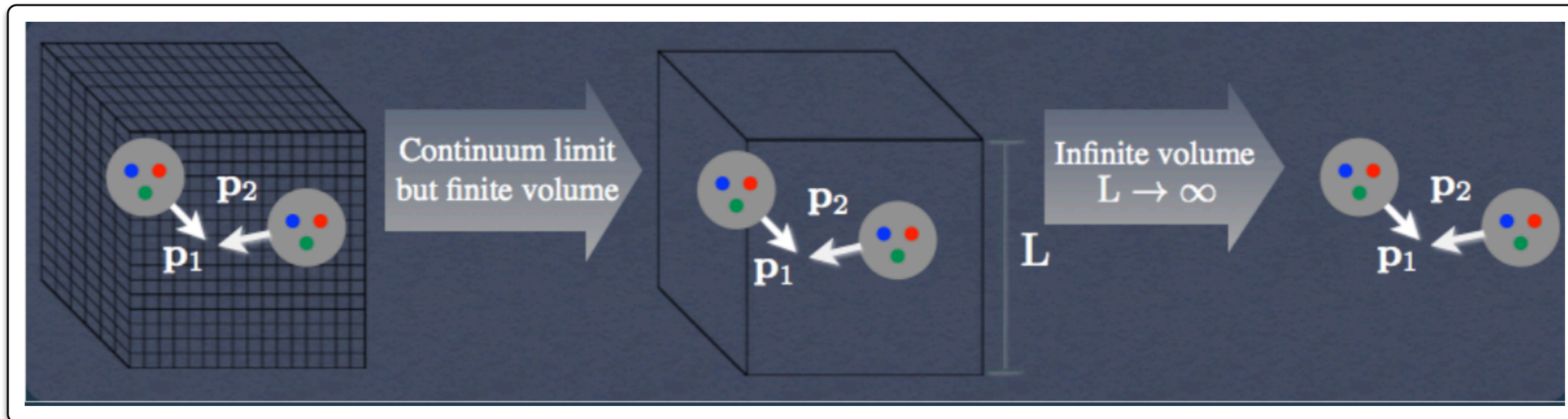
Step IV: Extract energies and matrix elements from correlation functions.

Step V: Make the connection to physical observables, such as scattering amplitudes, decay rates, etc.

See e.g., ZD, arXiv:1409.1966 [hep-lat]

Step V: Make the connection to physical observables, such as scattering amplitudes, decay rates, etc. Still not fully developed and presents challenge in multi-hadron systems.

Example: two-hadron scattering



Let's discuss in greater depth step V:

Step V: make the connection to physical observables, such as scattering amplitudes, decay rates, etc.

- i) Finite-volume effects in the single-hadron sector
- ii) Finite-volume formalism for two-hadron elastic scattering
- iii) Finite-volume formalism for coupled-channel two-hadron inelastic scattering and resonances
- iv) Finite-volume formalism for transition amplitudes and resonance form factors
- v) Finite-volume formalism for three-hadron scattering and resonances and decays
- vi) Finite-volume effects in lattice QED+QCD studies of hadrons

Let's discuss in greater depth step V:

Step V: make the connection to physical observables, such as scattering amplitudes, decay rates, etc.

i) Finite-volume effects in the single-hadron sector

ii) Finite-volume formalism for two-hadron elastic scattering

iii) Finite-volume formalism for coupled-channel two-hadron inelastic scattering and resonances

iv) Finite-volume formalism for transition amplitudes and resonance form factors

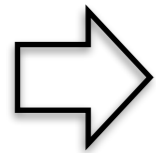
v) Finite-volume formalism for three-hadron scattering and resonances and decays

vi) Finite-volume effects in lattice QED+QCD studies of hadrons

Let's discuss in greater depth step V:

Step V: make the connection to physical observables, such as scattering amplitudes, decay rates, etc.

i) Finite-volume effects in the single-hadron sector



ii) Finite-volume formalism for two-hadron elastic scattering

iii) Finite-volume formalism for coupled-channel two-hadron inelastic scattering and resonances

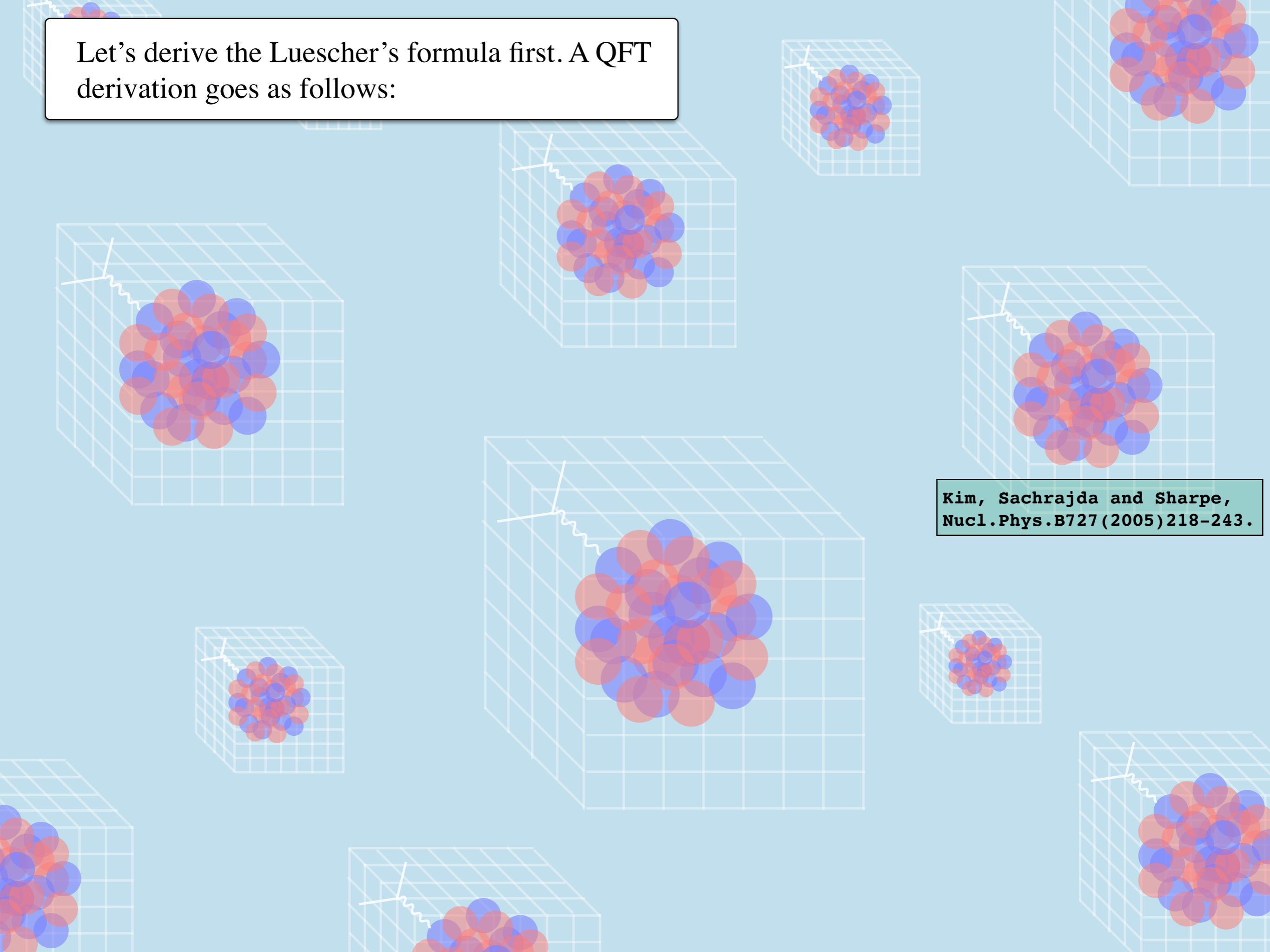
iv) Finite-volume formalism for transition amplitudes and resonance form factors

v) Finite-volume formalism for three-hadron scattering and resonances and decays

vi) Finite-volume effects in lattice QED+QCD studies of hadrons

See e.g., ZD, arXiv:1409.1966 [hep-lat, Briceno, Dudek and Young, Rev. Mod. Phys. 90.025001, Ann. Rev. Nucl. Part. Sci. 69 (2019).

Let's derive the Luescher's formula first. A QFT derivation goes as follows:



**Kim, Sachrajda and Sharpe,
Nucl.Phys.B727(2005)218-243.**

Let's derive the Luescher's formula first. A QFT derivation goes as follows:

$$C_V = \text{[diagram 1]} + \text{[diagram 2]} + \text{[diagram 3]} + \dots$$

The diagrammatic equation shows a series of terms representing the expansion of the vacuum expectation value of the operator V . Each term is a diagram with a central shaded region labeled V . The first term is a single circle with two green circles labeled σ' and σ on the left and right sides, and two black dots at the top and bottom. The second term consists of two such circles connected at their right side to the left side of the second circle, with a green circle labeled $-\kappa$ at the junction. The third term consists of three such circles connected in a chain, with green circles labeled $-\kappa$ at each junction. The terms are separated by plus signs and followed by an ellipsis.

$$T \rightarrow \infty, a \rightarrow 0$$

Kim, Sachrajda and Sharpe,
Nucl.Phys.B727(2005)218-243.

Let's derive the Luescher's formula first. A QFT derivation goes as follows:

$$C_V = \text{[diagram 1]} + \text{[diagram 2]} + \text{[diagram 3]} + \dots$$

The diagrammatic equation shows the expansion of the vacuum expectation value of the product of two operators σ' and σ in a volume V . The first term is a single circle with σ' and σ on the left and right, and V in the center. The second term is two such circles connected at their top and bottom vertices, with a $-\kappa$ label on the connecting line. The third term is three such circles connected in a chain, with $-\kappa$ labels on the connecting lines.

$$T \rightarrow \infty, a \rightarrow 0$$

Kim, Sachrajda and Sharpe,
Nucl.Phys.B727(2005)218-243.

$$(1) \text{ [diagram 1]} = \text{[diagram 2]} + \text{[diagram 3]}$$

The diagrammatic equation (1) shows a circle with two vertices and V in the center, equal to a circle with two vertices and an infinity symbol ∞ in the center, plus a circle with two vertices and V in the center, where the top and bottom vertices are connected by a dashed line.

Let's derive the Luescher's formula first. A QFT derivation goes as follows:

$$C_V = \text{[diagram 1]} + \text{[diagram 2]} + \text{[diagram 3]} + \dots$$

The diagrams represent a series expansion of the vacuum expectation value of the product of two operators σ' and σ in a volume V . Each term consists of a chain of circles representing interaction vertices V . The first term is a single circle with σ' on the left and σ on the right. The second term is two circles connected at a central vertex labeled $-\kappa$. The third term is three circles connected in a chain with two $-\kappa$ vertices. Each circle has two external black dots at the top and bottom.

$$T \rightarrow \infty, a \rightarrow 0$$

Kim, Sachrajda and Sharpe,
Nucl.Phys.B727(2005)218-243.

$$(1) \text{ [diagram 1]} = \text{[diagram 2]} + \text{[diagram 3]}$$

The first diagram is a circle with two external black dots and a central V . The second diagram is a circle with two external black dots and a central infinity symbol ∞ . The third diagram is a circle with two external black dots and a central V , with a dashed line extending from the top vertex.

$$(2) \text{ [diagram 1]} = \text{[diagram 2]} + \text{[diagram 3]} + \text{[diagram 4]} + \dots$$

The first diagram is a central blue circle with four external black lines and a central \mathcal{M}_∞ . The second diagram is a central green circle with two external black lines and a central $-\kappa$. The third diagram is a central grey circle with two external black lines and a central ∞ , with two green circles labeled $-\kappa$ on either side. The fourth diagram is a central grey circle with two external black lines and a central ∞ , with two green circles labeled $-\kappa$ on either side, and another grey circle with a central ∞ and two green circles labeled $-\kappa$ on either side.

Let's derive the Luescher's formula first. A QFT derivation goes as follows:

$$\begin{aligned}
 C_V &= \text{diagram}_1 + \text{diagram}_2 + \text{diagram}_3 + \dots \\
 &= C_\infty + \text{diagram}_4 + \text{diagram}_5 + \text{diagram}_6 + \dots
 \end{aligned}$$

The diagrams are as follows:

- Diagram 1: A circle with two black dots at the top and bottom. Inside, a green circle labeled σ' is on the left and a green circle labeled σ is on the right. A vertical line labeled V connects the two green circles.
- Diagram 2: Two circles as in Diagram 1, connected by a dashed line labeled $-\kappa$ between their green circles.
- Diagram 3: Three circles as in Diagram 1, connected by dashed lines labeled $-\kappa$ between their green circles.
- Diagram 4: A circle with two black dots at the top and bottom. Inside, a teal circle labeled A' is on the left and a teal circle labeled A is on the right. A vertical line labeled V connects the two teal circles.
- Diagram 5: Two circles as in Diagram 4, connected by a dashed line labeled M_∞ between their teal circles.
- Diagram 6: Three circles as in Diagram 4, connected by dashed lines labeled M_∞ between their teal circles.

$$T \rightarrow \infty, a \rightarrow 0$$

Kim, Sachrajda and Sharpe,
Nucl.Phys.B727(2005)218-243.

$$(1) \quad \text{diagram}_1 = \text{diagram}_2 + \text{diagram}_3$$

The diagrams are:

- Diagram 1: A circle with two black dots at the top and bottom. Inside, a vertical line labeled V connects the two dots.
- Diagram 2: A circle with two black dots at the top and bottom. Inside, an infinity symbol ∞ is centered.
- Diagram 3: A circle with two black dots at the top and bottom. Inside, a vertical line labeled V connects the two dots. A dashed line extends from the top dot upwards.

$$(2) \quad \text{diagram}_4 = \text{diagram}_5 + \text{diagram}_6 + \dots$$

The diagrams are:

- Diagram 4: A teal circle labeled M_∞ with four black dots on its sides.
- Diagram 5: A green circle labeled $-\kappa$ with two black dots on its top and bottom.
- Diagram 6: A circle with two black dots at the top and bottom. Inside, a vertical line labeled $-\kappa$ connects the two dots. A dashed line extends from the top dot upwards.
- Diagram 7: Two circles as in Diagram 6, connected by a dashed line labeled ∞ between their vertical lines.
- Diagram 8: Three circles as in Diagram 6, connected by dashed lines labeled ∞ between their vertical lines.

EXERCISE 2



By rearranging the diagrams in C_V (the first line in the upper panel) using the relations in the lower panel, verify the expansion in the second line in the upper panel. What is the relation between $\sigma(\sigma')$ and $A(A')$?

Let's derive the Luescher's formula first. A QFT derivation goes as follows:

$$\begin{aligned}
 C_V &= \text{diagram}_1 + \text{diagram}_2 + \text{diagram}_3 + \dots \\
 &= C_\infty + \text{diagram}_4 + \text{diagram}_5 + \text{diagram}_6 + \dots
 \end{aligned}$$

The diagrams are as follows:

- Diagram 1: A circle with two black dots at the top and bottom, and two green dots labeled σ' and σ on the left and right. Inside the circle is the letter V .
- Diagram 2: Two circles connected at their top and bottom dots. The left circle has σ' and σ on its left and right. The right circle has a green dot labeled $-\kappa$ on its left and σ on its right. Both circles contain the letter V .
- Diagram 3: Three circles connected in a chain. The left circle has σ' and σ . The middle circle has $-\kappa$ on its left and $-\kappa$ on its right. The right circle has $-\kappa$ on its left and σ on its right. All circles contain the letter V .
- Diagram 4: A circle with two black dots at the top and bottom, and two teal dots labeled A' and A on the left and right. Inside the circle is the letter V . A dashed line extends from the top dot.
- Diagram 5: Two circles connected at their top and bottom dots. The left circle has A' and A . The right circle has a teal dot labeled M_∞ on its left and A on its right. Both circles contain the letter V . Dashed lines extend from the top dots.
- Diagram 6: Three circles connected in a chain. The left circle has A' and A . The middle circle has M_∞ on its left and M_∞ on its right. The right circle has M_∞ on its left and A on its right. All circles contain the letter V . Dashed lines extend from the top dots.

$$T \rightarrow \infty, a \rightarrow 0$$

Kim, Sachrajda and Sharpe,
Nucl.Phys.B727(2005)218-243.

$$(1) \quad \text{diagram}_1 = \text{diagram}_2 + \text{diagram}_3$$

The diagrams are:

- Diagram 1: A circle with two black dots at the top and bottom, and the letter V inside.
- Diagram 2: A circle with two black dots at the top and bottom, and an infinity symbol ∞ inside.
- Diagram 3: A circle with two black dots at the top and bottom, and the letter V inside. A dashed line extends from the top dot.

$$(2) \quad \text{diagram}_4 = \text{diagram}_5 + \text{diagram}_6 + \dots$$

The diagrams are:

- Diagram 4: A teal circle with four black dots on its sides and the letter M_∞ inside.
- Diagram 5: A green circle with four black dots on its sides and the letter $-\kappa$ inside.
- Diagram 6: A circle with two black dots at the top and bottom, and two green dots labeled $-\kappa$ on the left and right. Inside the circle is an infinity symbol ∞ . A dashed line extends from the top dot.
- Diagram 7: Two circles connected at their top and bottom dots. Both have two black dots at the top and bottom, and two green dots labeled $-\kappa$ on the left and right. Both circles contain an infinity symbol ∞ .

Let's derive the Luescher's formula first. A QFT derivation goes as follows:

$$\begin{aligned}
 C_V &= \text{Diagram 1} + \text{Diagram 2} + \text{Diagram 3} + \dots \\
 &= C_\infty + \text{Diagram 4} + \text{Diagram 5} + \text{Diagram 6} + \dots
 \end{aligned}$$

The diagrams are Feynman diagrams representing the expansion of the vacuum energy C_V . The first row shows a series of diagrams with green circles labeled σ' and σ , and vertices labeled V and $-\kappa$. The second row shows the same series of diagrams with teal circles labeled A' and A , and vertices labeled V and \mathcal{M}_∞ . Dashed lines connect the vertices between the two rows.

$$\det [\delta\mathcal{G}^V(E^*) + \mathcal{M}_\infty^{-1}(E^*)] = 0$$

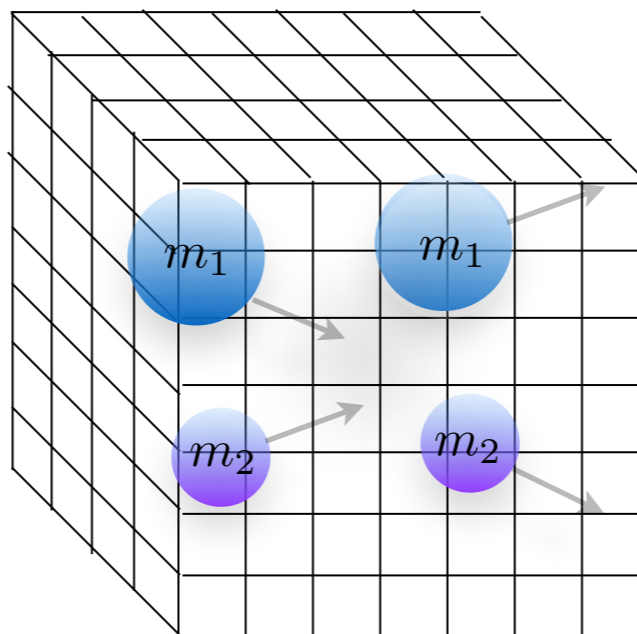
Kim, Sachrajda and Sharpe,
Nucl.Phys.B727(2005)218-243.

Finite-volume function Scattering amplitude

Poles of C_V which are the finite-volume CM energy eigenvalues.

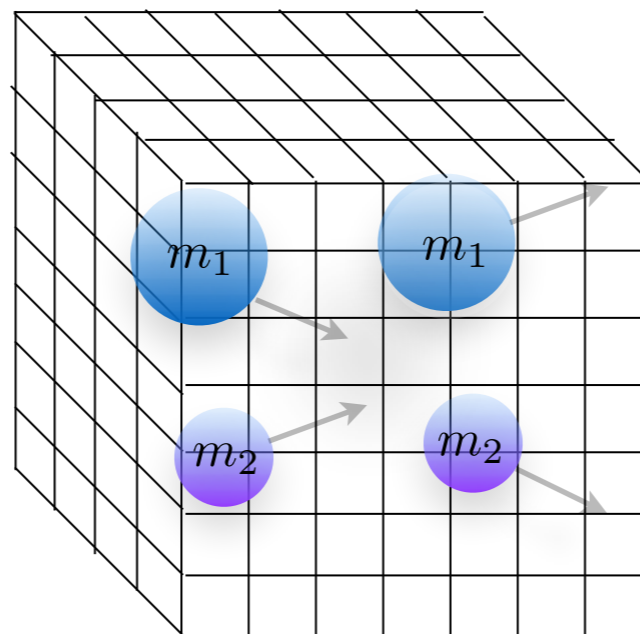
$$\det [\delta\mathcal{G}^V(E^*) + \mathcal{M}_\infty^{-1}(E^*)] = 0$$

Luescher (1986, 1991).



$$\det [\delta\mathcal{G}^V(E^*) + \mathcal{M}_\infty^{-1}(E^*)] = 0$$

Luescher (1986, 1991).



Elastic amplitude more closely...

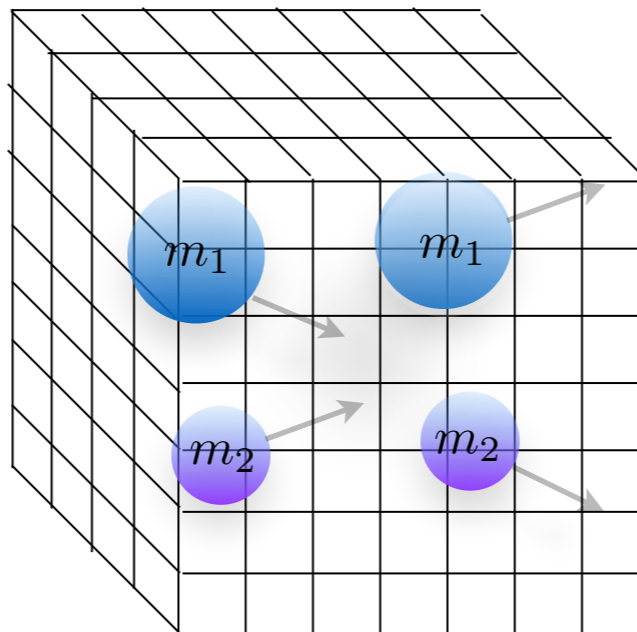
$$(\mathcal{M})_{l_1, m_1; l_2, m_2} = \delta_{l_1, l_2} \delta_{m_1, m_2} \frac{\delta \pi E^*}{n q^*} \frac{e^{2i\delta^{(l)}}(q^*) - 1}{2i}$$

CM energy
Phase shift

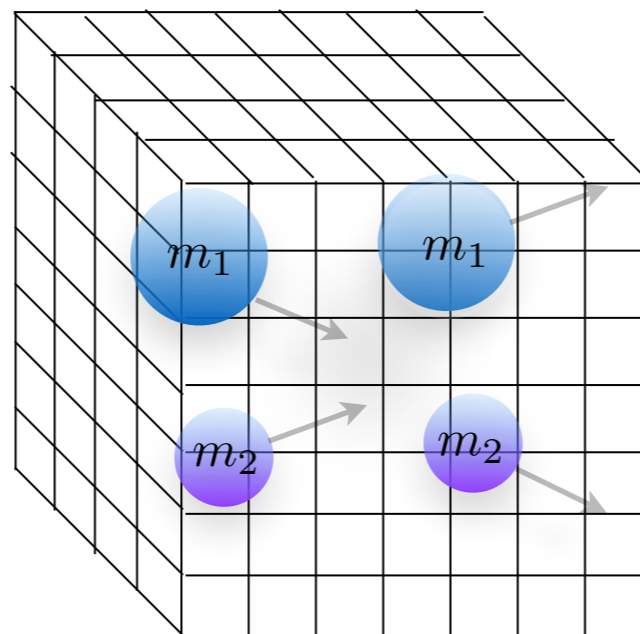
Symmetry factor
 nq^*

$$q^{*2} = \frac{1}{4} \left(E^{*2} - 2(m_1^2 + m_2^2) + \frac{(m_1^2 - m_2^2)^2}{E^{*2}} \right)$$

$$\det [\delta \mathcal{G}^V(E^*) + \mathcal{M}_\infty^{-1}(E^*)] = 0$$



$$\det [\delta \mathcal{G}^V(E^*) + \mathcal{M}_\infty^{-1}(E^*)] = 0$$



Finite-volume function more closely...

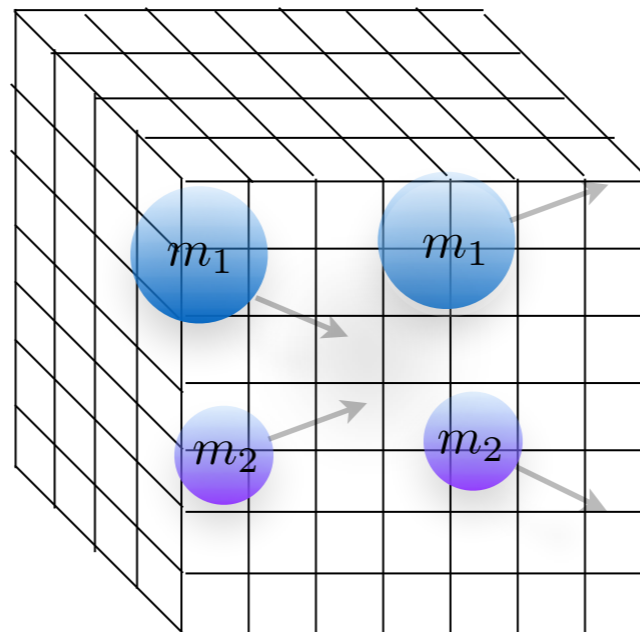
$$(\delta\mathcal{G}^V)_{l_1, m_1; l_2, m_2} = i \frac{q^* n}{8\pi E^*} \left(\delta_{l_1, l_2} \delta_{m_1, m_2} + i \frac{4\pi}{q^*} \sum_{l, m} \frac{\sqrt{4\pi}}{q^{*l}} c_{lm}^{\mathbf{P}}(q^{*2}) \int d\Omega^* Y_{l_1 m_1}^* Y_{lm}^* Y_{l_2 m_2} \right)$$

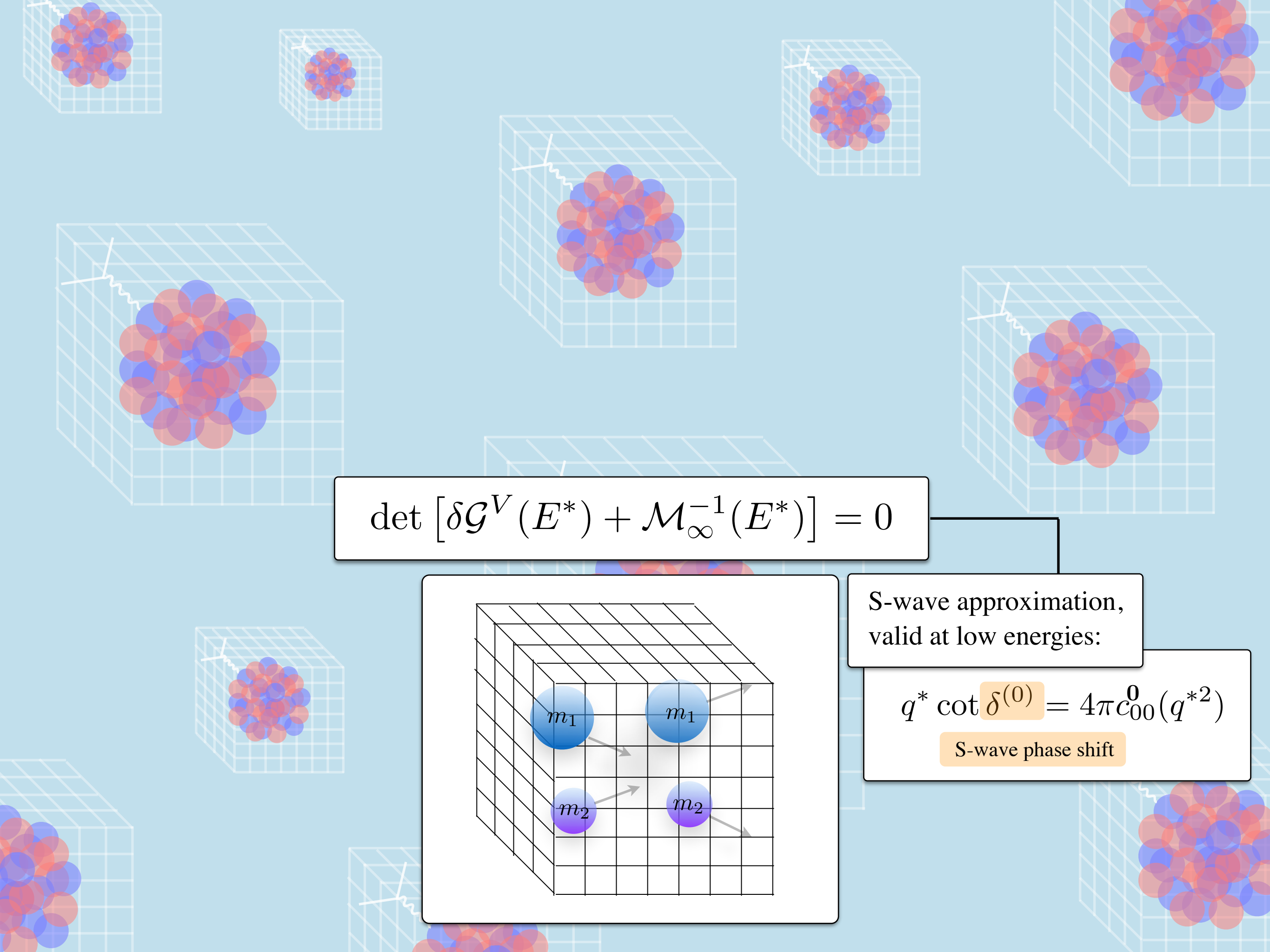
$$c_{lm}^{\mathbf{P}}(x) = \frac{1}{\gamma} \left[\frac{1}{L^3} \sum_{\mathbf{k}} -\mathcal{P} \int \frac{d^3\mathbf{k}}{(2\pi)^3} \frac{\sqrt{4\pi} Y_{lm}(\hat{\mathbf{k}}^*) k^{*l}}{k^{*2} - x} \right]$$

$$\mathbf{k}^* = \gamma^{-1} \left[\mathbf{k}_{\parallel} - \frac{1}{2} \left(1 + \frac{m_1^2 - m_2^2}{E^{*2}} \right) \mathbf{P} \right] + \mathbf{k}_{\perp}$$

ZD and Savage, Phys. Rev. D84, 114502 (2011).

$$\det [\delta\mathcal{G}^V(E^*) + \mathcal{M}_{\infty}^{-1}(E^*)] = 0$$

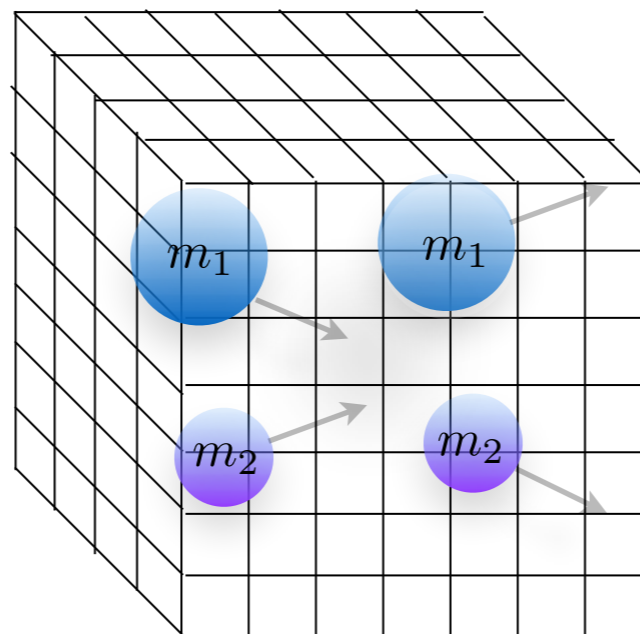



$$\det [\delta \mathcal{G}^V (E^*) + \mathcal{M}_\infty^{-1} (E^*)] = 0$$

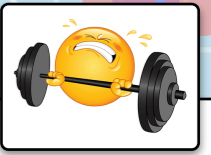
S-wave approximation,
valid at low energies:

$$q^* \cot \delta^{(0)} = 4\pi c_{00}^0 (q^{*2})$$

S-wave phase shift



EXERCISE 3



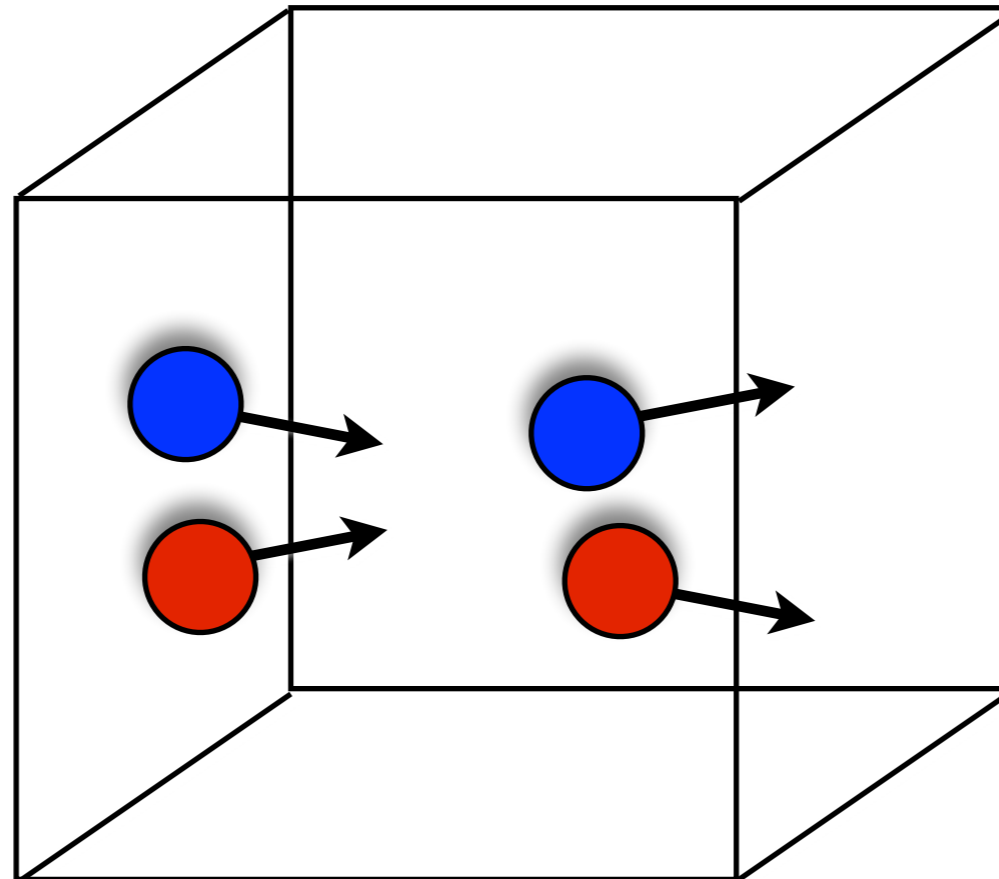
Derive the S-wave limit of Luescher's quantization condition from the master relation.

BONUS EXERCISE 2



Plot the S-wave finite-volume function c_{00}^0 for a range of momenta q^{*2} , including negative values. At what values of q^{*2} do you observe singularities? What do these momenta correspond to?

Now let's see an application of Luescher's method to obtain elastic scattering amplitudes of two nucleon from lattice QCD (at a large quark mass!):

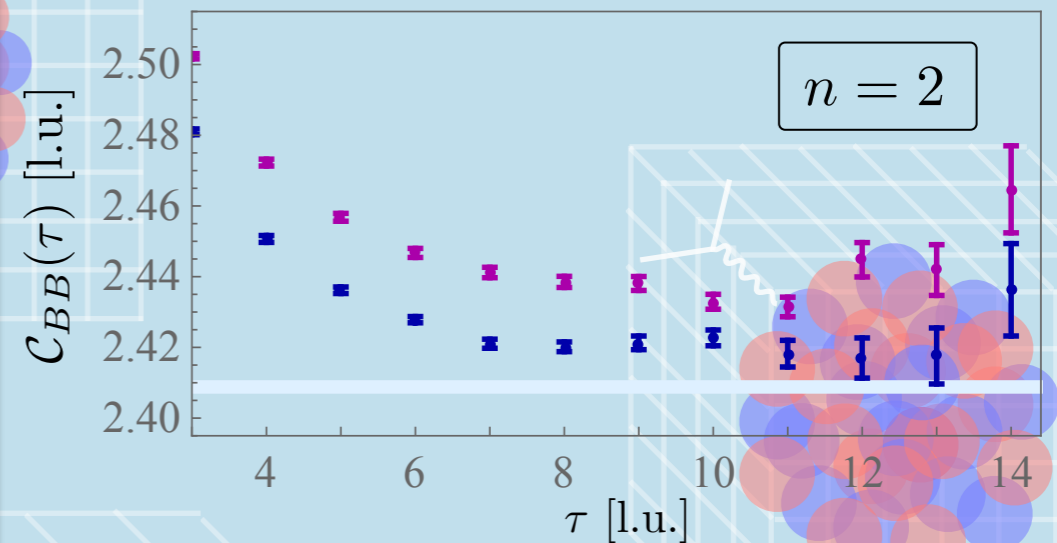
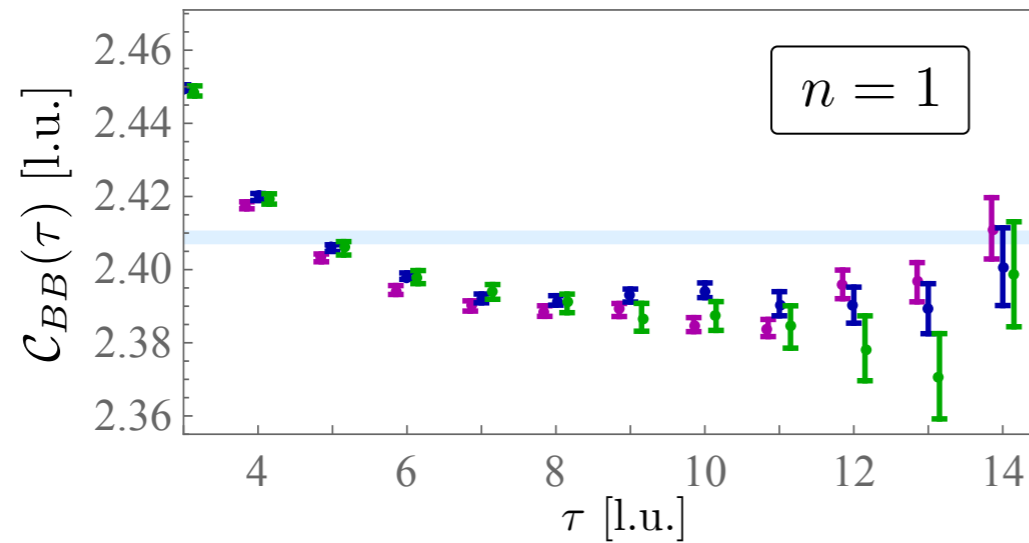


Wagman et al. (NPLQCD), Phys.Rev.D 96,114510(2017).

Step 1: Obtain the lowest-lying spectra

$N_f = 3, m_\pi = 0.806 \text{ GeV}, a = 0.145(2) \text{ fm}$

$NN (^3S_1)$



$24^3 \times 48$

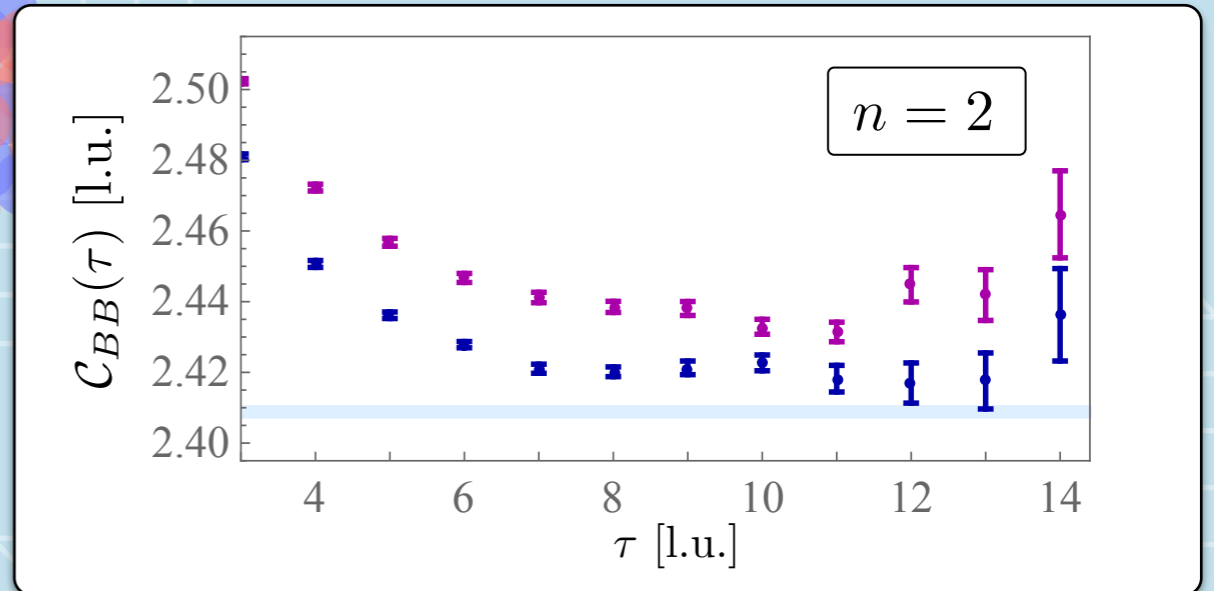
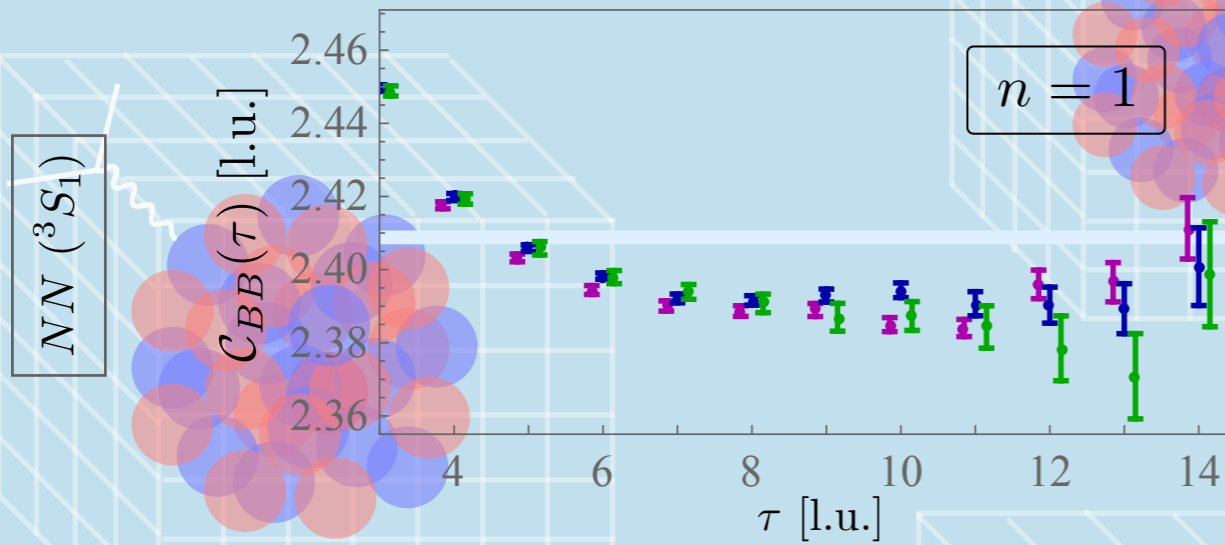
$32^3 \times 48$

$48^3 \times 64$

$2M_N$

Step 1: Obtain the lowest-lying spectra

$N_f = 3$, $m_\pi = 0.806$ GeV, $a = 0.145(2)$ fm



$24^3 \times 48$

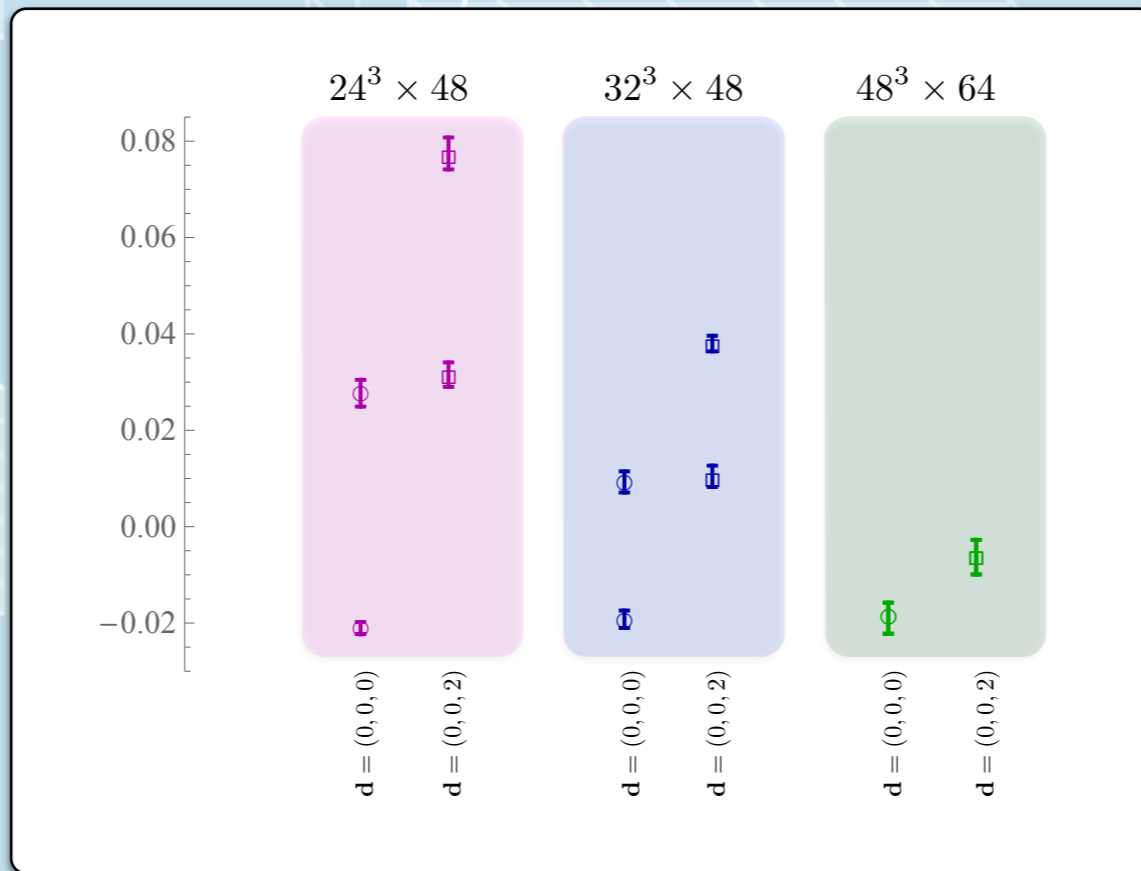
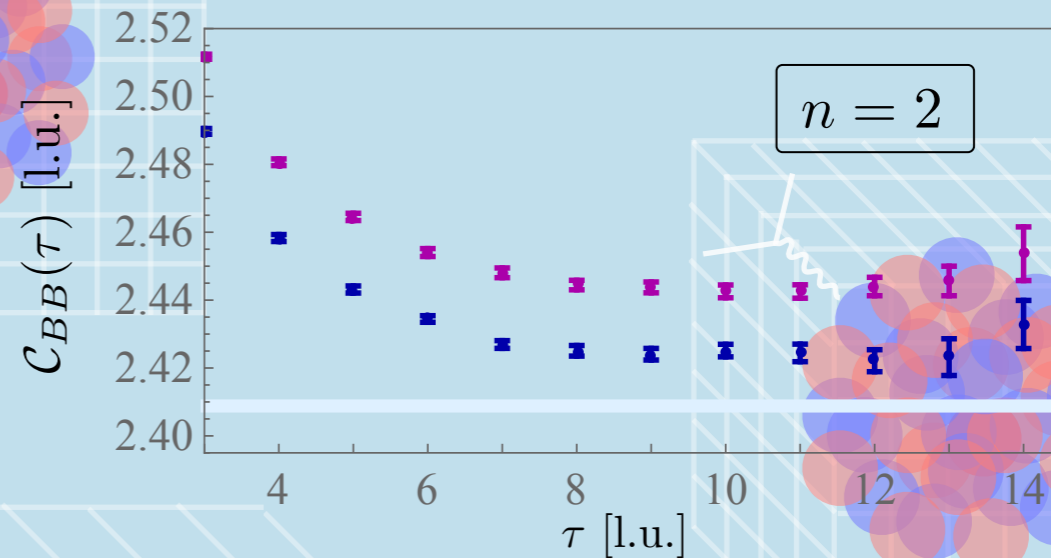
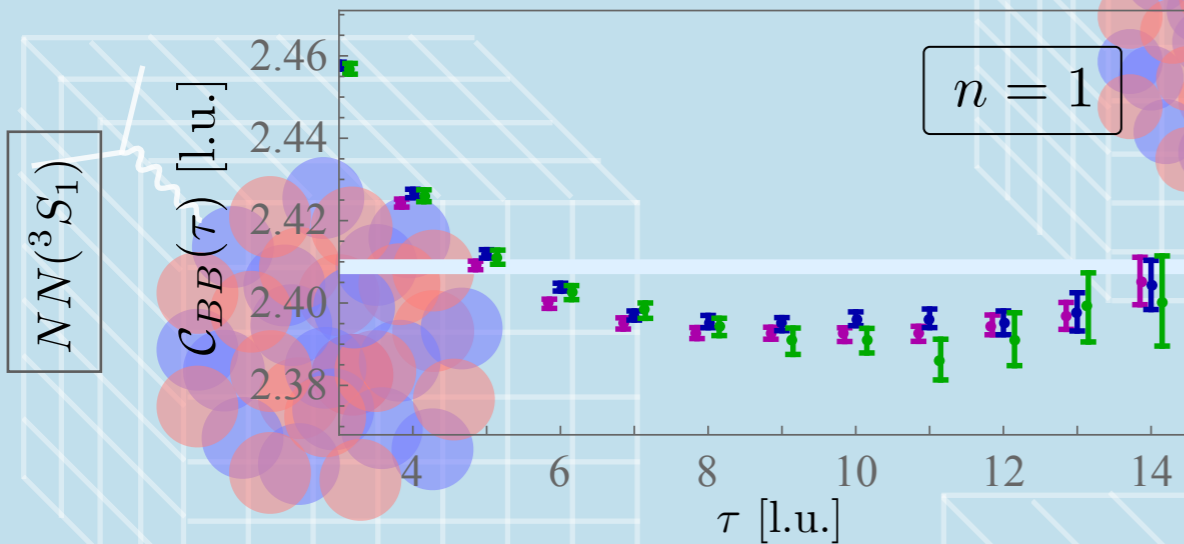
$32^3 \times 48$

$48^3 \times 64$

$2M_N$

Step 1: Obtain the lowest-lying spectra

$N_f = 3$, $m_\pi = 0.806$ GeV, $a = 0.145(2)$ fm



Step 2: Feed the energies to the Luescher's equation and obtain the S-wave scattering phase shifts.

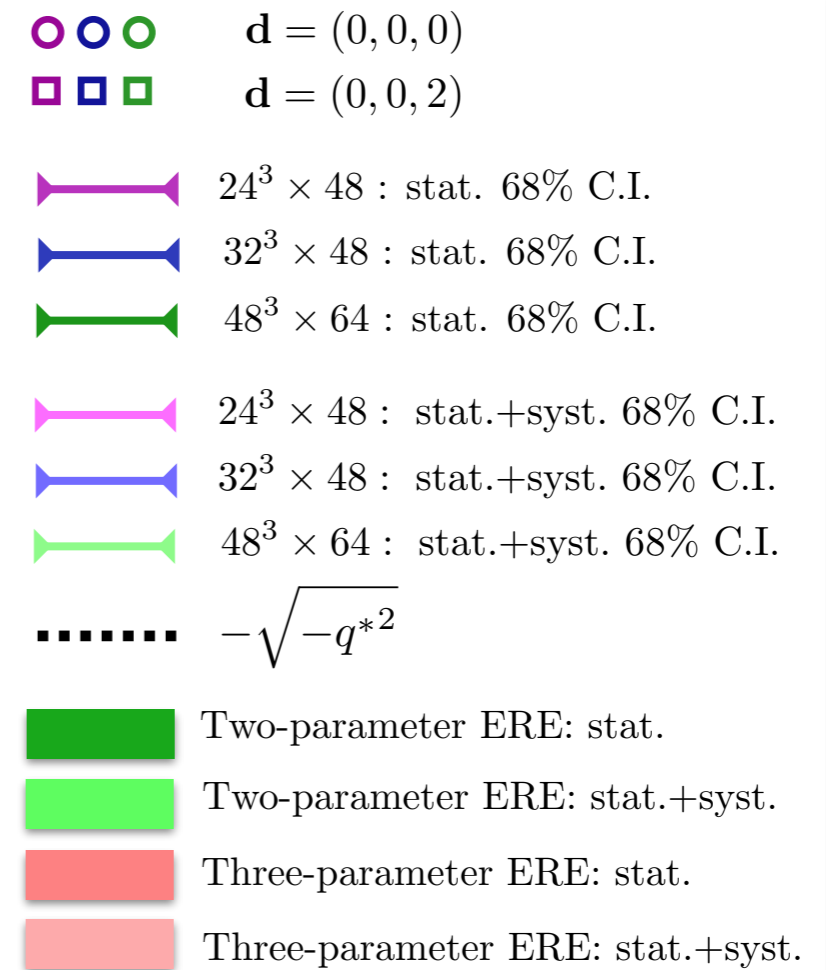
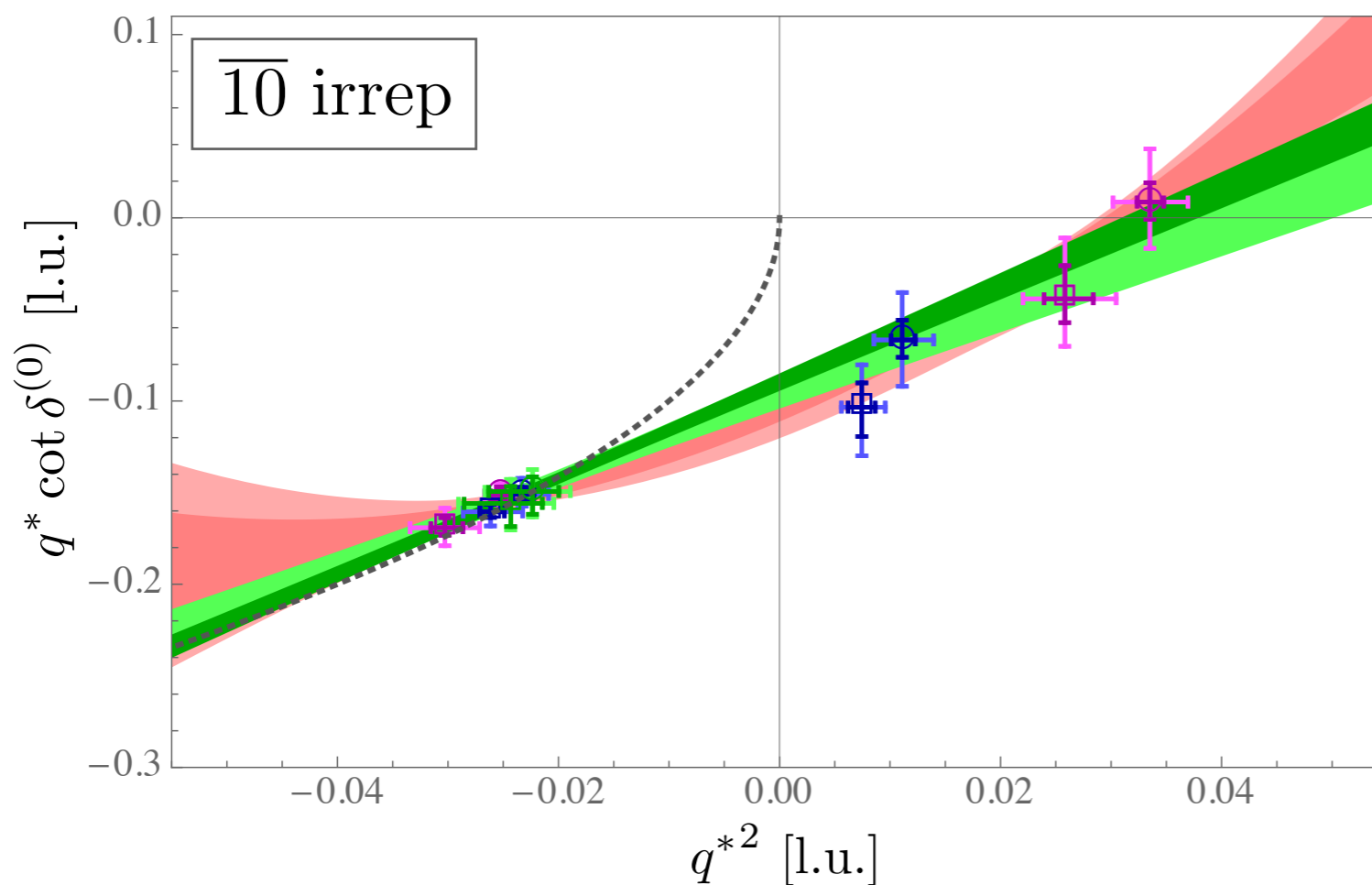
$$q^* \cot \delta^{(0)} = 4\pi c_{00}^0(q^{*2})$$

S-wave phase shift

Step 2: Feed the energies to the Luescher's equation and obtain the S-wave scattering phase shifts.

$N_f = 3, m_\pi = 0.806 \text{ GeV}, a = 0.145(2) \text{ fm}$

$$q^* \cot \delta^{(0)} = -\frac{1}{a} + \frac{1}{2} r q^{*2} + \dots$$



$$B = 27.9^{(+3.1)(+2.2)}_{(-2.3)(-1.4)} \text{ MeV}$$

Let's discuss in greater depth step V:

Step V: make the connection to physical observables, such as scattering amplitudes, decay rates, etc.

i) Finite-volume effects in the single-hadron sector

ii) Finite-volume formalism for two-hadron elastic scattering



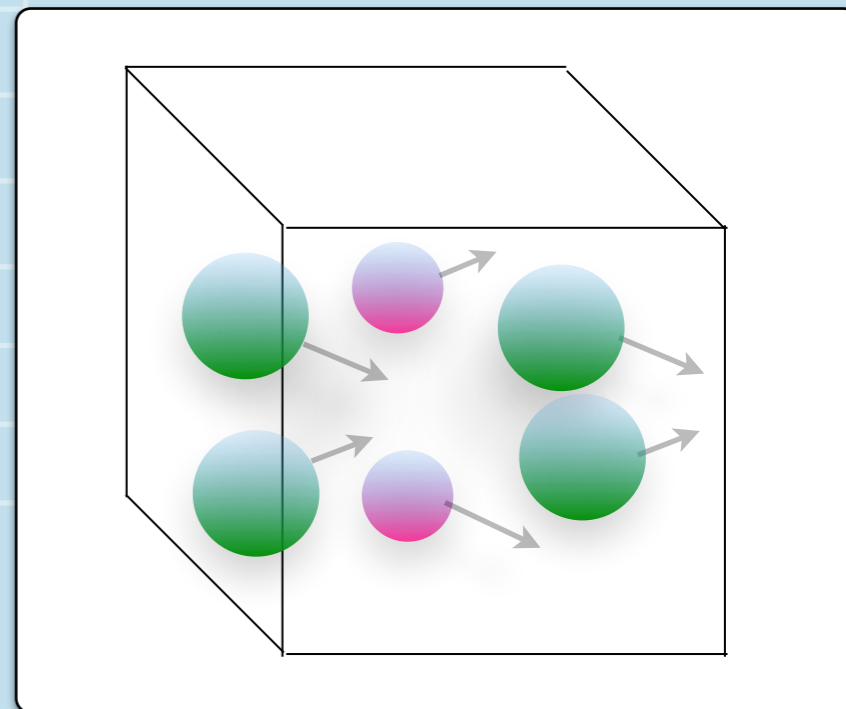
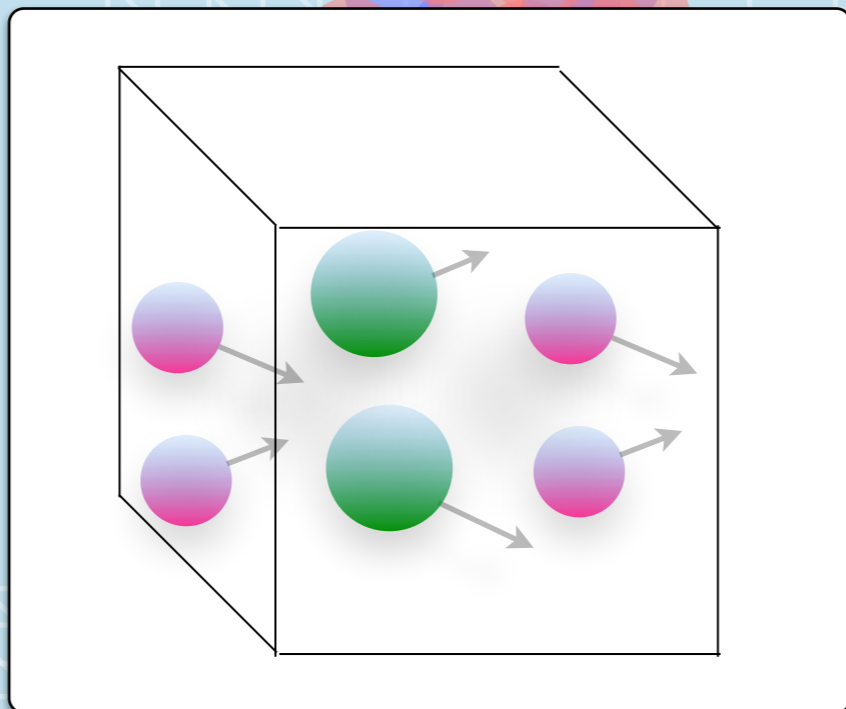
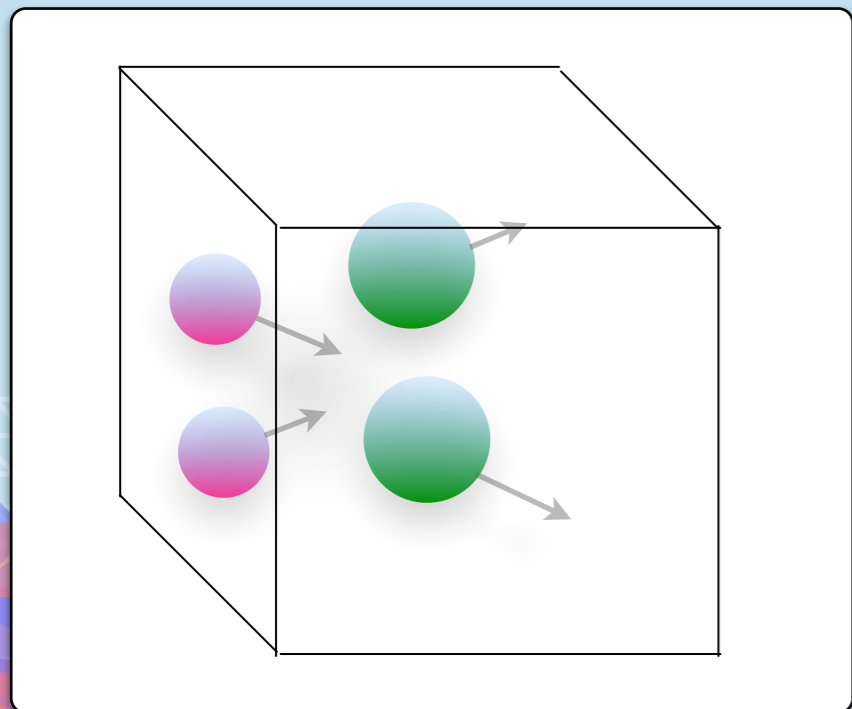
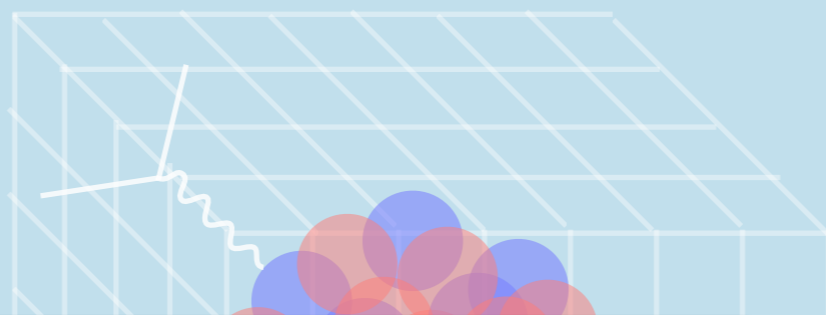
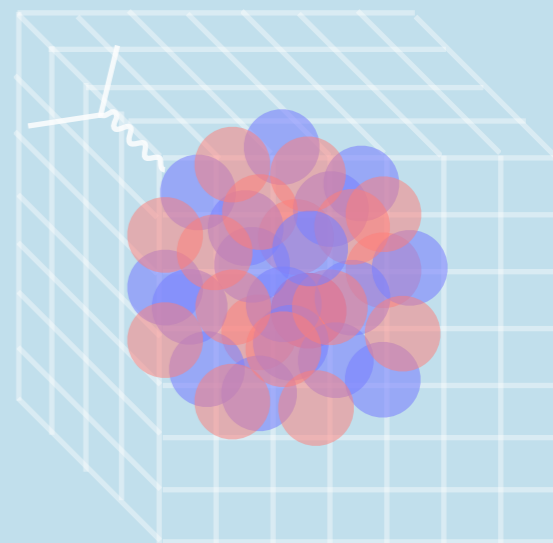
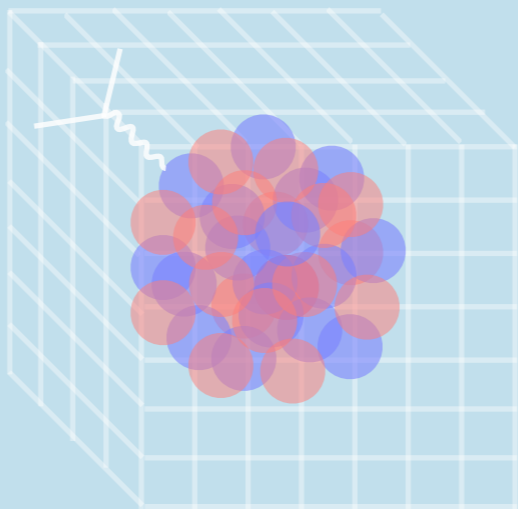
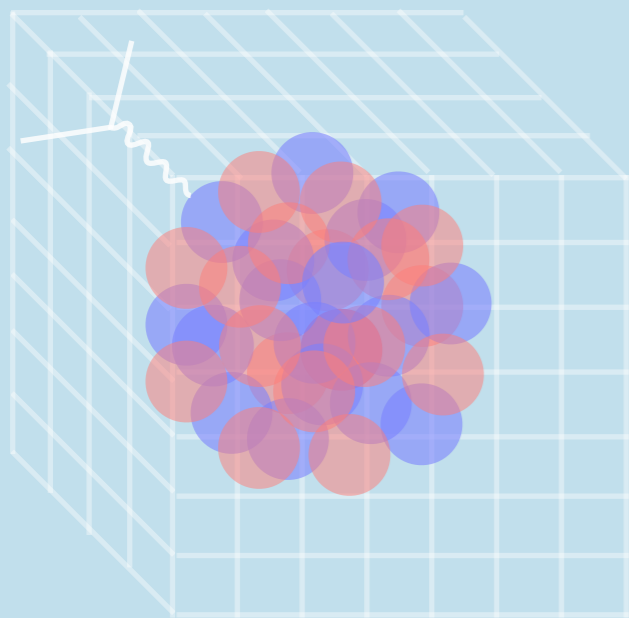
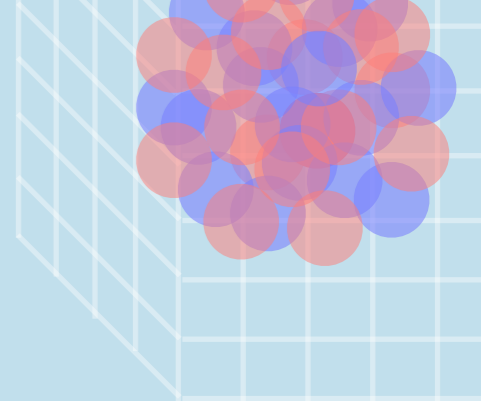
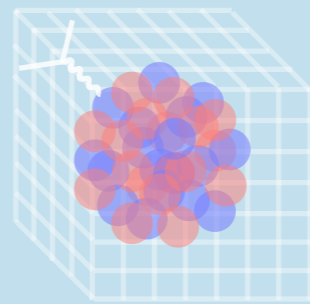
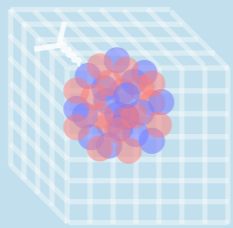
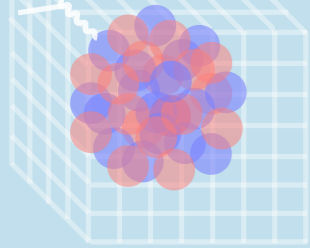
iii) Finite-volume formalism for coupled-channel two-hadron elastic scattering and resonances

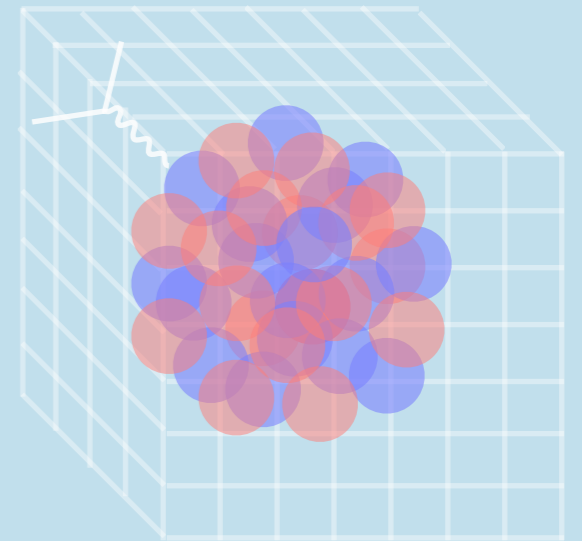
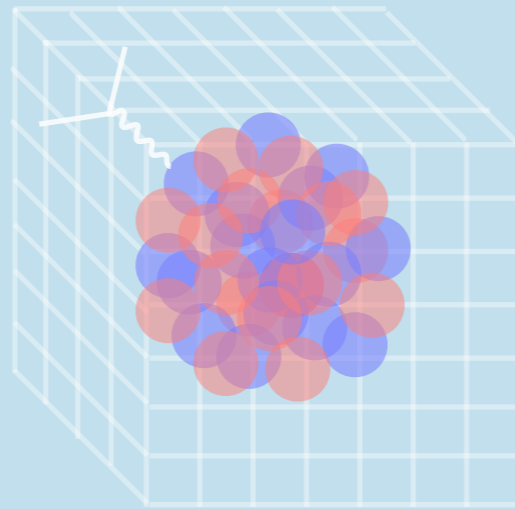
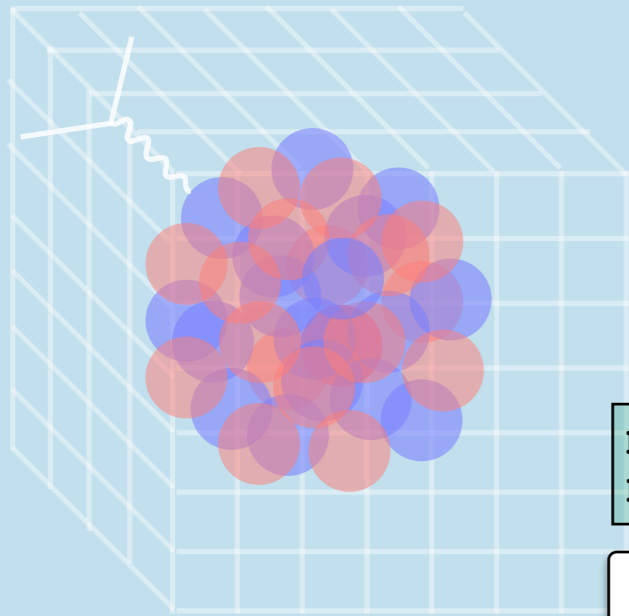
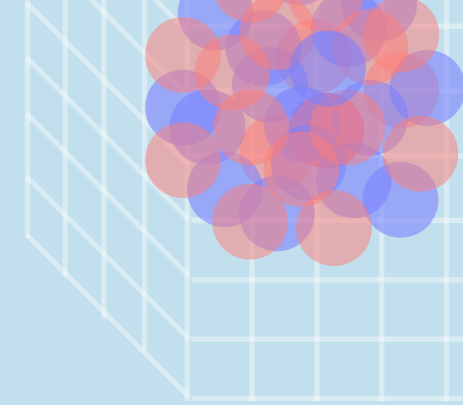
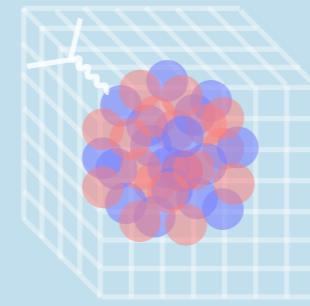
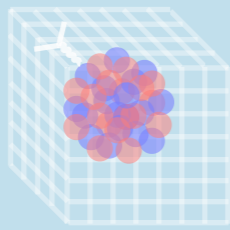
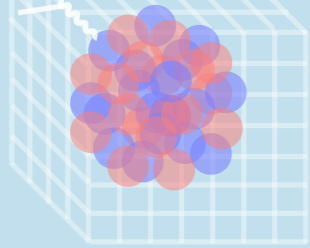
iv) Finite-volume formalism for transition amplitudes and resonance form factors

v) Finite-volume formalism for three-hadron scattering and resonances

vi) Finite-volume effects in lattice QED+QCD studies of hadrons

See e.g., ZD, arXiv:1409.1966 [hep-lat, Briceno, Dudek and Young, Rev. Mod. Phys. 90.025001, Ann. Rev. Nucl. Part. Sci. 69 (2019).

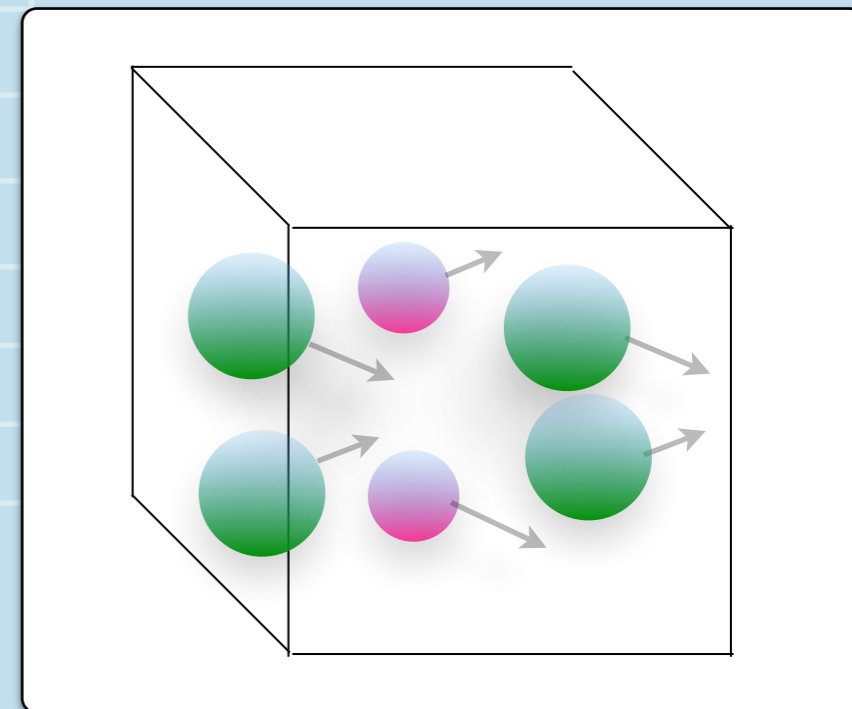
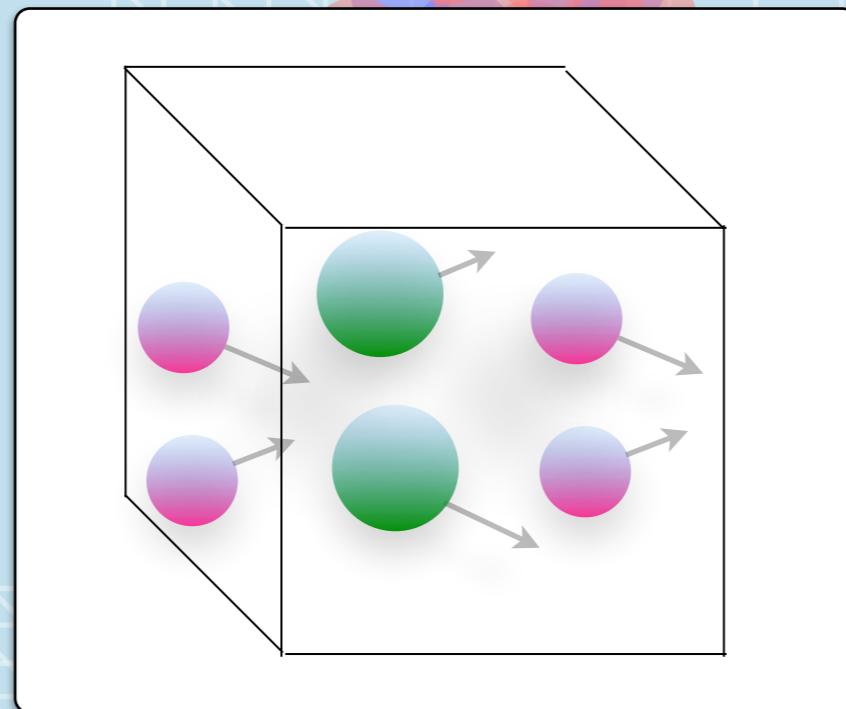
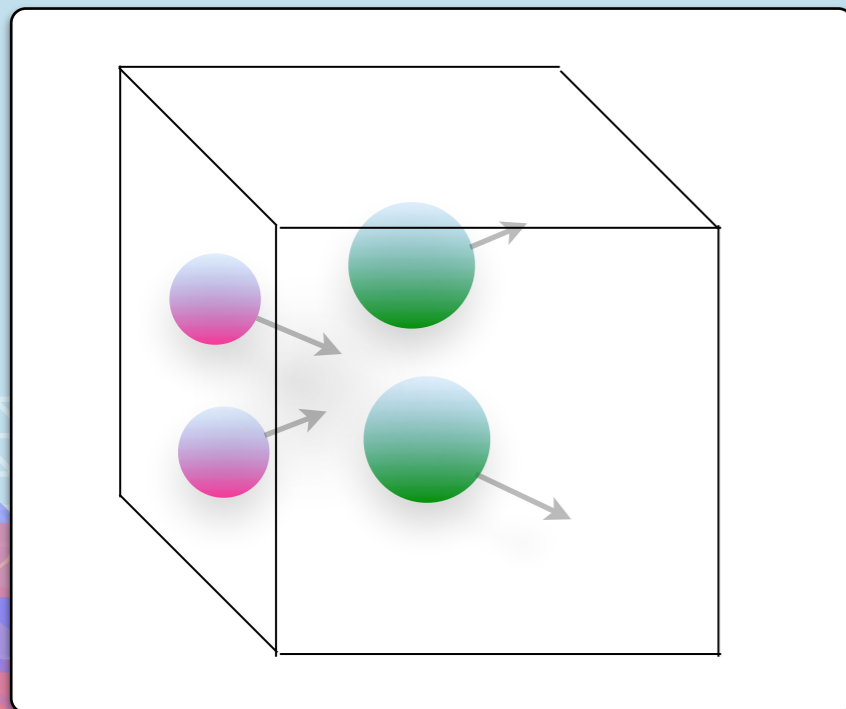




Briceno and ZD, Phys. Rev. D88, 094507 (2013).

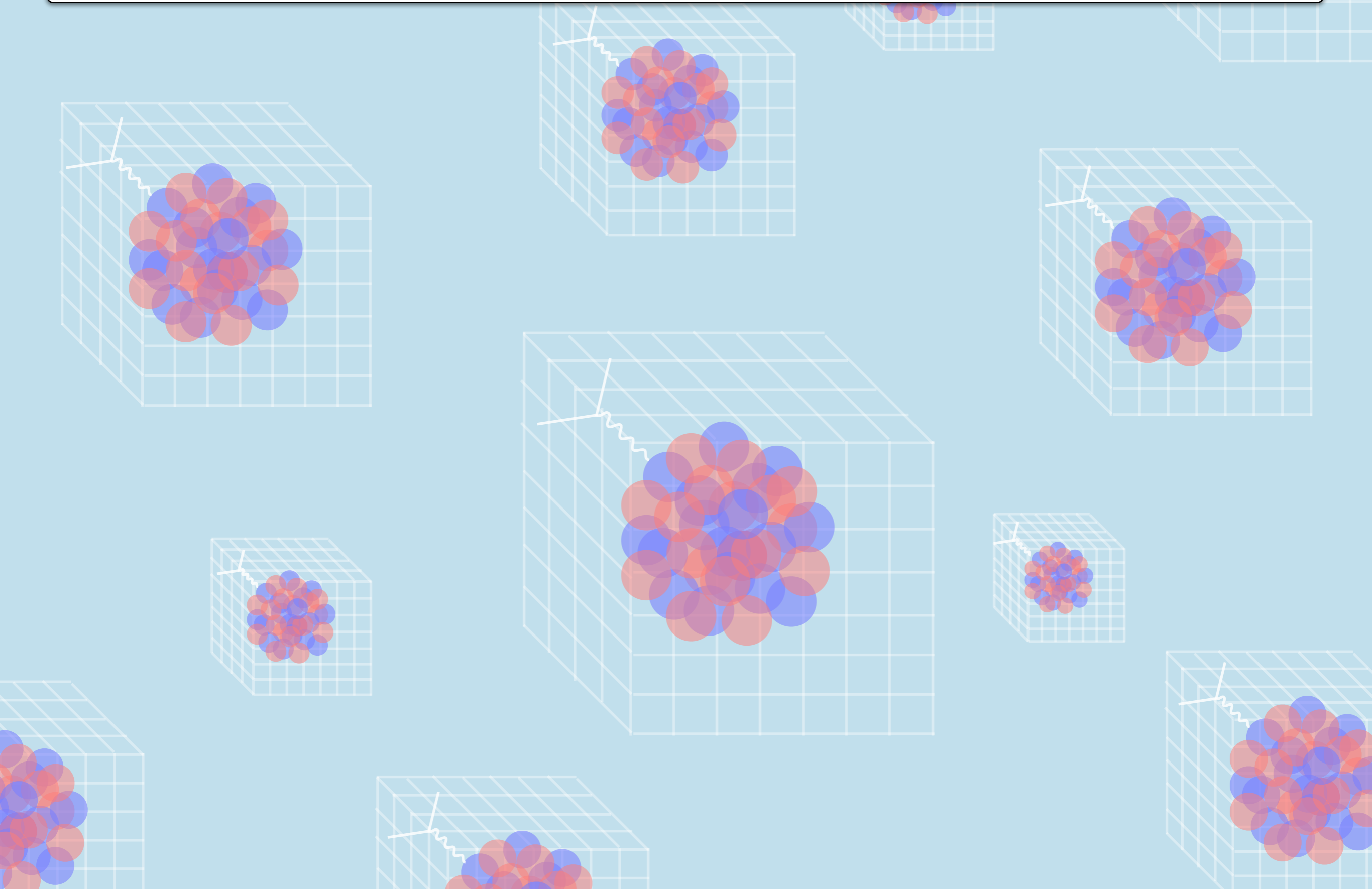
Hansen and Sharpe, Phys. Rev. D86, 016007 (2012).

$$\text{Det} [\delta\mathcal{G}^V (E^*) + \mathcal{M}_{\infty}^{-1}(E^*)] = 0$$



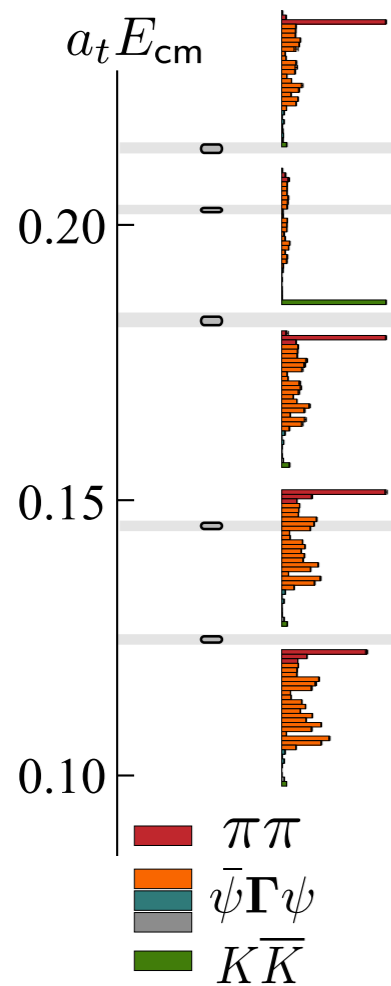
Now let's see an application of the coupled-channel formalism: Hunting resonances using lattice QCD in the P-wave coupled $\pi\pi - K\bar{K}$ channel

Wilson et al. (HadSpec),
Phys.Rev. D92 (2015), 094502



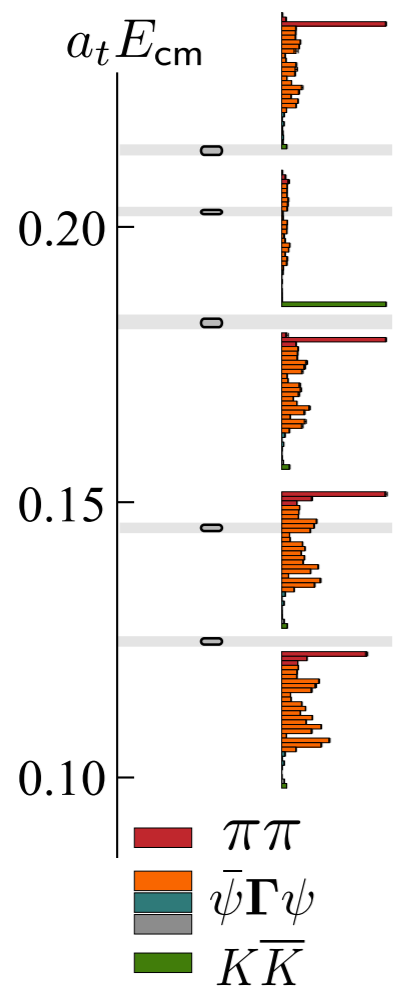
Now let's see an application of the coupled-channel formalism: Hunting resonances using lattice QCD in the P-wave coupled $\pi\pi - K\bar{K}$ channel

Wilson et al. (HadSpec),
Phys.Rev. D92 (2015), 094502

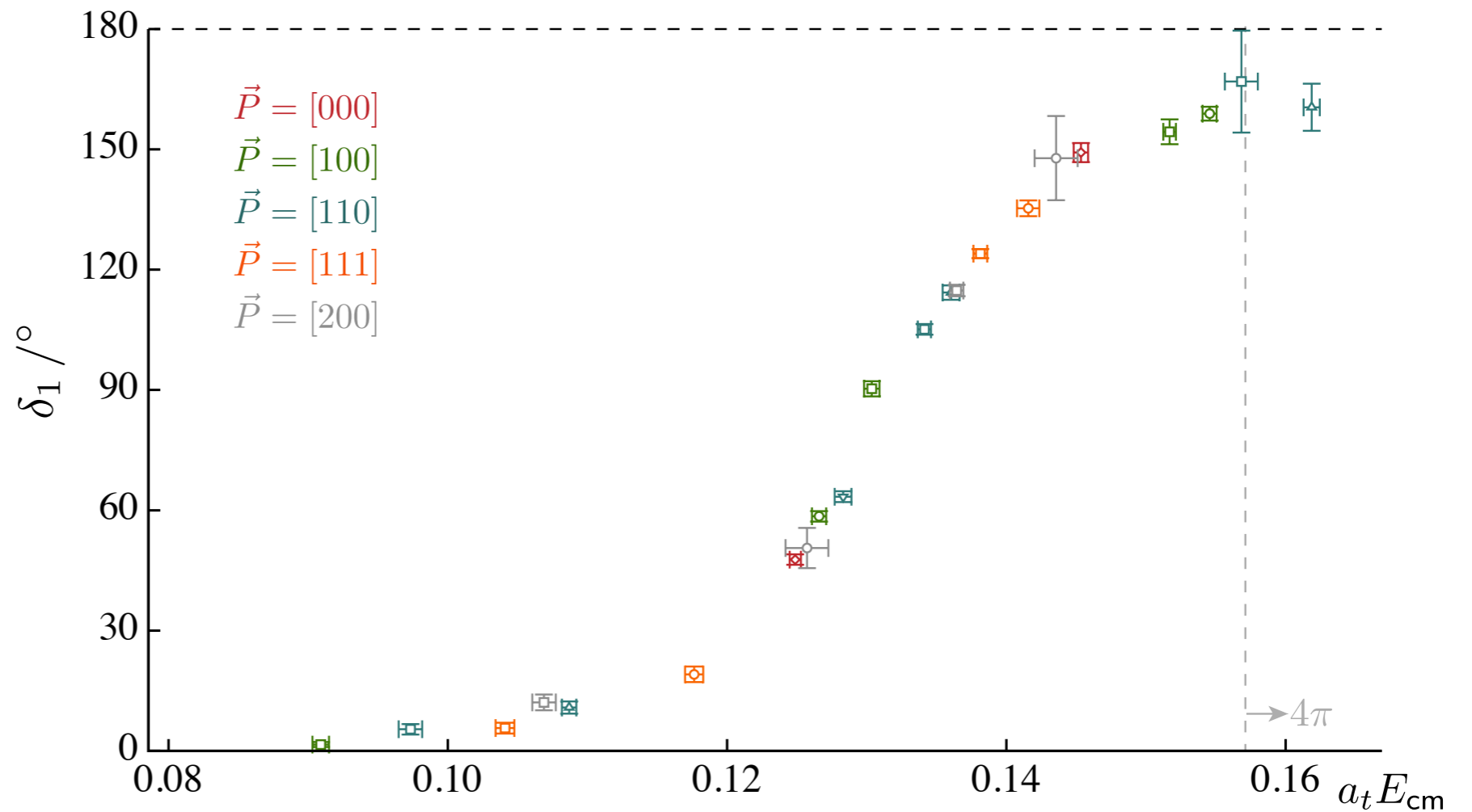


Example: T1 irrep
energies

$$N_f = 2 + 1, m_\pi = 236 \text{ MeV}, V \approx (4 \text{ fm})^3$$

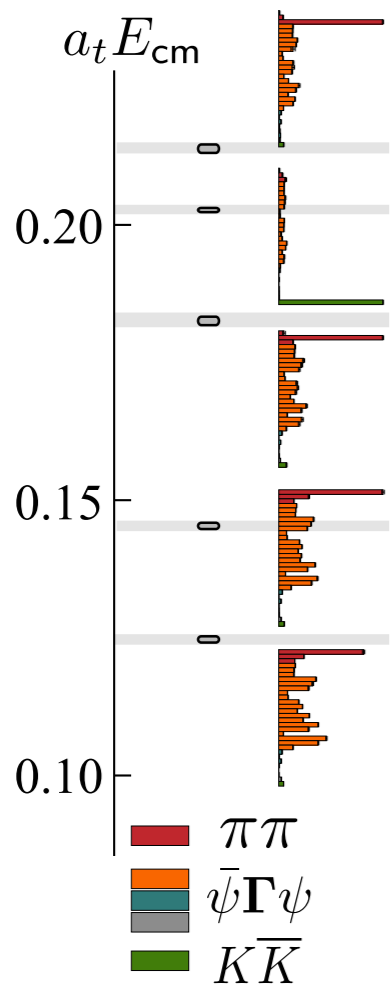


Example: T1 irrep
 energies

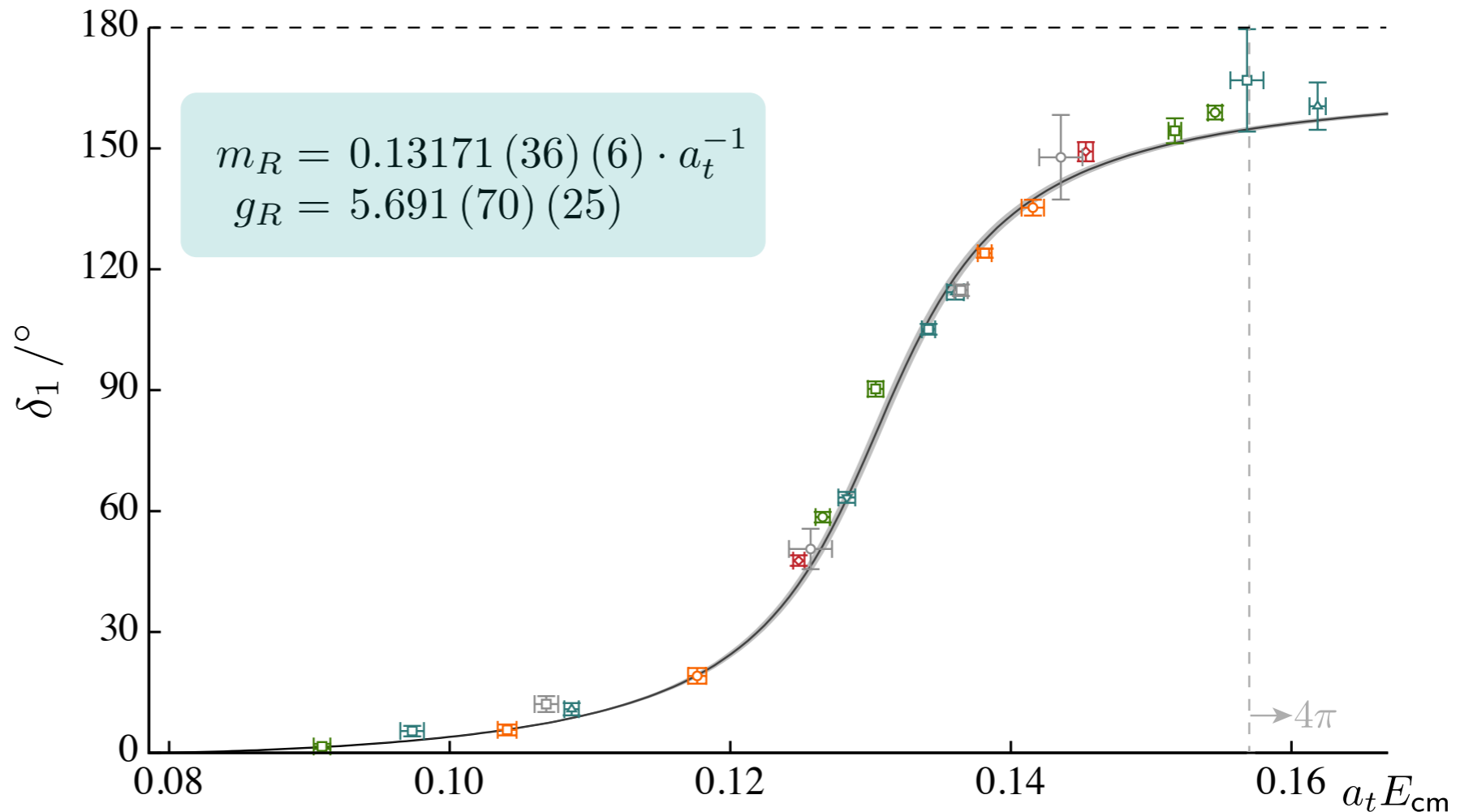


P-wave $\pi\pi$ phase shift as a function of energy

$$N_f = 2 + 1, m_\pi = 236 \text{ MeV}, V \approx (4 \text{ fm})^3$$



Example: T1 irrep energies



Fit to a Breit-Wigner form

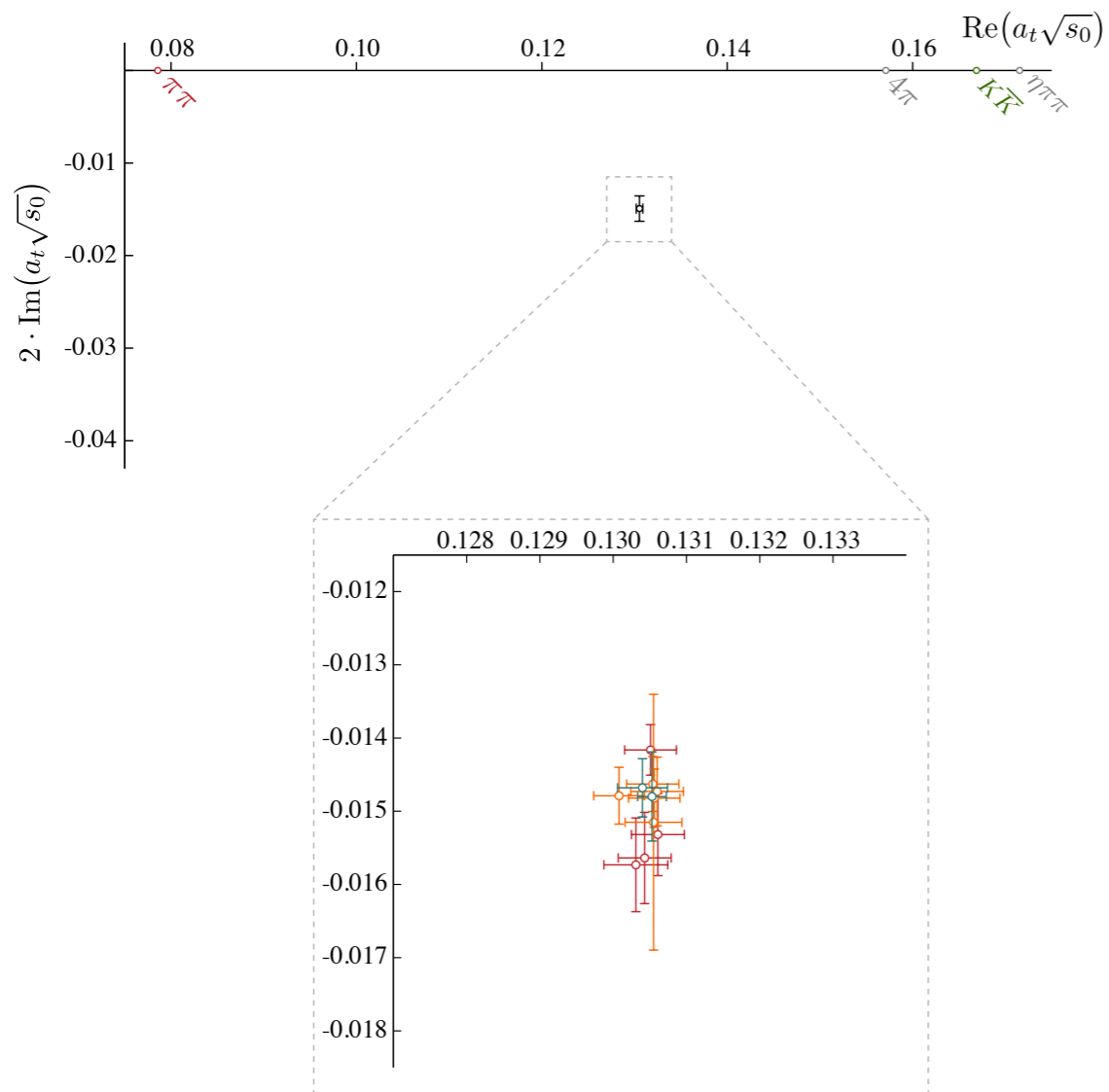
$$\mathcal{M}(s) = \frac{1}{\rho(s)} \frac{\sqrt{s} \Gamma(s)}{m_R^2 - s - i\sqrt{s} \Gamma(s)}$$

$$\begin{aligned} \rho_i(E_{\text{cm}}) &= 2\bar{k}_i/E_{\text{cm}} \\ s &= E_{\text{cm}}^2 \\ \Gamma(s) &= \frac{g_R^2 k^3}{6\pi s} \end{aligned}$$

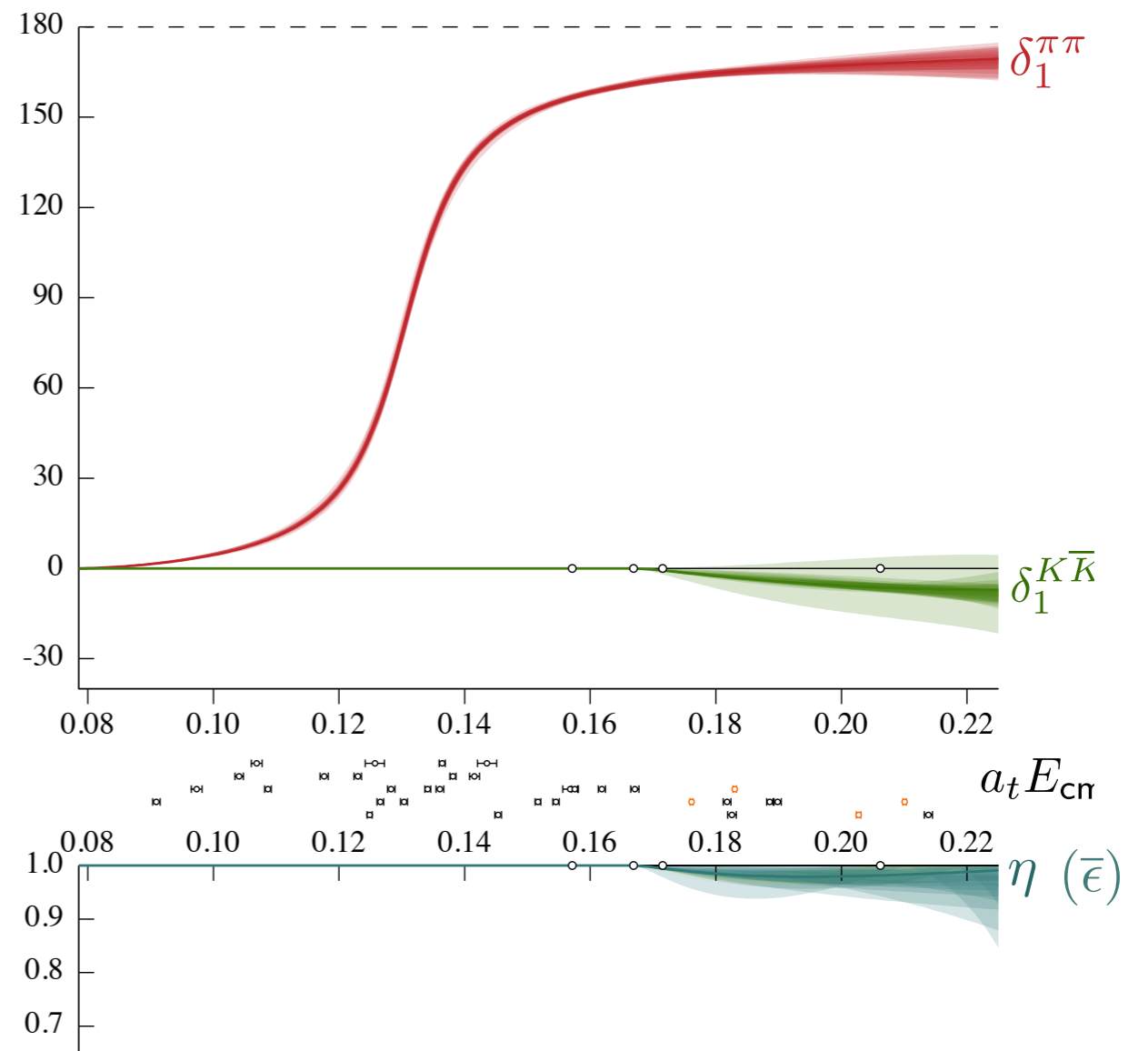
$$N_f = 2 + 1, m_\pi = 236 \text{ MeV}, V \approx (4 \text{ fm})^3$$

Using a range of parametrizations:

Pole position:



All three scattering parameters:



$$N_f = 2 + 1, m_\pi = 236 \text{ MeV}, V \approx (4 \text{ fm})^3$$

SUMMARY OF LECTURE I

Lattice QCD workflow

GENERATE A
SAMPLE OF
VACUUM
CONFIGURATIONS

- Hybrid Monte Carlo to sample gauge configurations
- Determinant of a high-dimensional matrix required

COMPUTE
EUCLIDEAN
CORRELATION
FUNCTIONS

- Quark contractions
- Inverting a high-dimensional matrix required (to get the quark propagators)

ANALYZE
CORRELATION
FUNCTIONS:
NUMERICS AND
ANALYTICAL WORK

- Assess stat. and sys. uncertainties (take the continuum and infinite-volume limits)
- Connect to physical observables

LECTURE II: NUCLEON STRUCTURE FROM LATTICE QCD...

The background of the slide features a repeating pattern of nucleon clusters. Each cluster is represented as a collection of overlapping red and blue spheres, resembling a nucleus, situated within a white 3D wireframe cube that represents a lattice. The clusters vary in size and orientation across the background. A central white rectangular box with a black border contains the title text.

LECTURE II: NUCLEON STRUCTURE FROM LATTICE QCD

Let's enumerate some of the methods that give access to structure quantities in general:

Three(four)-point functions

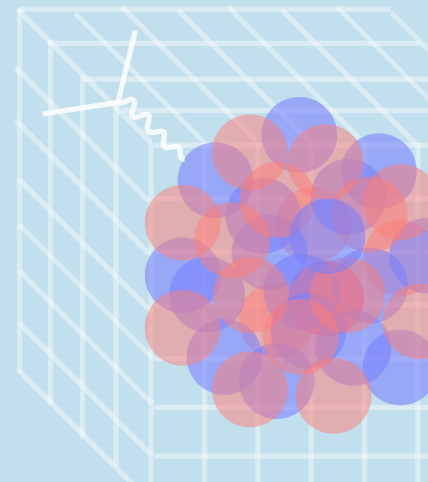
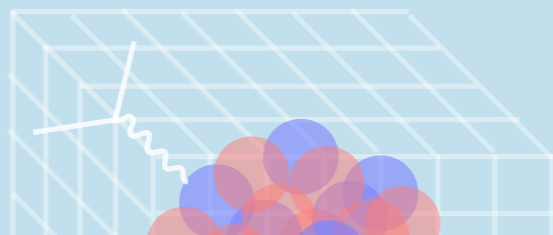
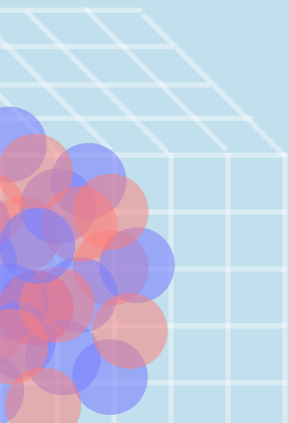
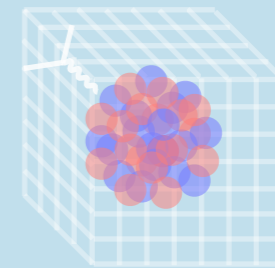
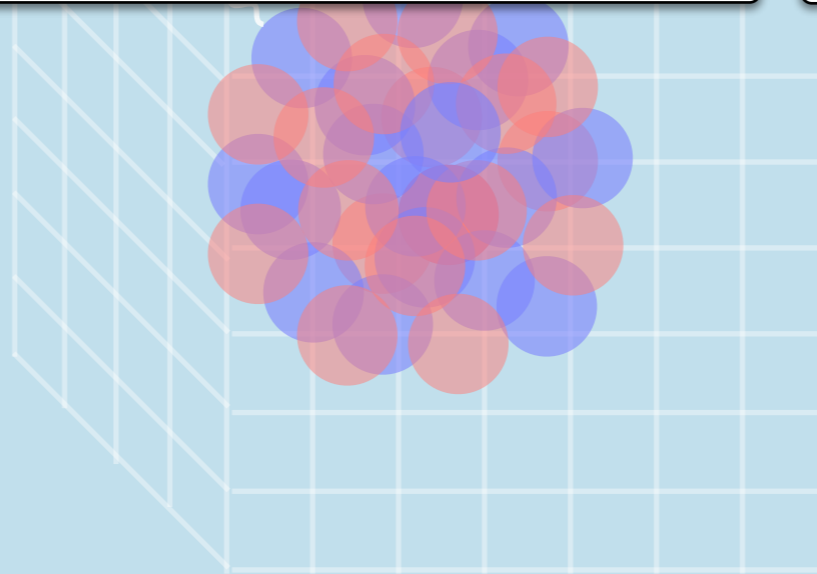
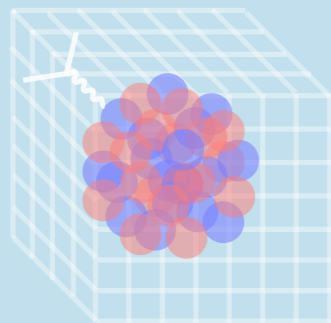
For e.g., form factors, moments of structure functions, Compton amplitude, transition amplitudes

Background-field methods

For e.g., EM moments and polarizabilities, charge radius, form factors and transition amplitudes.

Feynman-Hellmann inspired methods

Similar to background fields. For e.g., axial charge, form factors, EM moments, transition amplitudes



Let's enumerate some of the methods that give access to structure quantities in general:

Three(four)-point functions

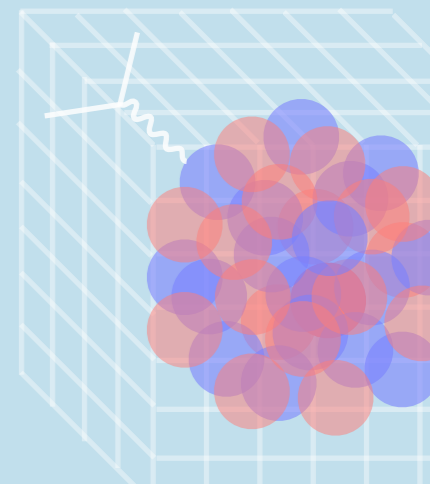
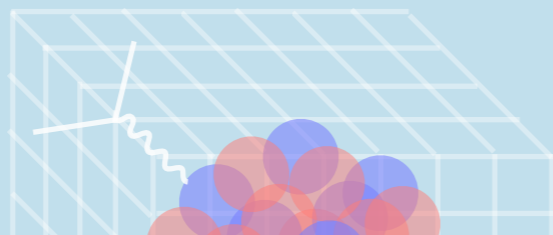
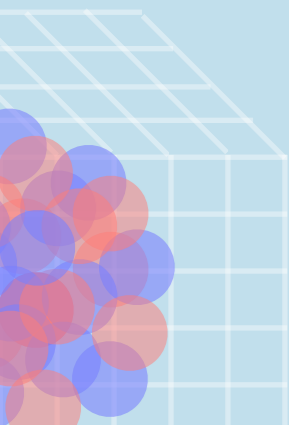
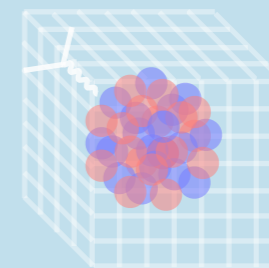
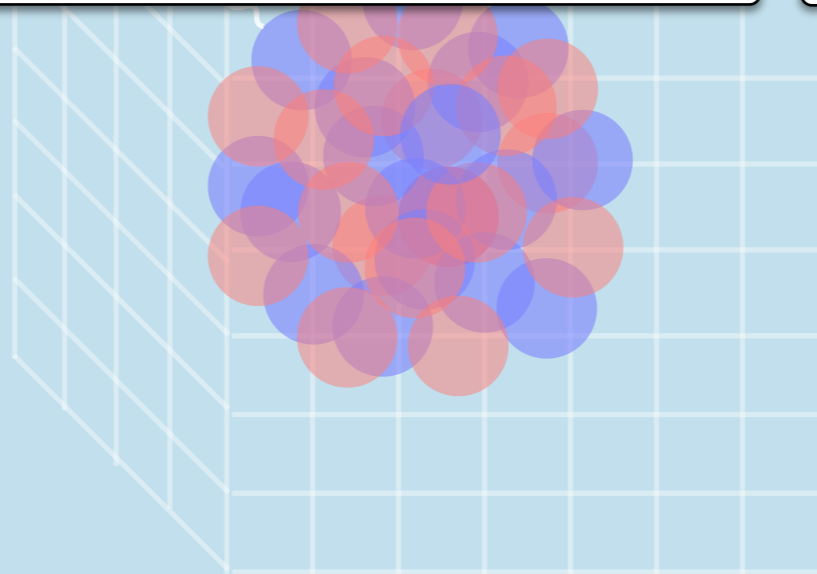
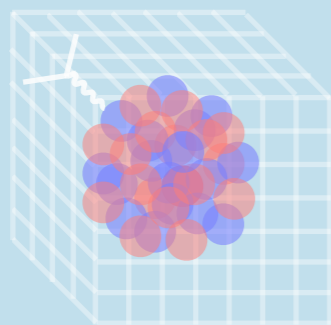
For e.g., form factors, moments of structure functions, Compton amplitude, transition amplitudes

Background-field methods

For e.g., EM moments and polarizabilities, charge radius, form factors and transition amplitudes.

Feynman-Hellmann inspired methods

Similar to background fields. For e.g., axial charge, form factors, EM moments, transition amplitudes



A three-point (3pt)
function:

$$C_{\tilde{\chi}O\chi}(x', y, x) \equiv \langle \chi(x') \mathcal{O}(y) \tilde{\chi}(x) \rangle$$

Chambers, <http://inspirehep.net/record/1744874/>

Annihilate the state

Insert the
operator

Create the state

A three-point (3pt) function:

$$C_{\tilde{\chi}\mathcal{O}\chi}(x', y, x) \equiv \langle \chi(x') \mathcal{O}(y) \tilde{\chi}(x) \rangle$$

Chambers, <http://inspirehep.net/record/1744874/>

Annihilate the state

Insert the operator

Create the state

Spectral decomposition of the 3pt function in Euclidean spacetime

$$G_{\chi\mathcal{O}\tilde{\chi}}(\mathbf{p}', \mathbf{p}; t', \tau, t) = \sum_{X, Y} \frac{e^{-E_X(\mathbf{p}')(t'-\tau)} e^{-E_Y(\mathbf{p})(\tau-t)}}{2E_X(\mathbf{p}') 2E_Y(\mathbf{p})} \langle \Omega | \chi(0) | X(\mathbf{p}') \rangle \langle X(\mathbf{p}') | \mathcal{O}(0) | Y(\mathbf{p}) \rangle \langle Y(\mathbf{p}) | \tilde{\chi}(0) | \Omega \rangle$$

A complete set of states

Another complete set of states

A three-point (3pt) function:

$$C_{\tilde{\chi}\mathcal{O}\chi}(x', y, x) \equiv \langle \chi(x') \mathcal{O}(y) \tilde{\chi}(x) \rangle$$

Annihilate the state

Insert the operator

Create the state

Spectral decomposition of the 3pt function in Euclidean spacetime

$$G_{\chi\mathcal{O}\tilde{\chi}}(\mathbf{p}', \mathbf{p}; t', \tau, t) = \sum_{X, Y} \frac{e^{-E_X(\mathbf{p}')(t'-\tau)}}{2E_X(\mathbf{p}')} \frac{e^{-E_Y(\mathbf{p})(\tau-t)}}{2E_Y(\mathbf{p})} \langle \Omega | \chi(0) | X(\mathbf{p}') \rangle \langle X(\mathbf{p}') | \mathcal{O}(0) | Y(\mathbf{p}) \rangle \langle Y(\mathbf{p}) | \tilde{\chi}(0) | \Omega \rangle$$

A complete set of states

Another complete set of states

Long-separation behavior dominated by ground states

$$G_{\chi\mathcal{O}\tilde{\chi}}(\mathbf{p}', \mathbf{p}; t', \tau, t) \xrightarrow{\text{large } t'-\tau, \tau-t} \frac{e^{-E_{X_0}(\mathbf{p}')(t'-\tau)}}{2E_{X_0}(\mathbf{p}')} \frac{e^{-E_{X_0}(\mathbf{p})(\tau-t)}}{2E_{X_0}(\mathbf{p})} \sum_{r', r} \langle \Omega | \chi(0) | X_0(\mathbf{p}', r') \rangle \langle X_0(\mathbf{p}', r') | \mathcal{O}(0) | X_0(\mathbf{p}, r) \rangle \langle X_0(\mathbf{p}, r) | \tilde{\chi}(0) | \Omega \rangle$$

If there are degenerate ground states

Desired ground state to ground state matrix element (unrenormalized and in a finite volume)

A three-point (3pt) function:

$$C_{\tilde{\chi}\mathcal{O}\chi}(x', y, x) \equiv \langle \chi(x') \mathcal{O}(y) \tilde{\chi}(x) \rangle$$

Annihilate the state

Insert the operator

Create the state

Spectral decomposition of the 3pt function in Euclidean spacetime

$$G_{\chi\mathcal{O}\tilde{\chi}}(\mathbf{p}', \mathbf{p}; t', \tau, t) = \sum_{X, Y} \frac{e^{-E_X(\mathbf{p}')(t'-\tau)}}{2E_X(\mathbf{p}')} \frac{e^{-E_Y(\mathbf{p})(\tau-t)}}{2E_Y(\mathbf{p})} \langle \Omega | \chi(0) | X(\mathbf{p}') \rangle \langle X(\mathbf{p}') | \mathcal{O}(0) | Y(\mathbf{p}) \rangle \langle Y(\mathbf{p}) | \tilde{\chi}(0) | \Omega \rangle$$

A complete set of states

Another complete set of states

Long-separation behavior dominated by ground states

$$G_{\chi\mathcal{O}\tilde{\chi}}(\mathbf{p}', \mathbf{p}; t', \tau, t) \xrightarrow{\text{large } t'-\tau, \tau-t} \frac{e^{-E_{X_0}(\mathbf{p}')(t'-\tau)}}{2E_{X_0}(\mathbf{p}')} \frac{e^{-E_{X_0}(\mathbf{p})(\tau-t)}}{2E_{X_0}(\mathbf{p})} \sum_{r', r} \langle \Omega | \chi(0) | X_0(\mathbf{p}', r') \rangle \langle X_0(\mathbf{p}', r') | \mathcal{O}(0) | X_0(\mathbf{p}, r) \rangle \langle X_0(\mathbf{p}, r) | \tilde{\chi}(0) | \Omega \rangle$$

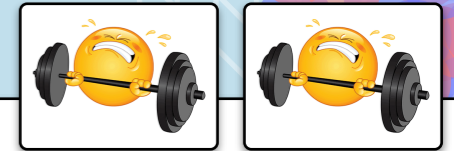
If there are degenerate ground states

Desired ground state to ground state matrix element (unrenormalized and in a finite volume)

Taking a proper ratio to 2pt functions

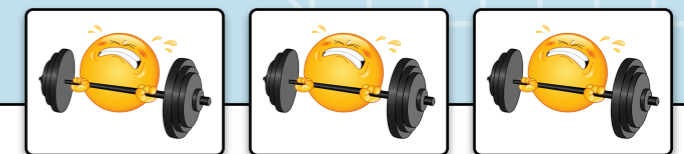
$$R_{\chi\mathcal{O}\tilde{\chi}}(\mathbf{p}', \mathbf{p}; t', \tau, t) \xrightarrow{\text{large } t'-\tau, \tau-t} \propto \langle X_0(\mathbf{p}', r') | \mathcal{O}(0) | X_0(\mathbf{p}, r) \rangle$$

EXERCISE 4



If the computational resources do not allow large source, operator and sink time separations to be achieved, one should worry about the effect of excited states. One way to have more confidence over the extracted ground state to ground state matrix element is to perform a multi-exponential fits to the ratio of 3pt to 2pt functions as a function of both the source-sink and the source-operator separations. Assume that both the ground state and the first excited states contribute significantly to such a ratio. Write down a generic form for such a multi-exponential function.

BONUS EXERCISE 3



In the above exercise, sum over the time insertions of the operator and write down a new form for the ratio of 3pt to 2pt functions, which now is only a function of the source-sink time separation. This is referred to as the summation method in literature.

Example: The application of 3pt function method to obtain the axial charge/form factors of the nucleon

Constantinou, arXiv:1411.0078 [hep-lat].

$$\langle N(p', s') | \bar{\psi}(x) \gamma_\mu \gamma_5 \psi(x) | N(p, s) \rangle = i \left(\frac{m_N^2}{E_N(\mathbf{p}') E_N(\mathbf{p})} \right)^{1/2} \bar{u}_N(p', s') \left[G_A(q^2) \gamma_\mu \gamma_5 + \frac{q_\mu \gamma_5}{2m_N} G_P(q^2) \right] u_N(p, s)$$

Axial-vector current

Nucleon spinor

Axial and pseudo scalar form factors

$$G_A(0) = g_A$$

Example: The application of 3pt function method to obtain the axial charge/form factors of the nucleon

Constantinou, arXiv:1411.0078 [hep-lat].

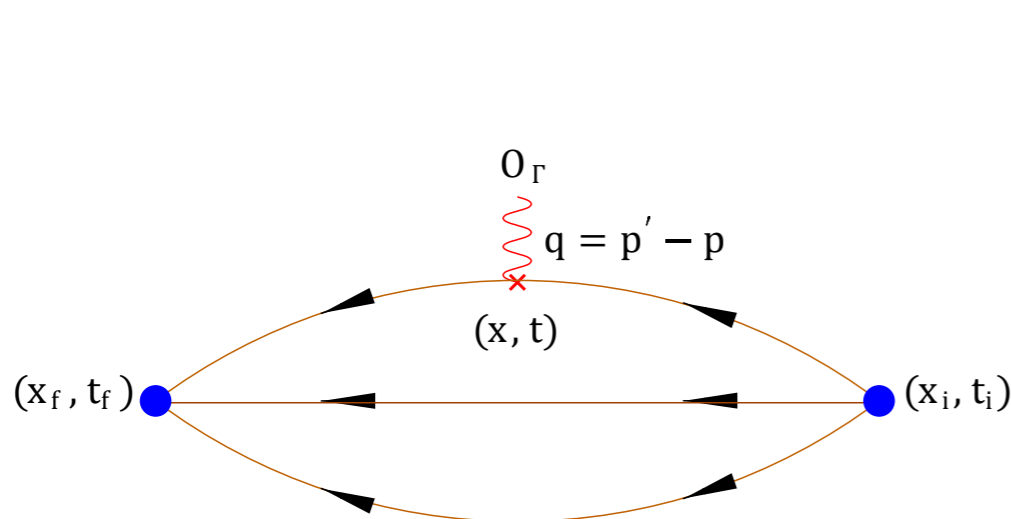
$$\langle N(p', s') | \bar{\psi}(x) \gamma_\mu \gamma_5 \psi(x) | N(p, s) \rangle = i \left(\frac{m_N^2}{E_N(\mathbf{p}') E_N(\mathbf{p})} \right)^{1/2} \bar{u}_N(p', s') \left[G_A(q^2) \gamma_\mu \gamma_5 + \frac{q_\mu \gamma_5}{2m_N} G_P(q^2) \right] u_N(p, s)$$

Axial-vector current

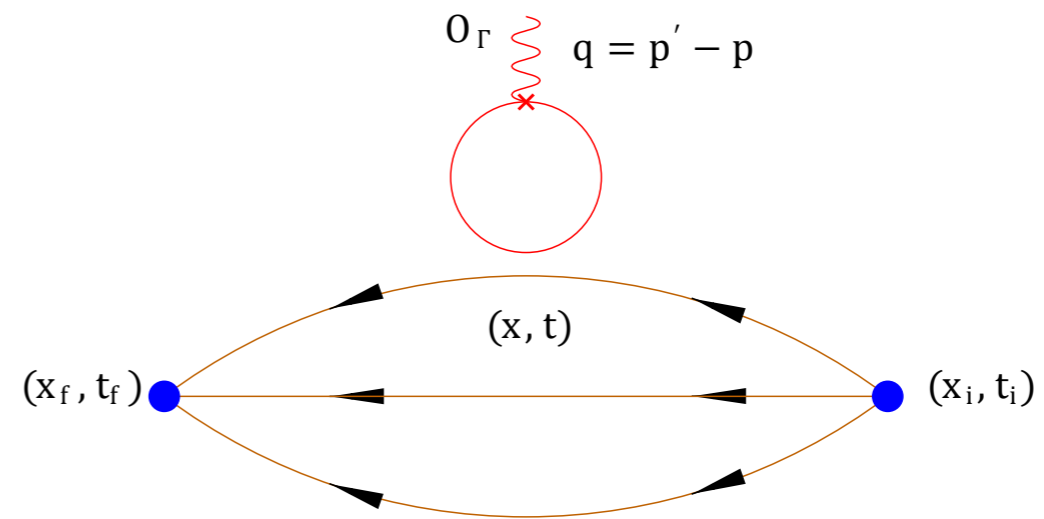
Nucleon spinor

Axial and pseudo scalar form factors

$$G_A(0) = g_A$$



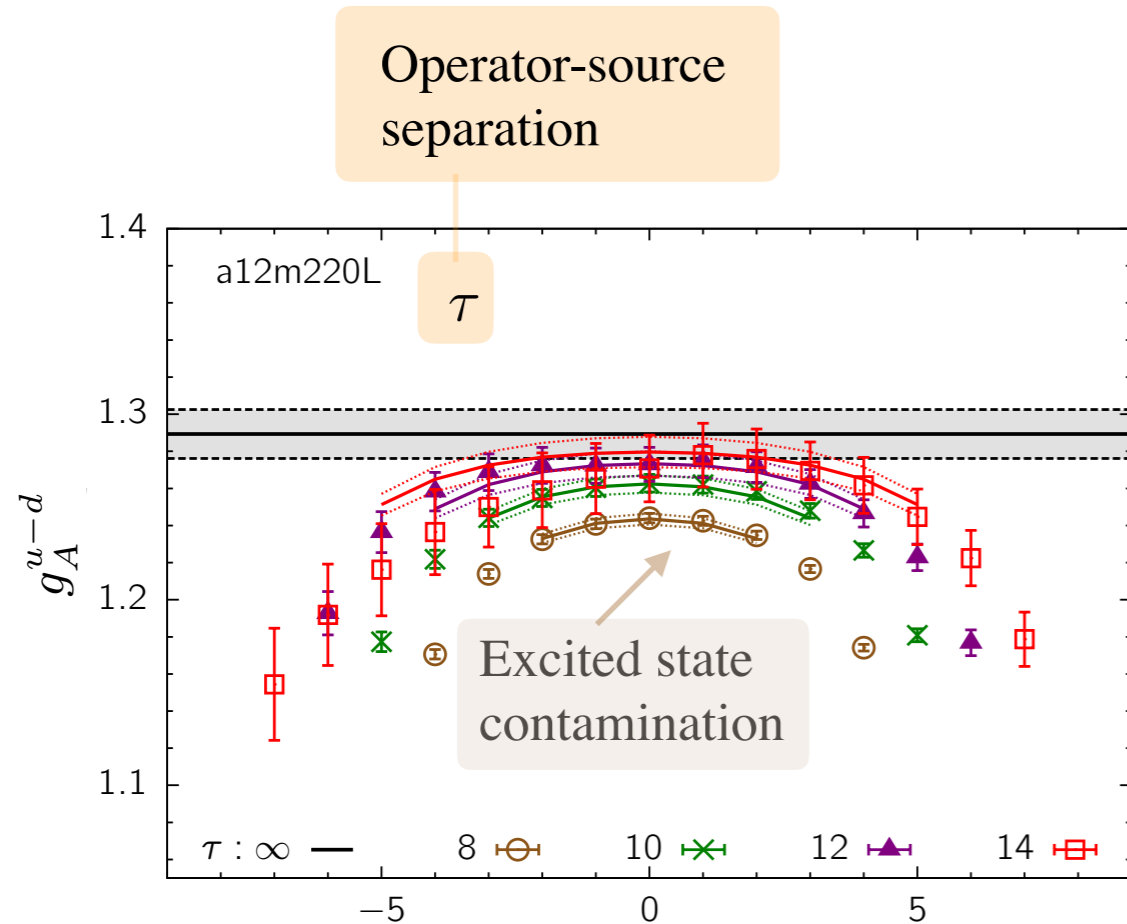
Connected contribution



Disconnected contribution
(vanishes at isospin limit for isovector quantities)

Example: The application of 3pt function method to obtain the axial charge/form factors of the nucleon

Gupta et al (PNDME), Phys. Rev. D 98, 034503 (2018)



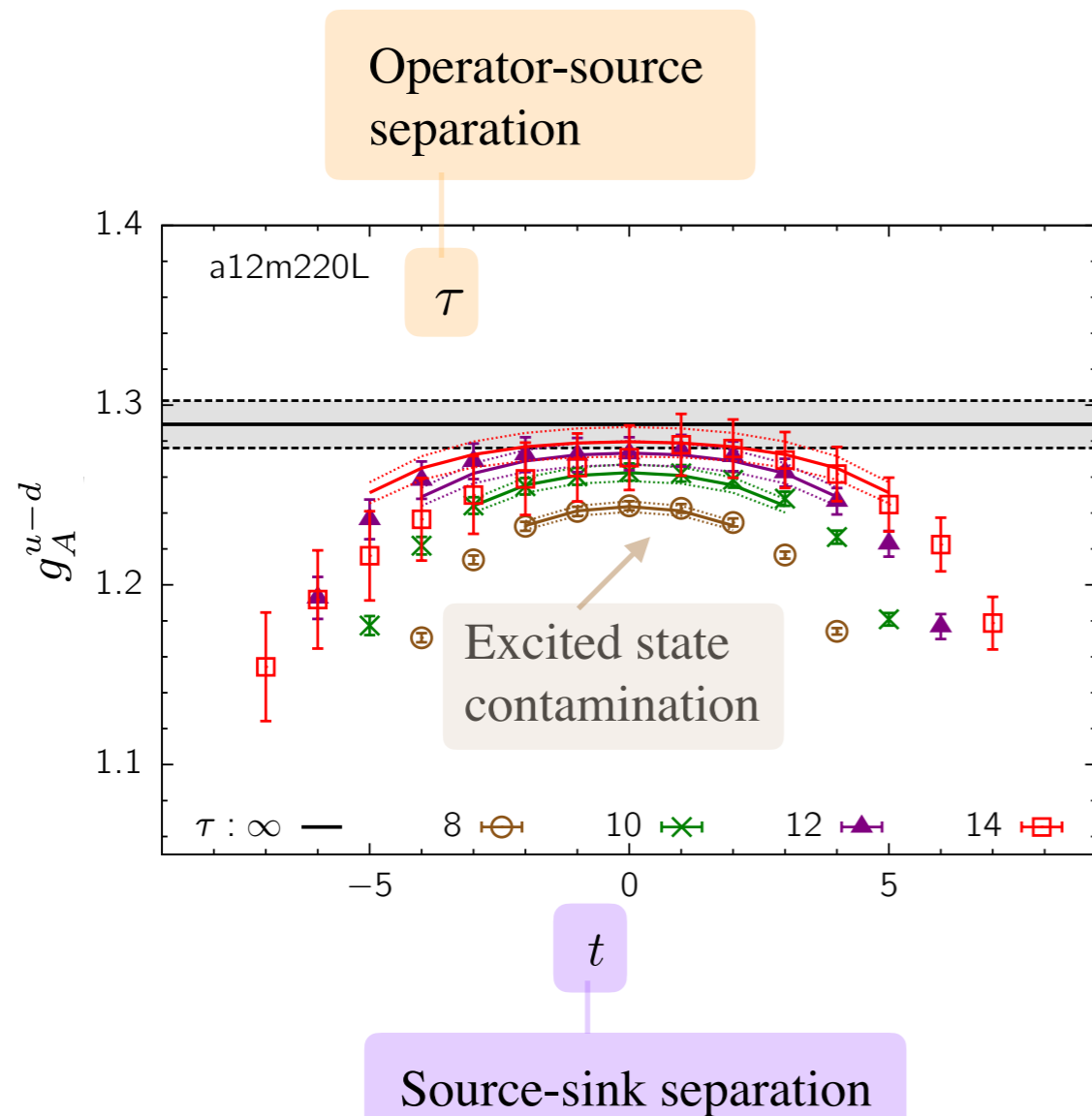
Operator-source separation

Source-sink separation

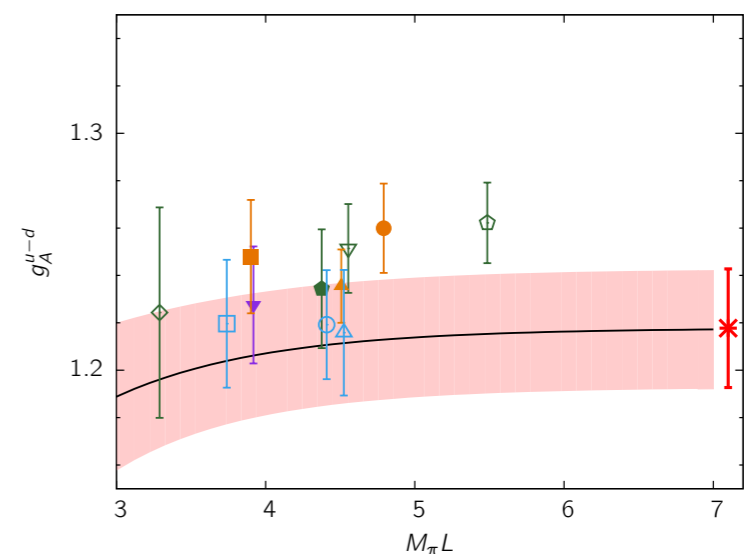
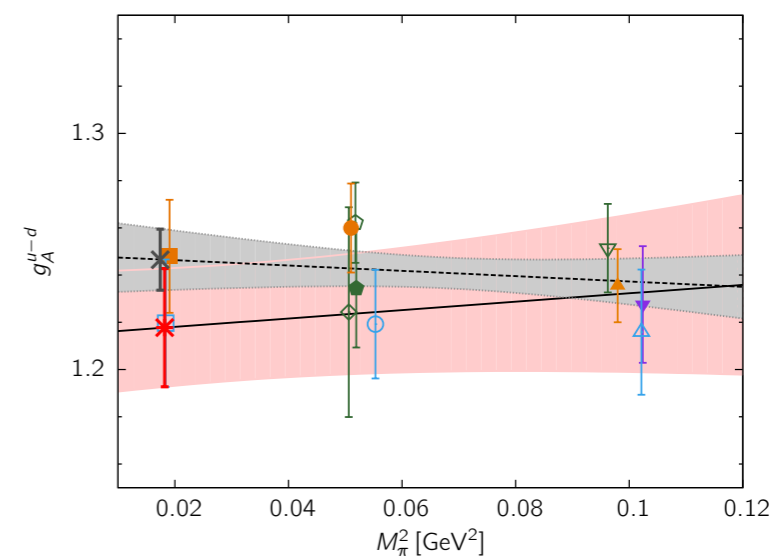
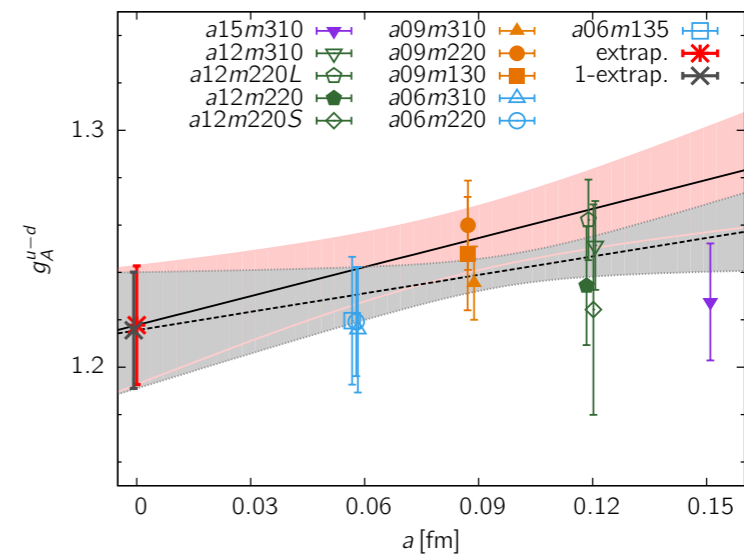
3pt function for a single lattice spacing, volume and quark masses

Example: The application of 3pt function method to obtain the axial charge/form factors of the nucleon

Gupta et al (PNDME), Phys. Rev. D 98, 034503 (2018)



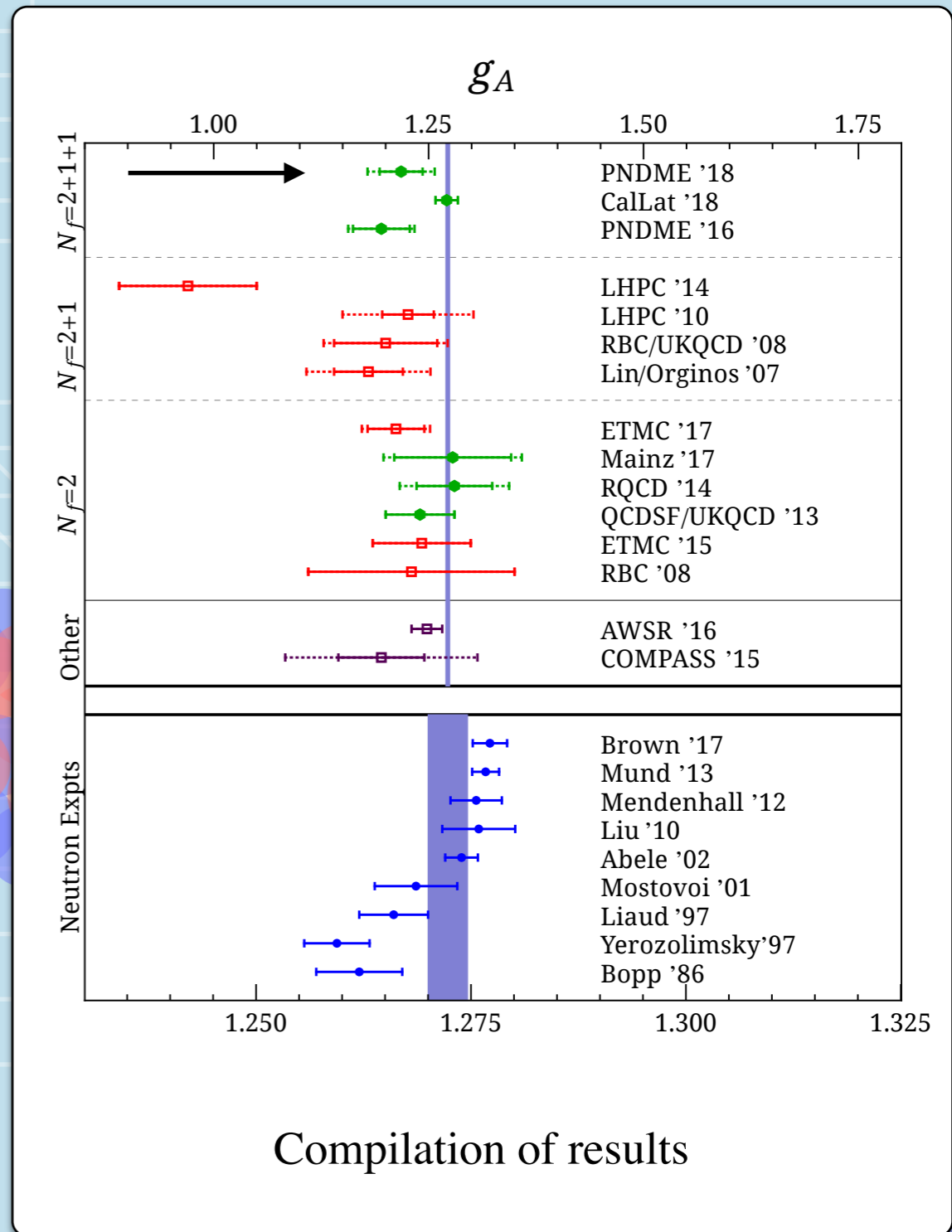
3pt function for a single lattice spacing, volume and quark masses



Extrapolation to continuum, infinite volume and physical quark masses

Example: The application of 3pt function method to obtain the axial charge/form factors of the nucleon

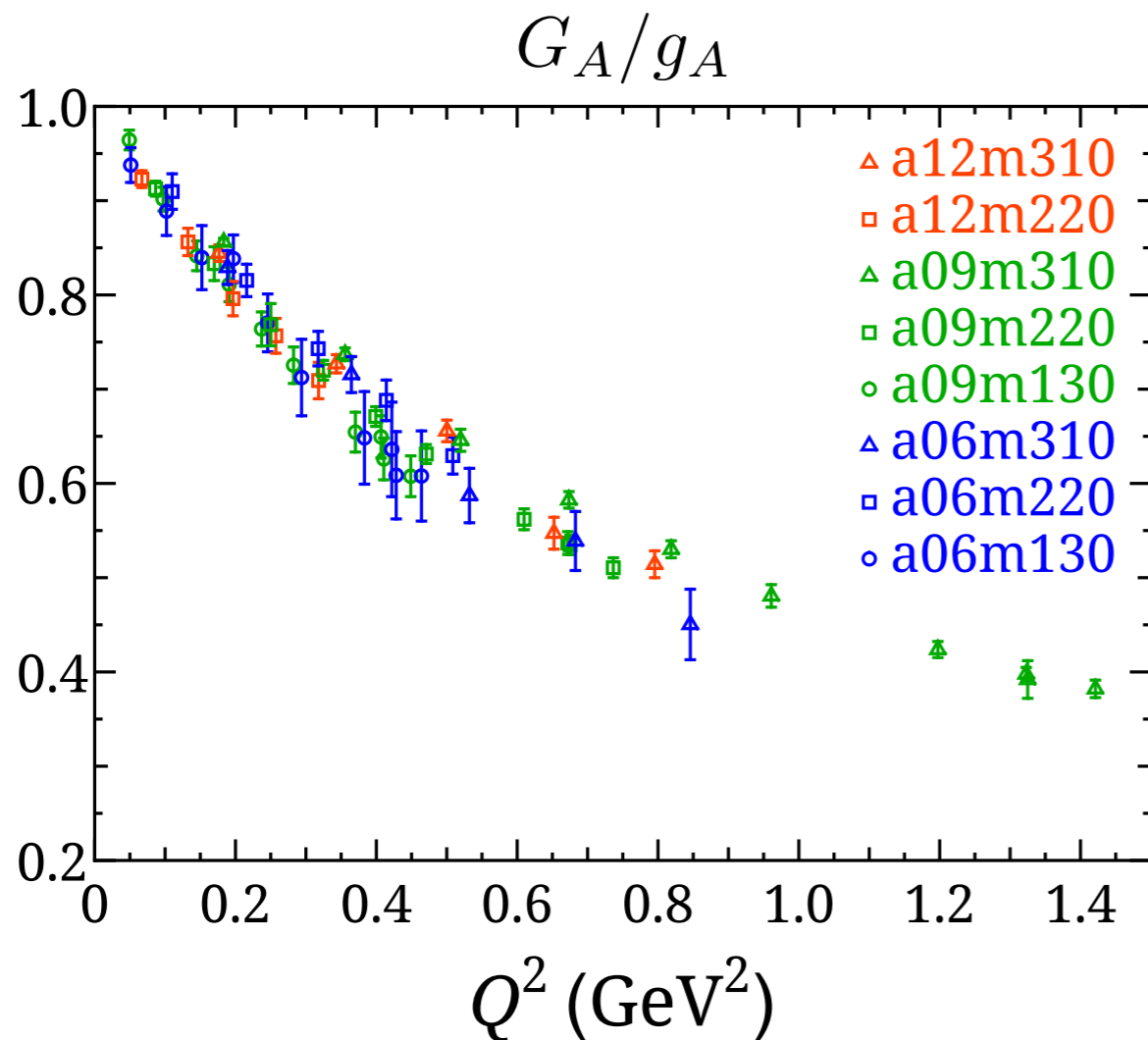
Gupta et al (PNDME), Phys. Rev. D 98, 034503 (2018)



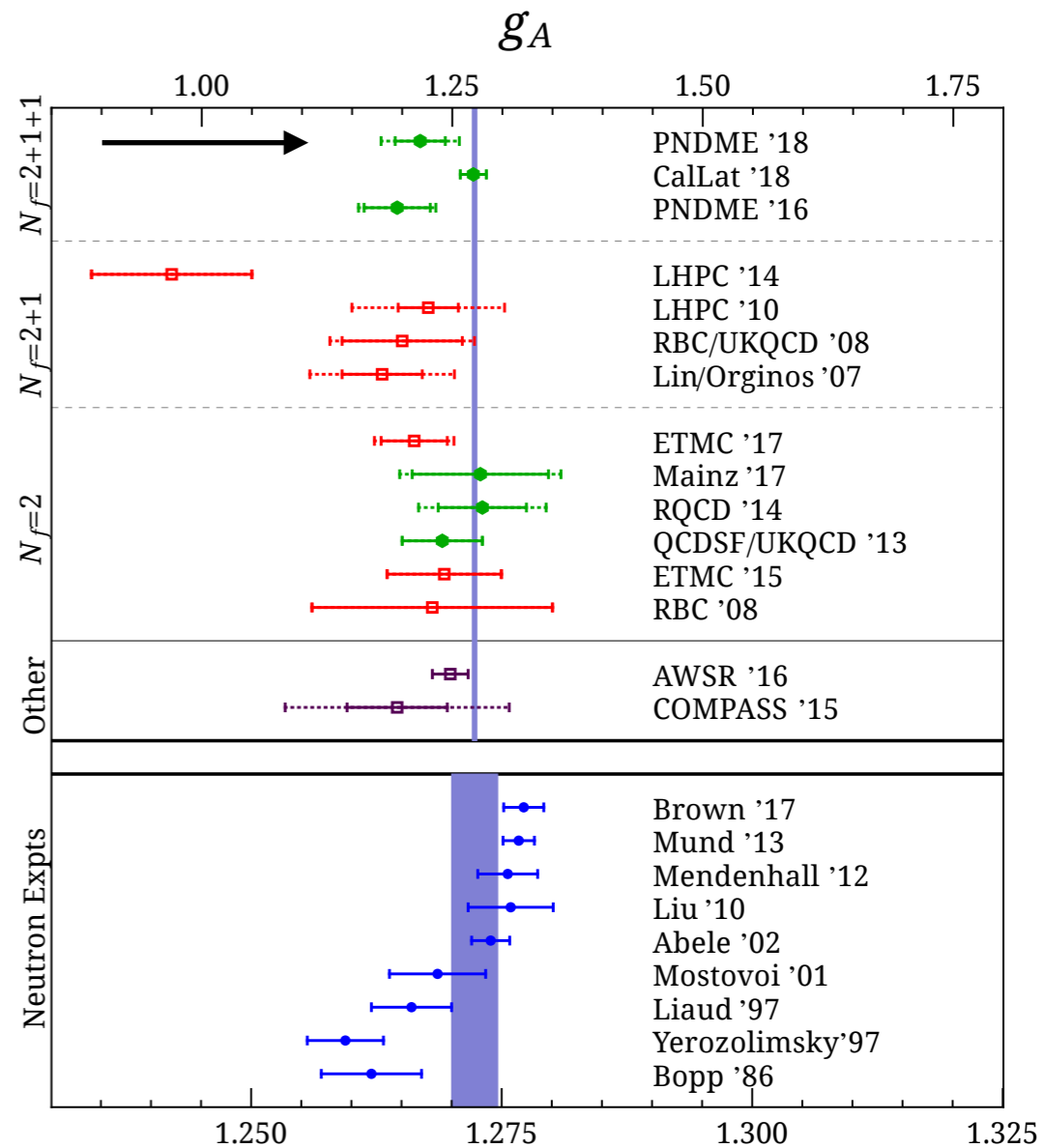
Example: The application of 3pt function method to obtain the axial charge/form factors of the nucleon

Gupta et al (PNDME), Phys. Rev. D 98, 034503 (2018)

Jang et al, EPJ Web Conf. 175, 06033 (2018)



Axial form factor results



Compilation of results

Example: The spin decomposition of the nucleon

Alexandru, Phys. Rev. Lett. 119, 142002 (2017).

$$J_N = \sum_{q=u,d,s,c,\dots} \left(\frac{1}{2} \Delta \Sigma_q + L_q \right) + J_g$$

Quark spin

Quark orbital
angular
momentum

Total gluon
angular
momentum

Ji, Phys. Rev. Lett. 78, 610 (1997).

Example: The spin decomposition of the nucleon

Alexandru, Phys. Rev. Lett. 119, 142002 (2017).

$$J_N = \sum_{q=u,d,s,c,\dots} \left(\frac{1}{2} \Delta\Sigma_q + L_q \right) + J_g$$

Quark spin

Quark orbital angular momentum

Total gluon angular momentum

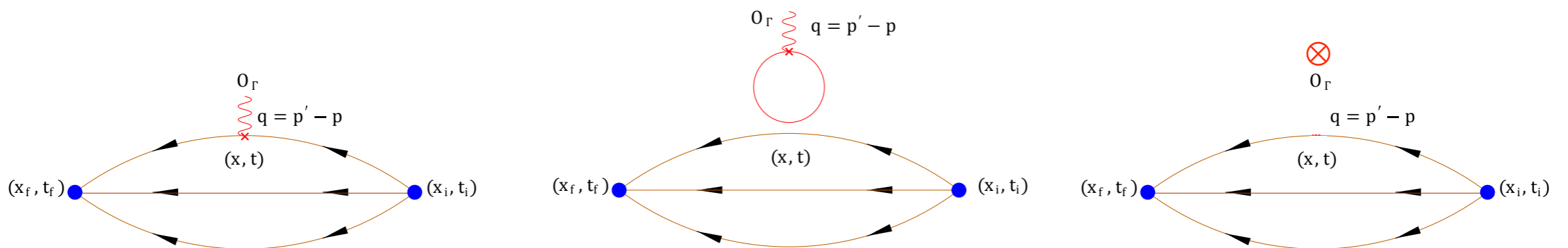
Ji, Phys. Rev. Lett. 78, 610 (1997).

Matrix elements needed

$$\begin{aligned} \langle N(p, s') | \mathcal{O}_A^\mu | N(p, s) \rangle &= \bar{u}_N(p, s') \left[g_A^q \gamma^\mu \gamma_5 \right] u_N(p, s) \\ \langle N(p', s') | \mathcal{O}_V^{\mu\nu} | N(p, s) \rangle &= \bar{u}_N(p', s') \Lambda_{\mu\nu}^q(Q^2) u_N(p, s) \\ \langle N(p', s') | \mathcal{O}_g^{\mu\nu} | N(p, s) \rangle &= \bar{u}_N(p', s') \Lambda_{\mu\nu}^g(Q^2) u_N(p, s) \end{aligned}$$

With operators

$$\begin{aligned} \mathcal{O}_A^\mu &= \bar{q} \gamma^\mu \gamma_5 q \\ \mathcal{O}_V^{\mu\nu} &= \bar{q} \gamma^{\{\mu} \overleftrightarrow{D}^{\nu\}} q \\ \mathcal{O}_g^{\mu\nu} &= 2 \text{Tr} [G_{\mu\sigma} G_{\nu\sigma}] \end{aligned}$$

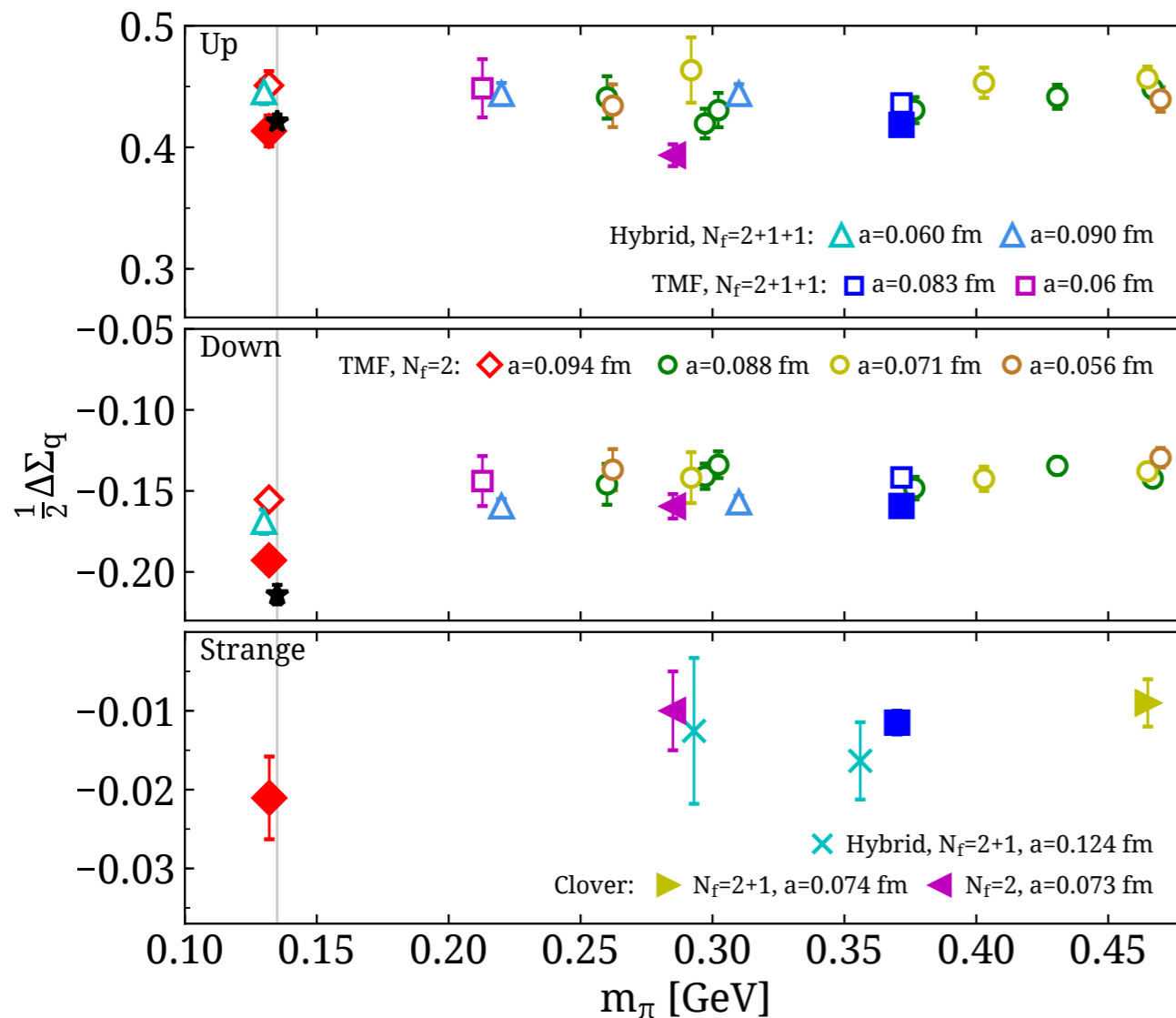


Quark contributions

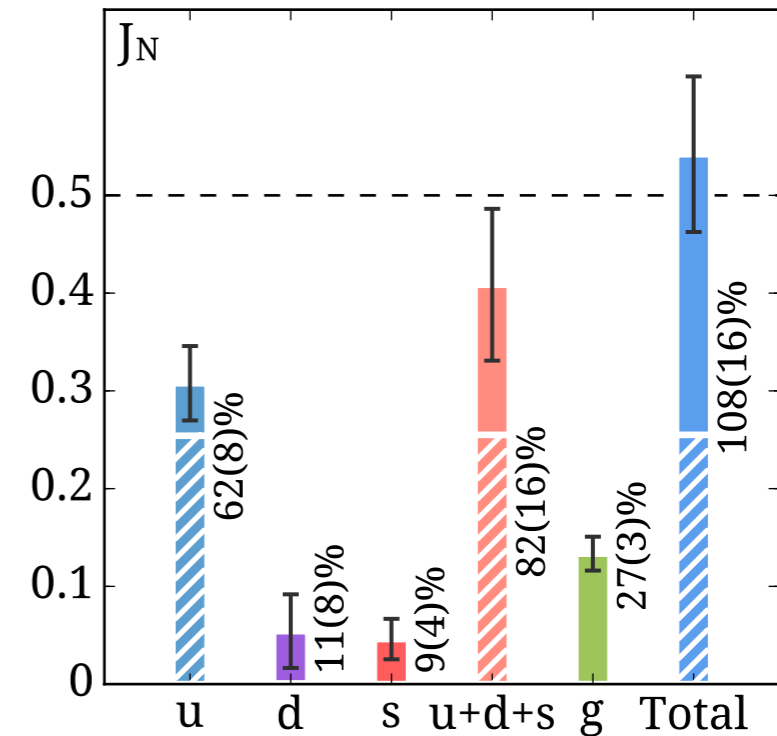
Gluonic contribution

Example: The spin decomposition of the nucleon

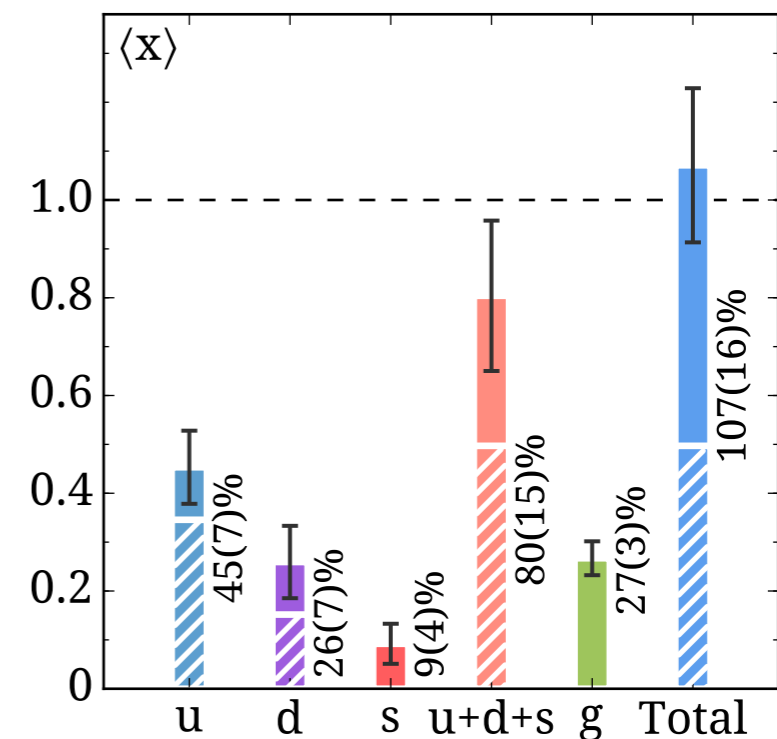
Alexandru, Phys. Rev. Lett. 119, 142002 (2017).



Quark spin contributions



Nucleon spin decomposition



Longitudinal momentum decomposition

The background of the slide features a repeating pattern of 3D wireframe cubes. Inside each cube, there is a cluster of overlapping spheres in shades of blue and red, representing a nucleon. A white zigzag line, symbolizing a gluon, is attached to the top-left corner of each cube. The cubes are arranged in a staggered, isometric grid across the light blue background.

**[STILL CONTINUING ON] LECTURE II:
NUCLEON STRUCTURE FROM LATTICE QCD**

Let's enumerate a some of the methods that give access to structure quantities in general:

Three(four)-point functions

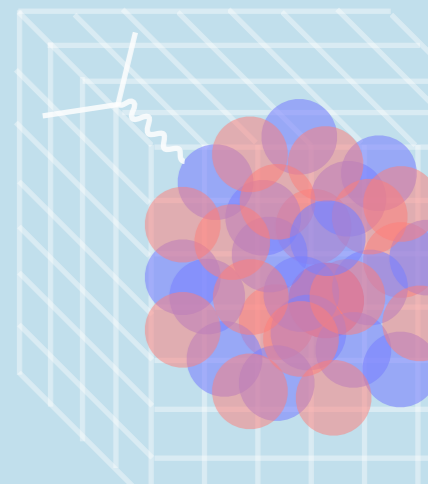
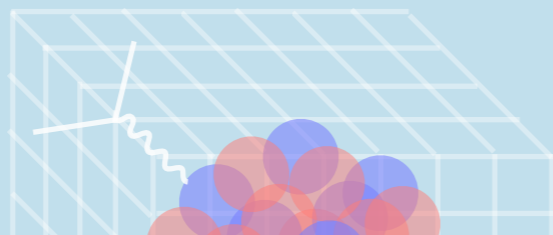
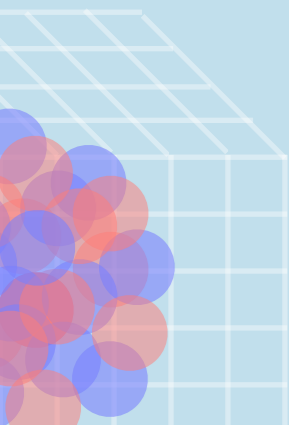
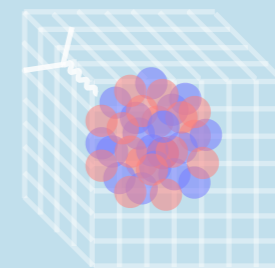
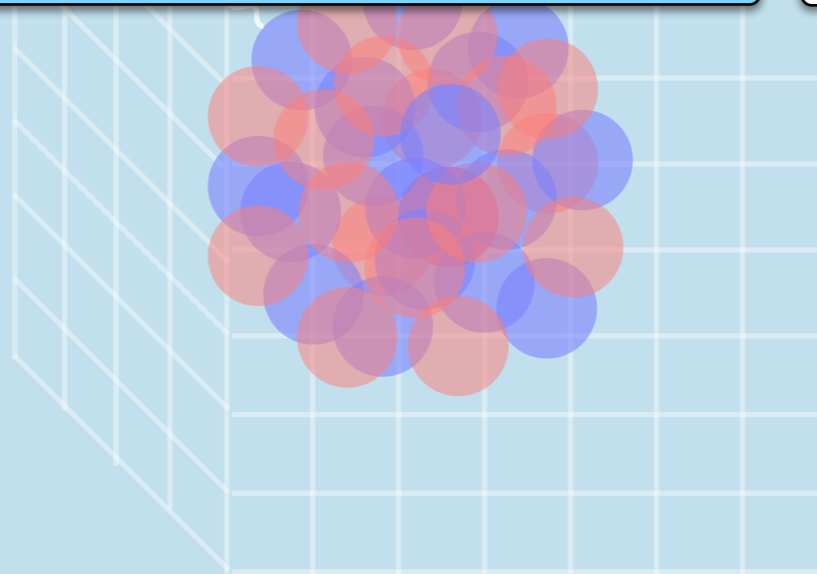
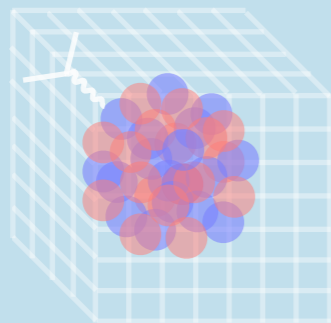
For e.g., form factors, moments of structure functions, Compton amplitude, transition amplitudes

Background-field methods

For e.g., EM moments and polarizabilities, charge radius, form factors and transition amplitudes.

Feynman-Hellmann inspired methods

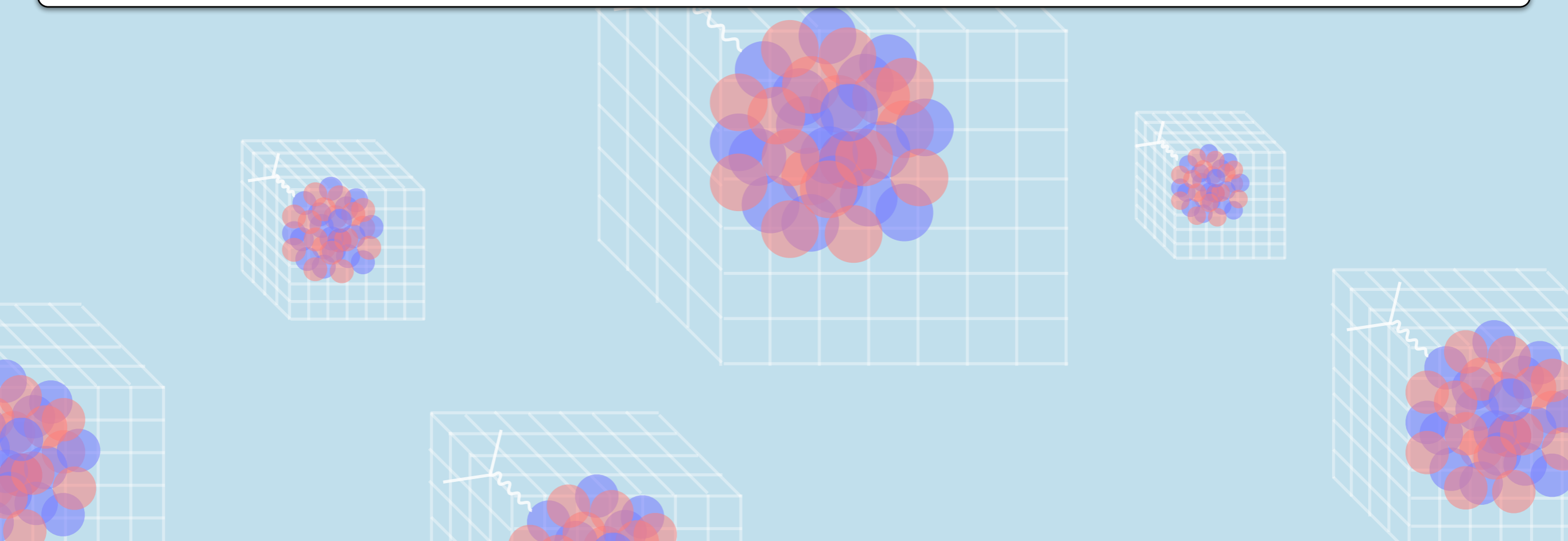
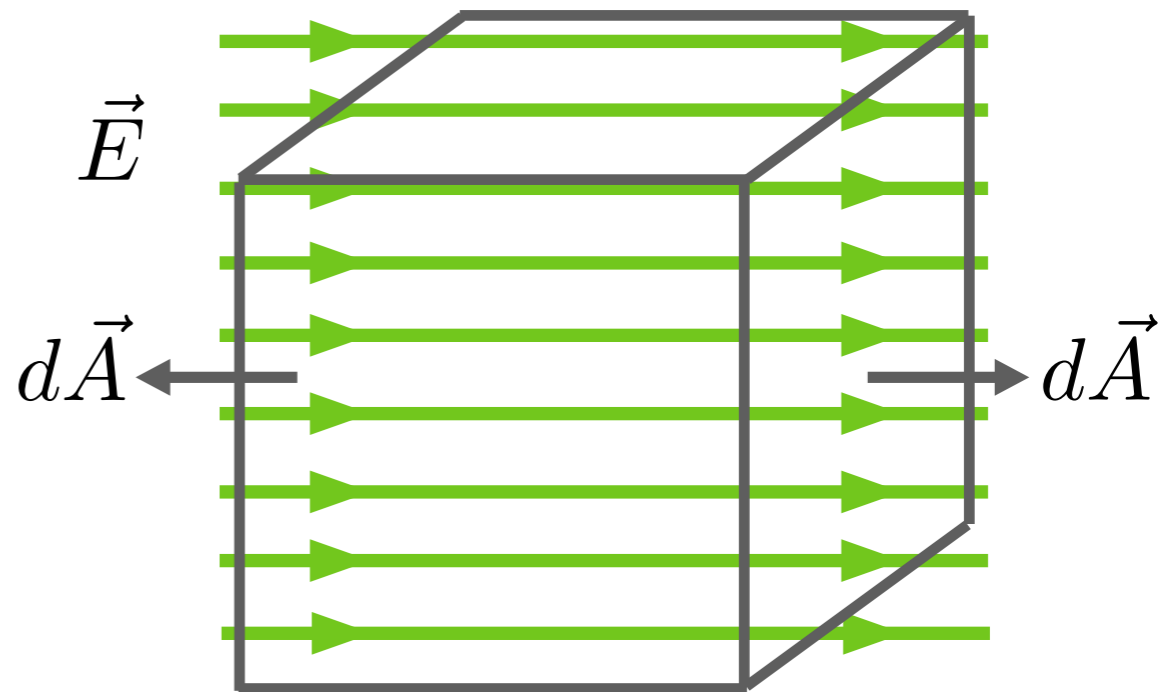
Similar to background fields. For e.g., axial charge, form factors, EM moments, transition amplitudes



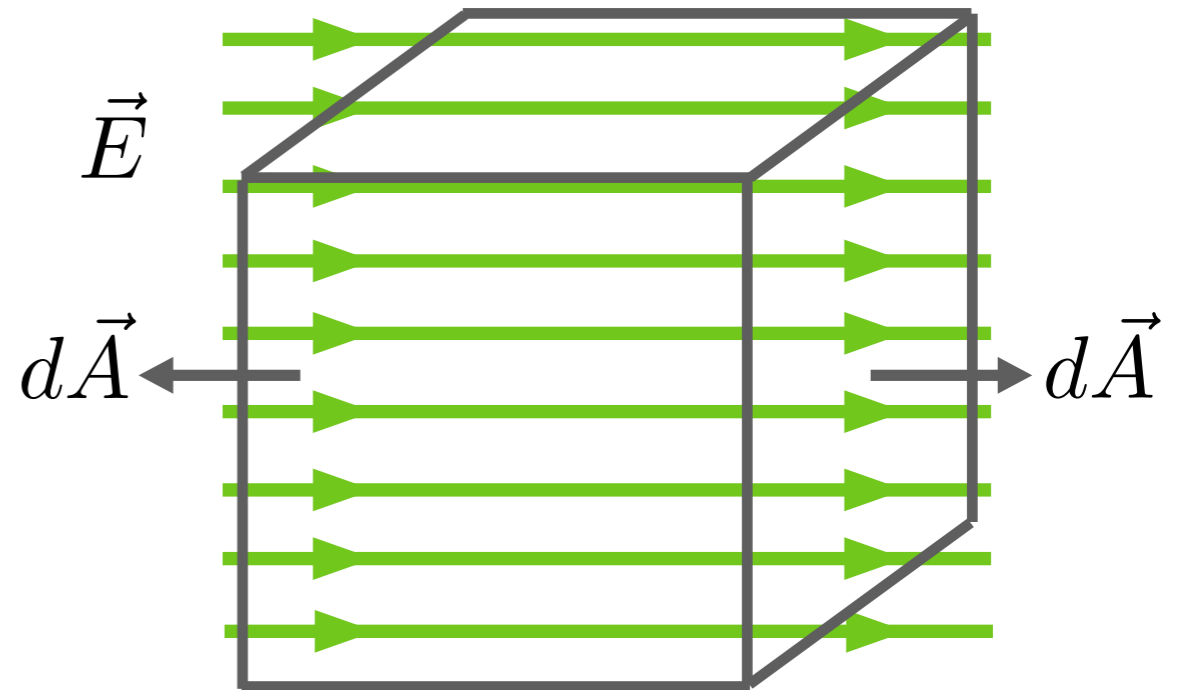
Background fields are non-dynamical, i.e., there will be no pair creation and annihilation in vacuum with a classical EM background field. This means the photon zero mode is no problem: it is absent in the calculation!

$$U(\text{QCD}) \rightarrow U(\text{QCD}) \times U(\text{QED})$$

Modify the links when forming the quark propagators (quench approx).



Background fields are non-dynamical, i.e., there will be no pair creation and annihilation in vacuum with a classical EM background field. This means the photon zero mode is no problem: it is absent in the calculation!

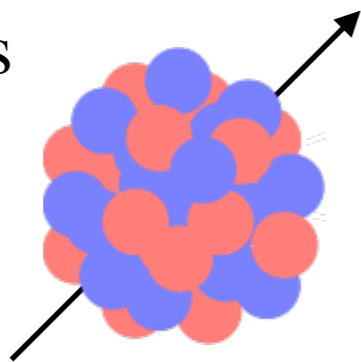


$$U(\text{QCD}) \rightarrow U(\text{QCD}) \times U(\text{QED})$$

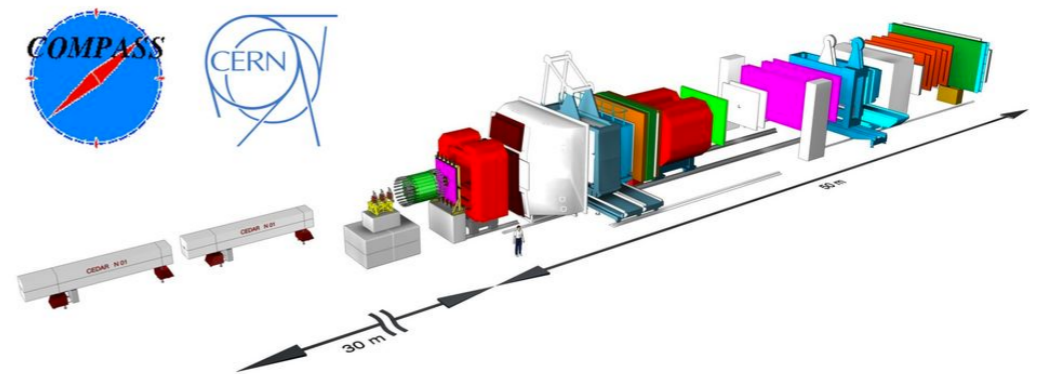
Modify the links when forming the quark propagators (quench approx).

Traditionally they are used for constraining the response of hadrons/nuclei to external probes:

Magnetic moments



Electric and magnetic polarizabilities



See e.g., BEANE et al (NPLQCD), Phys.Rev.Lett. 113 (2014) 25, 252001 and Phys.Rev. D92 (2015) 11, 114502. for nuclear-physics calculations.

Various other structure properties of hadrons and nuclei, as well as their transitions, can be studied using more complex background fields:

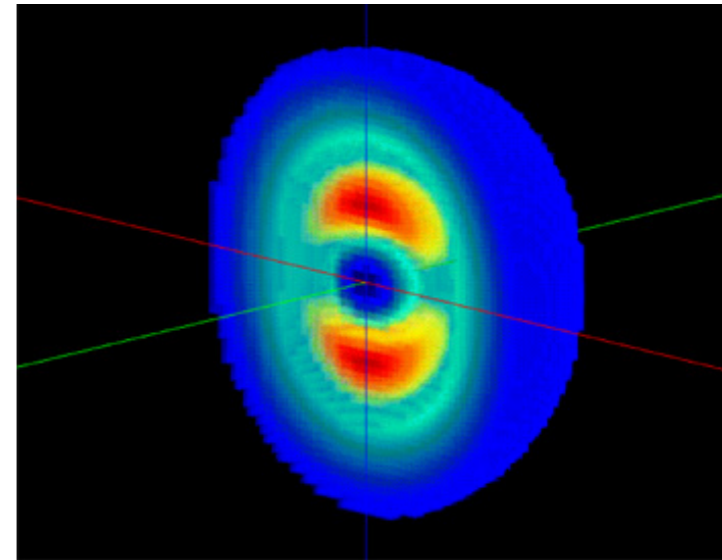
1) EM charge radius

ZD and Detmold, Phys. Rev. D 93, 014509 (2016).



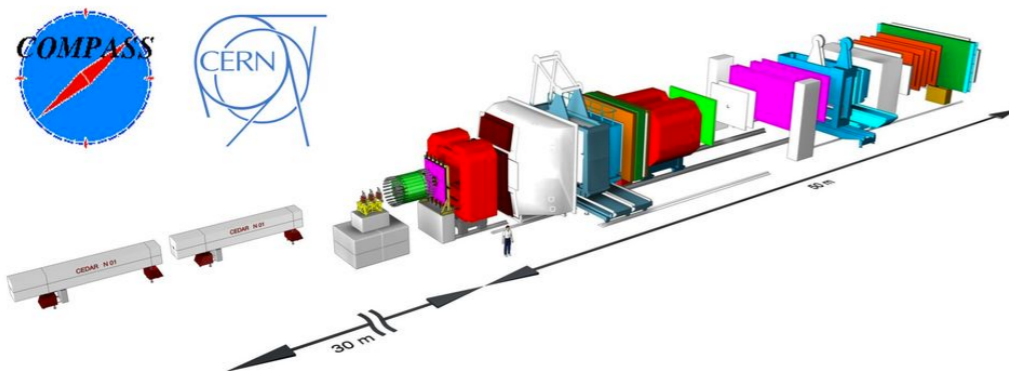
2) Electric quadrupole moment

ZD and Detmold, Phys. Rev. D 93, 014509 (2016).



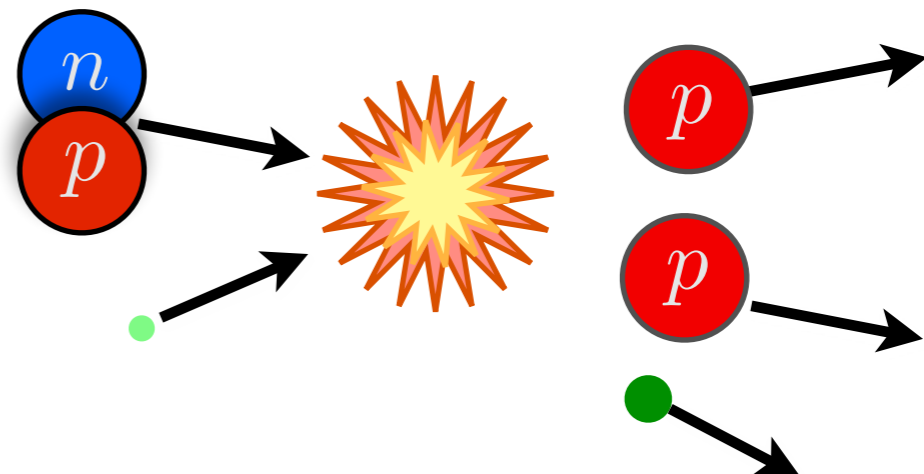
3) Form factors

Detmold, Phys. Rev. D 71, 054506 (2005).



4) Axial background fields

Beane et al, Phys. Rev. Lett, 115 132001 (2015).



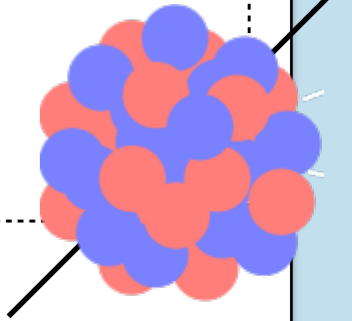
Here's an application of the background-field technique to obtain magnetic moment and polarizabilities of the nucleon:

$$E_{h;j_z}(\mathbf{B}) = \sqrt{M_h^2 + P_{\parallel}^2} + (2n_L + 1)|Q_h e \mathbf{B}| - \boldsymbol{\mu}_h \cdot \mathbf{B} - 2\pi\beta_h^{(M0)}|\mathbf{B}|^2 - 2\pi\beta_h^{(M2)}\langle\hat{T}_{ij}B_iB_j\rangle + \dots$$

Landau levels for
charged particles

Magnetic
moment

Magnetic polarizabilities



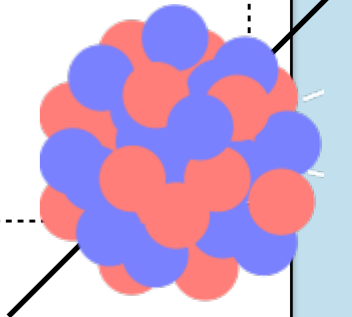
Here's an application of the background-field technique to obtain magnetic moment and polarizabilities of the nucleon:

$$E_{h;j_z}(\mathbf{B}) = \sqrt{M_h^2 + P_{\parallel}^2} + (2n_L + 1)|Q_h e \mathbf{B}| - \boldsymbol{\mu}_h \cdot \mathbf{B} - 2\pi\beta_h^{(M0)}|\mathbf{B}|^2 - 2\pi\beta_h^{(M2)}\langle \hat{T}_{ij} B_i B_j \rangle + \dots$$

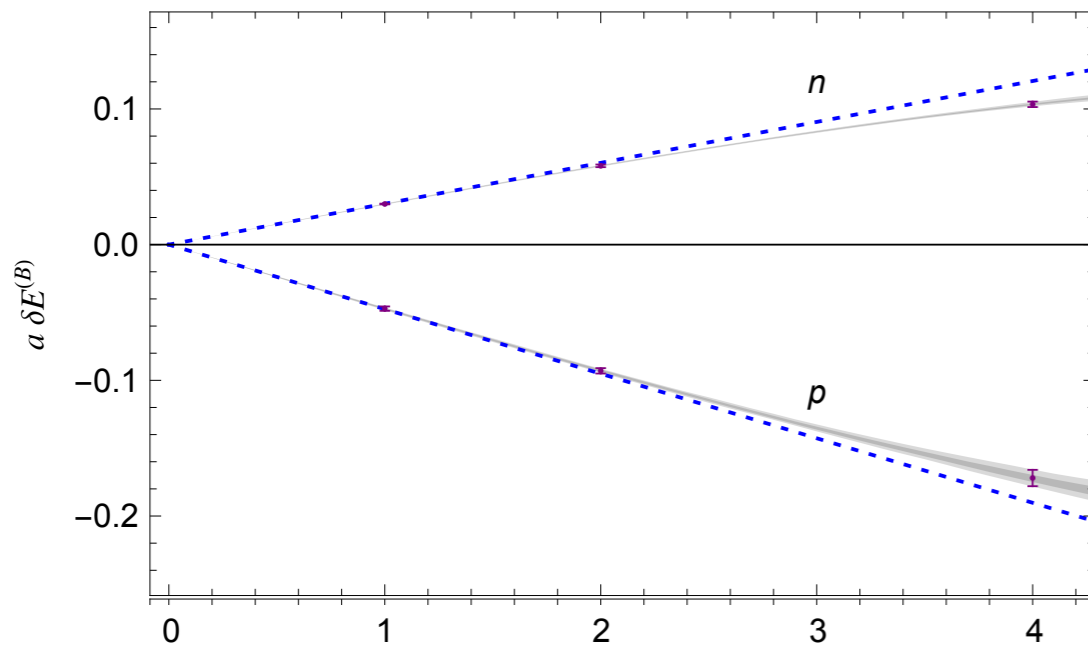
Landau levels for charged particles

Magnetic moment

Magnetic polarizabilities



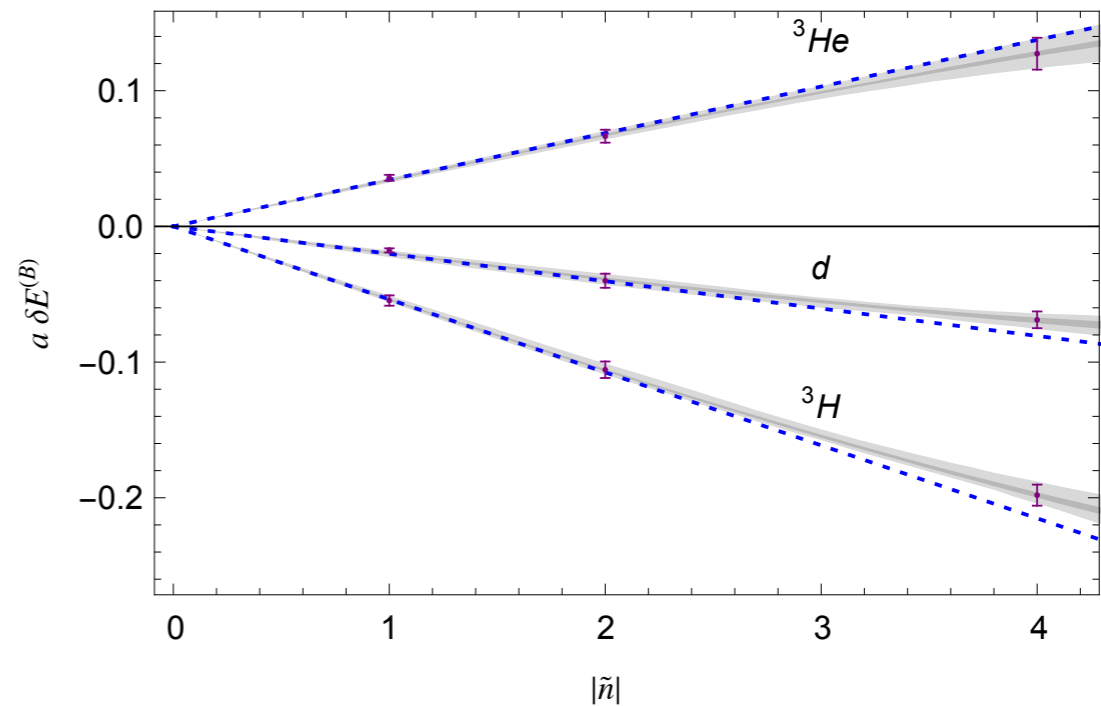
Nucleon



$|\tilde{n}|$

A quanta of magnetic field

Light nuclei



$$N_f = 3, m_\pi = 0.806 \text{ GeV}, a = 0.145(2) \text{ fm}$$

Beane et al. (NPLQCD), *phys.rev.lett.* 113 (2014) 25, 252001.
 Beane et al. (NPLQCD), *phys.rev.* D92 (2015) 11, 114502.

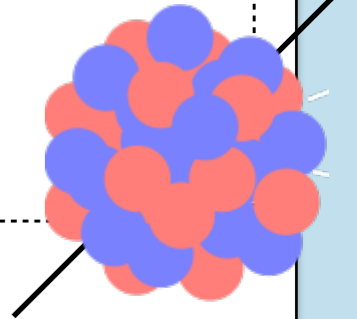
Here's an application of the background-field technique to obtain magnetic moment and polarizabilities of the nucleon:

$$E_{h;j_z}(\mathbf{B}) = \sqrt{M_h^2 + P_{\parallel}^2} + (2n_L + 1)|Q_h e \mathbf{B}| - \boldsymbol{\mu}_h \cdot \mathbf{B} - 2\pi\beta_h^{(M0)}|\mathbf{B}|^2 - 2\pi\beta_h^{(M2)}\langle \hat{T}_{ij} B_i B_j \rangle + \dots$$

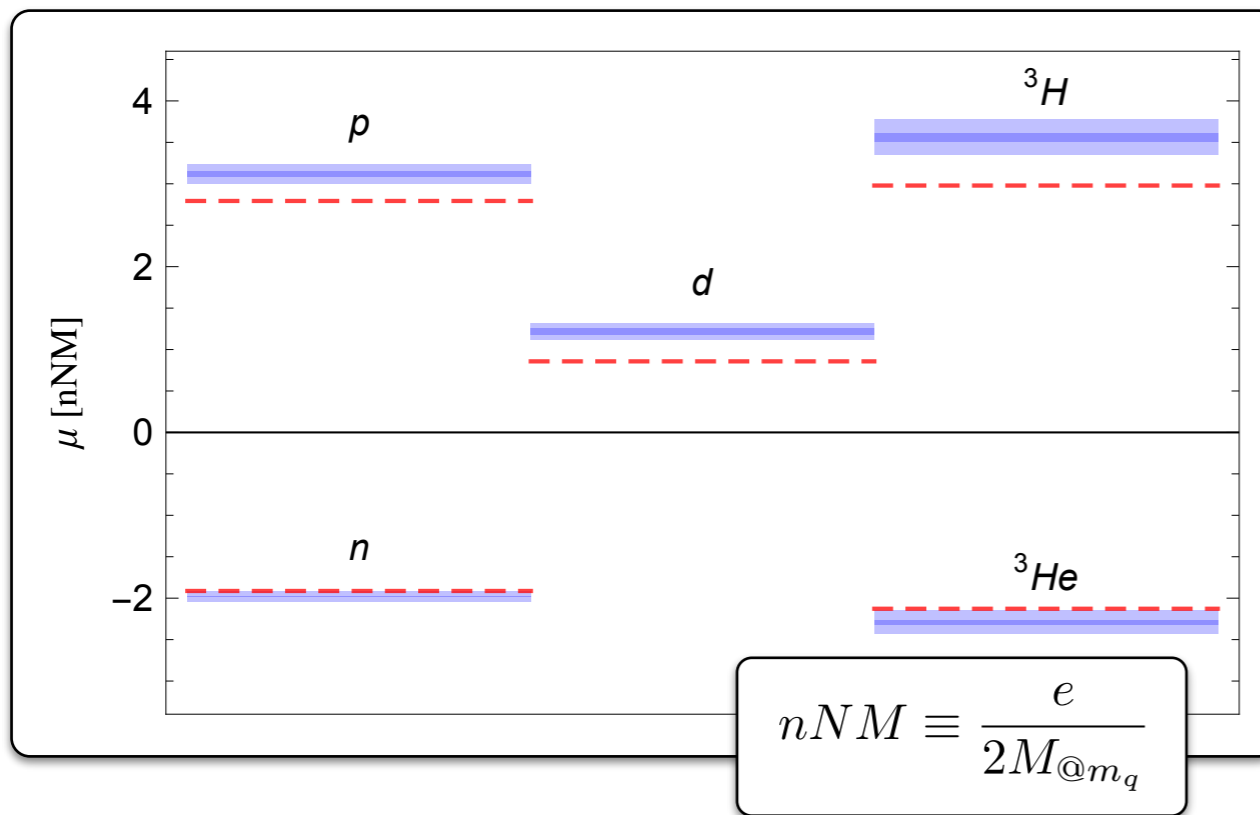
Landau levels for charged particles

Magnetic moment

Magnetic polarizabilities



Magnetic moment



$$N_f = 3, m_\pi = 0.806 \text{ GeV}, a = 0.145(2) \text{ fm}$$

Beane et al. (NPLQCD), *phys.rev.lett.* 113 (2014) 25, 252001.
 Beane et al. (NPLQCD), *phys.rev.* D92 (2015) 11, 114502.

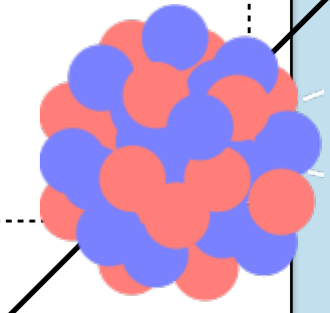
Here's an application of the background-field technique to obtain magnetic moment and polarizabilities of the nucleon:

$$E_{h;j_z}(\mathbf{B}) = \sqrt{M_h^2 + P_{\parallel}^2} + (2n_L + 1)|Q_h e \mathbf{B}| - \boldsymbol{\mu}_h \cdot \mathbf{B} - 2\pi\beta_h^{(M0)}|\mathbf{B}|^2 - 2\pi\beta_h^{(M2)}\langle \hat{T}_{ij} B_i B_j \rangle + \dots$$

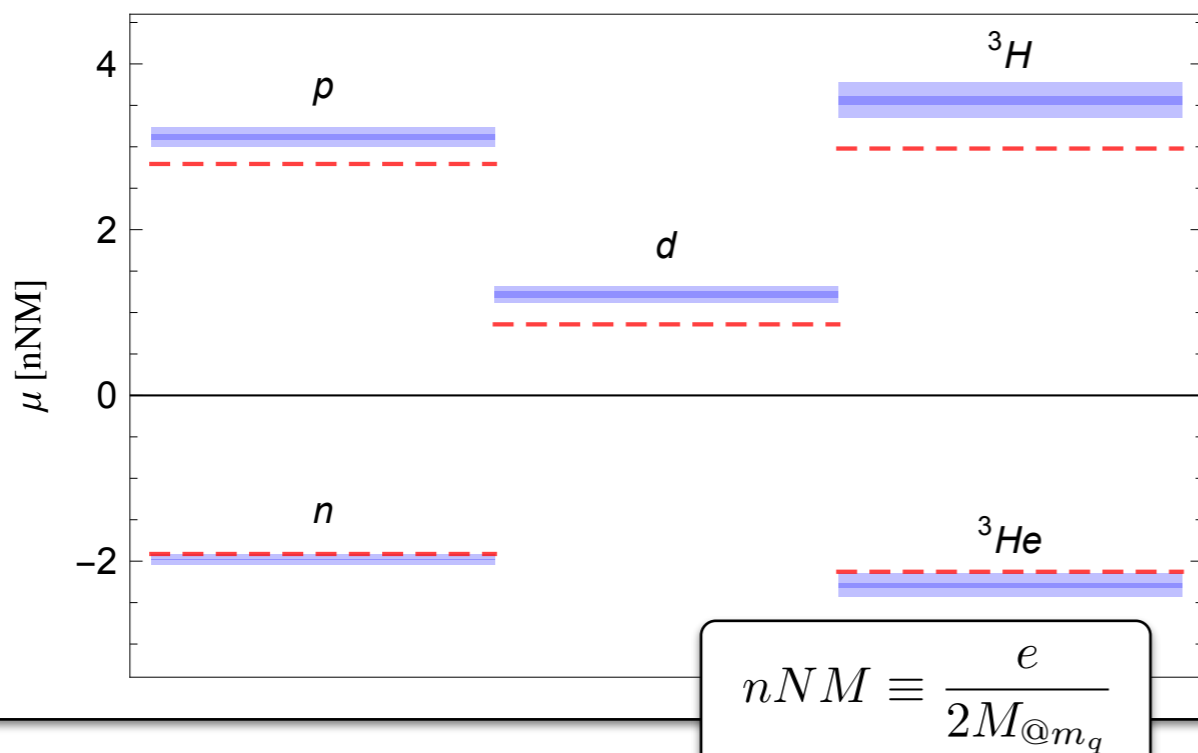
Landau levels for charged particles

Magnetic moment

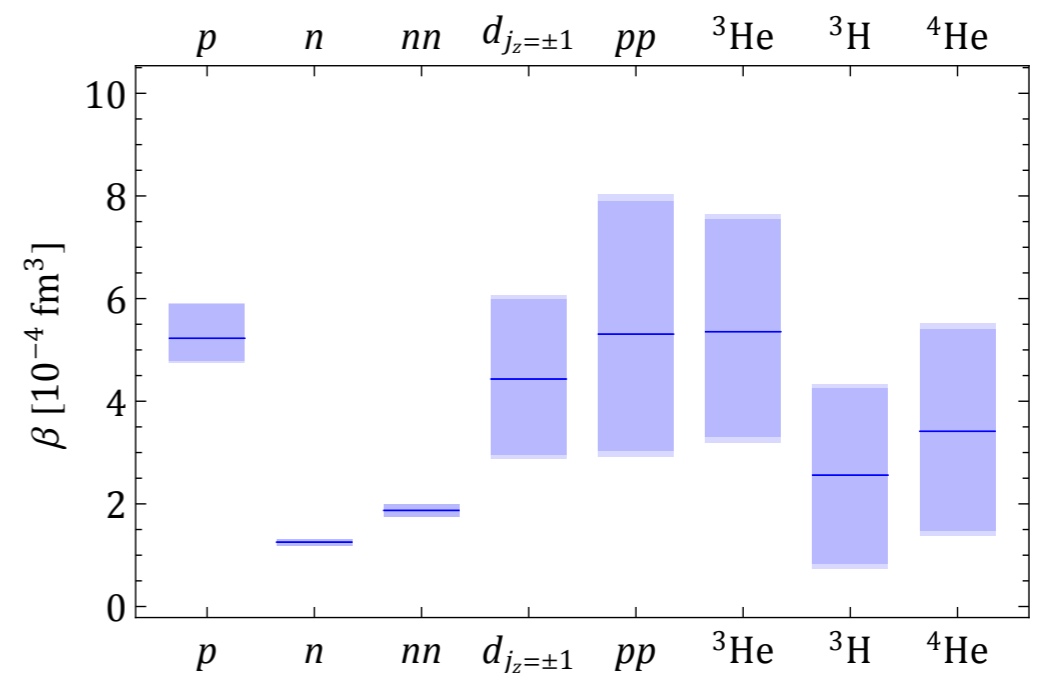
Magnetic polarizabilities



Magnetic moment



Magnetic polarizability



$$N_f = 3, m_\pi = 0.806 \text{ GeV}, a = 0.145(2) \text{ fm}$$

Beane et al. (NPLQCD), *phys.rev.lett.* 113 (2014) 25, 252001.
 Beane et al. (NPLQCD), *phys.rev.* D92 (2015) 11, 114502.

Let's enumerate a some of the methods that give access to structure quantities in general:

Three(four)-point functions

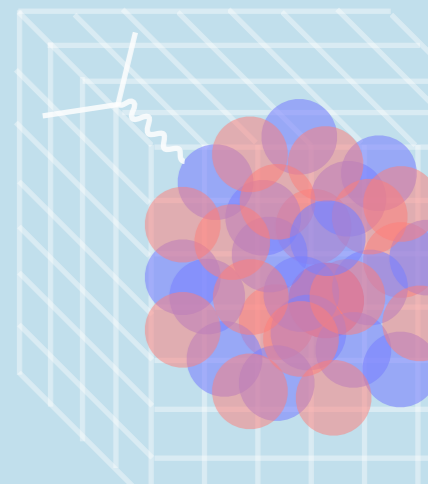
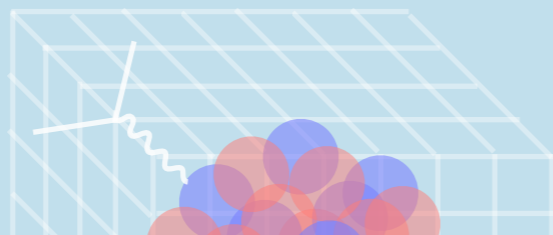
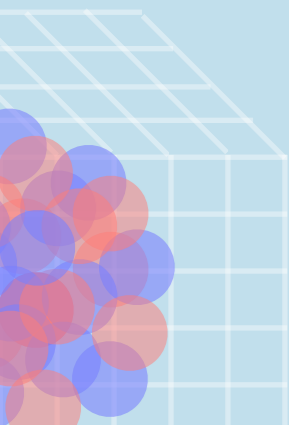
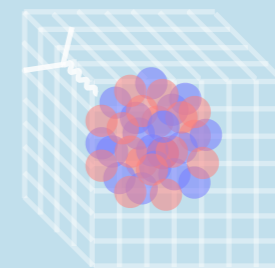
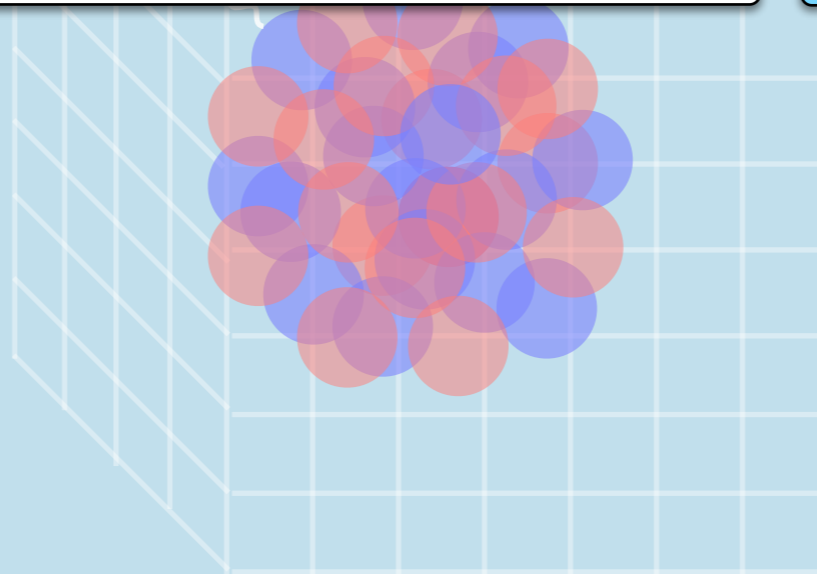
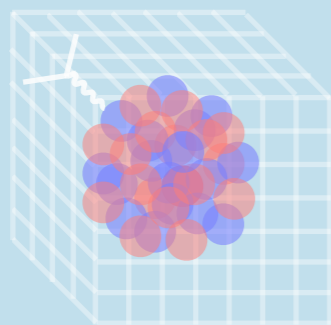
For e.g., form factors, moments of structure functions, Compton amplitude, transition amplitudes

Background-field methods

For e.g., EM moments and polarizabilities, charge radius, form factors and transition amplitudes.

Feynman-Hellmann inspired methods

Similar to background fields. For e.g., axial charge, form factors, EM moments, transition amplitudes



Hamiltonian as a
function of a
variable parameter

$$\hat{H}(\lambda) = \hat{H} + \lambda \hat{V}$$

Energy eigenvalue

$$\frac{dE_n}{d\lambda} = \frac{\langle \psi_n | \frac{d\hat{H}}{d\lambda} | \psi_n \rangle}{\langle \psi_n | \psi_n \rangle}$$

Energy eigenstate

Example: sigma term

$$m_q \frac{\partial m_N}{\partial m_q} \Big|_{m_q = m_q^{\text{phy}}} = \langle \mathcal{N} | m_q \bar{q} q | \mathcal{N} \rangle$$

Hamiltonian as a function of a variable parameter

$$\hat{H}(\lambda) = \hat{H} + \lambda \hat{V}$$

Energy eigenvalue

$$\frac{dE_n}{d\lambda} = \frac{\langle \psi_n | \frac{d\hat{H}}{d\lambda} | \psi_n \rangle}{\langle \psi_n | \psi_n \rangle}$$

Energy eigenstate

Example: sigma term

$$m_q \frac{\partial m_N}{\partial m_q} \Big|_{m_q = m_q^{\text{phy}}} = \langle \mathcal{N} | m_q \bar{q} q | \mathcal{N} \rangle$$

Generalization to correlation functions

$$C_\lambda(t) = \langle \lambda | \mathcal{O}(t) \mathcal{O}^\dagger(0) | \lambda \rangle = \frac{1}{\mathcal{Z}_\lambda} \int D\Phi e^{-S - S_\lambda} \mathcal{O}(t) \mathcal{O}^\dagger(0)$$

Just a 2pt function

$$S_\lambda = \lambda \int d^4x j(x)$$

Integrated matrix element

$$-\frac{\partial C_\lambda(t)}{\partial \lambda} \Big|_{\lambda=0} = -C(t) \int dt' \langle \Omega | \mathcal{J}(t') | \Omega \rangle + \int dt' \langle \Omega | T \{ \mathcal{O}(t) \mathcal{J}(t') \mathcal{O}^\dagger(0) \} | \Omega \rangle$$

$$\mathcal{J}(t) = \int d^3x j(t, \vec{x})$$

Example: axial charge of the nucleon and triton!

Since the operator here is a quark bilinear, a clever to implement this is by modifying the quark propagator.

$$S_{\lambda_q; \Gamma}^{(q)}(x, y) = S^{(q)}(x, y) + \lambda_q \int dz S^{(q)}(x, z) \Gamma S^{(q)}(z, y)$$



Savage et al (NPLQCD), Phys.Rev.Lett.119,062002(2017).

Buochard et al (CALLATT), Phys.Rev.D96,014504(2017).

Example: axial charge of the nucleon and triton!

Since the operator here is a quark bilinear, a clever to implement this is by modifying the quark propagator.

$$S_{\lambda_q; \Gamma}^{(q)}(x, y) = S^{(q)}(x, y) + \lambda_q \int dz S^{(q)}(x, z) \Gamma S^{(q)}(z, y)$$

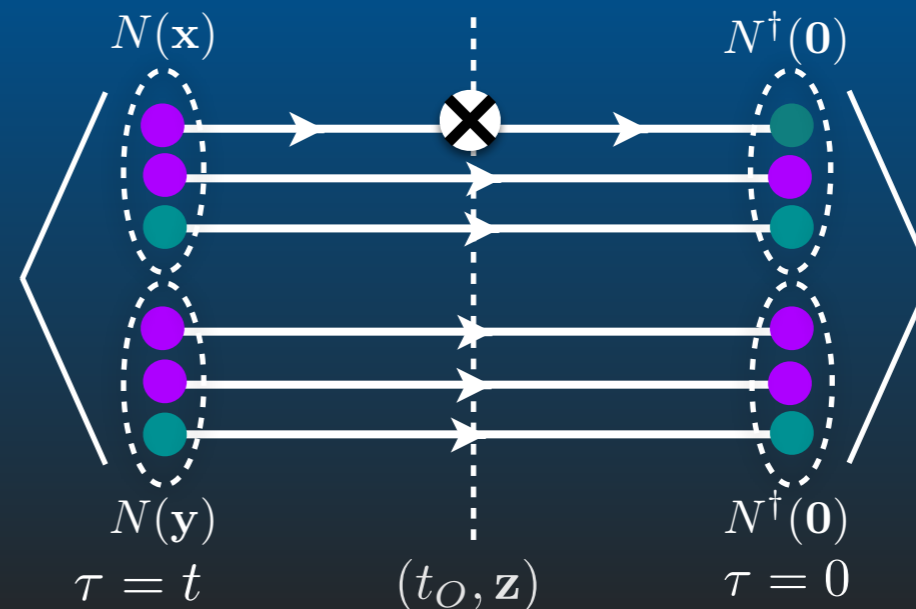


Savage et al (NPLQCD), Phys.Rev.Lett.119,062002(2017).

Buochard et al (CALLATT), Phys.Rev.D96,014504(2017).

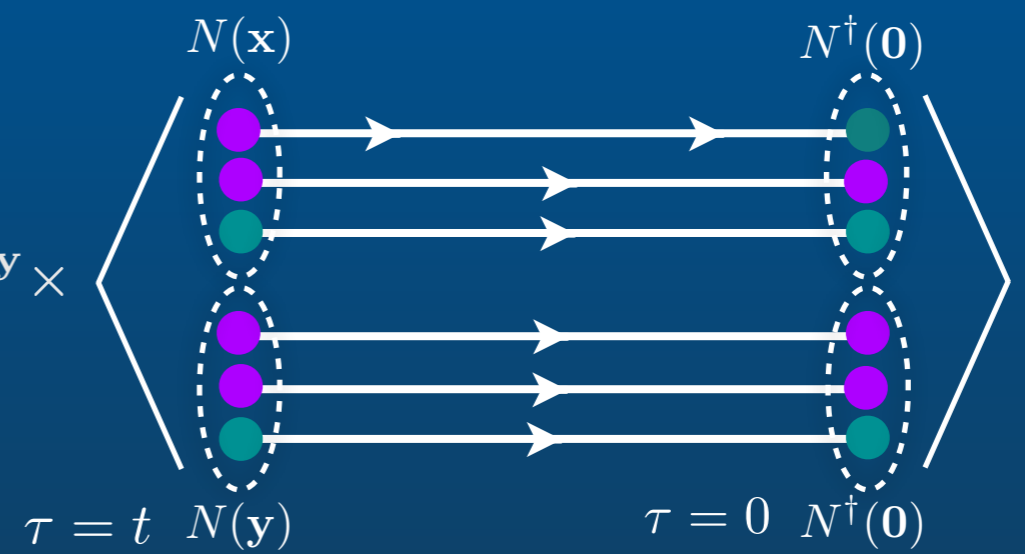
e.g.,

$$C(\mathbf{P}; t, t_0) = \sum_{\mathbf{p}_1 + \mathbf{p}_2 = \mathbf{P}} \sum_{\mathbf{x}, \mathbf{y}, \mathbf{z}} e^{i\mathbf{p}_1 \cdot \mathbf{x} + i\mathbf{p}_2 \cdot \mathbf{y}} \times$$

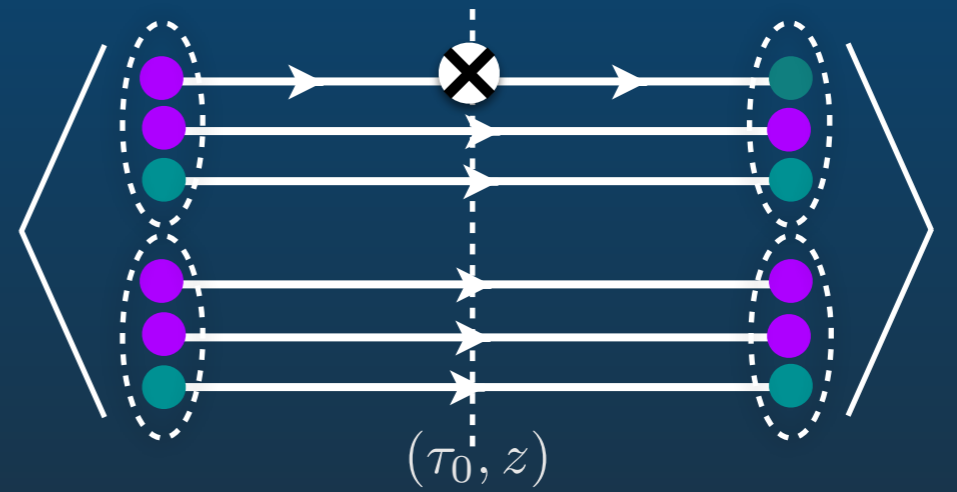


This gives more generally:

$$C_\lambda(\mathbf{P}; t, t_0) = \sum_{\mathbf{p}_1 + \mathbf{p}_2 = \mathbf{P}} \sum_{\mathbf{x}, \mathbf{y}, \mathbf{z}} e^{i\mathbf{p}_1 \cdot \mathbf{x} + i\mathbf{p}_2 \cdot \mathbf{y}} \times$$

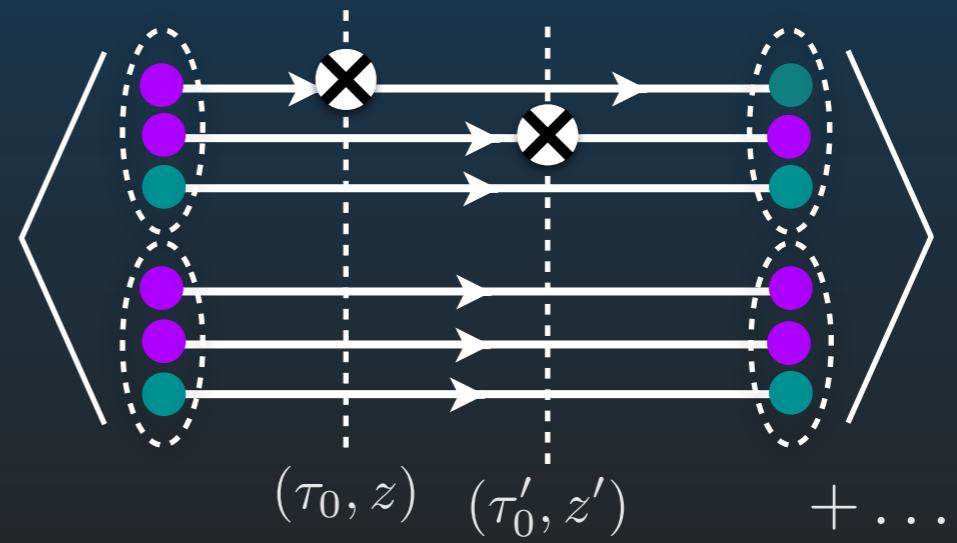


All possibilities $\longrightarrow + \lambda \sum_{\tau_0=0}^T \sum_z$



time-ordered product T

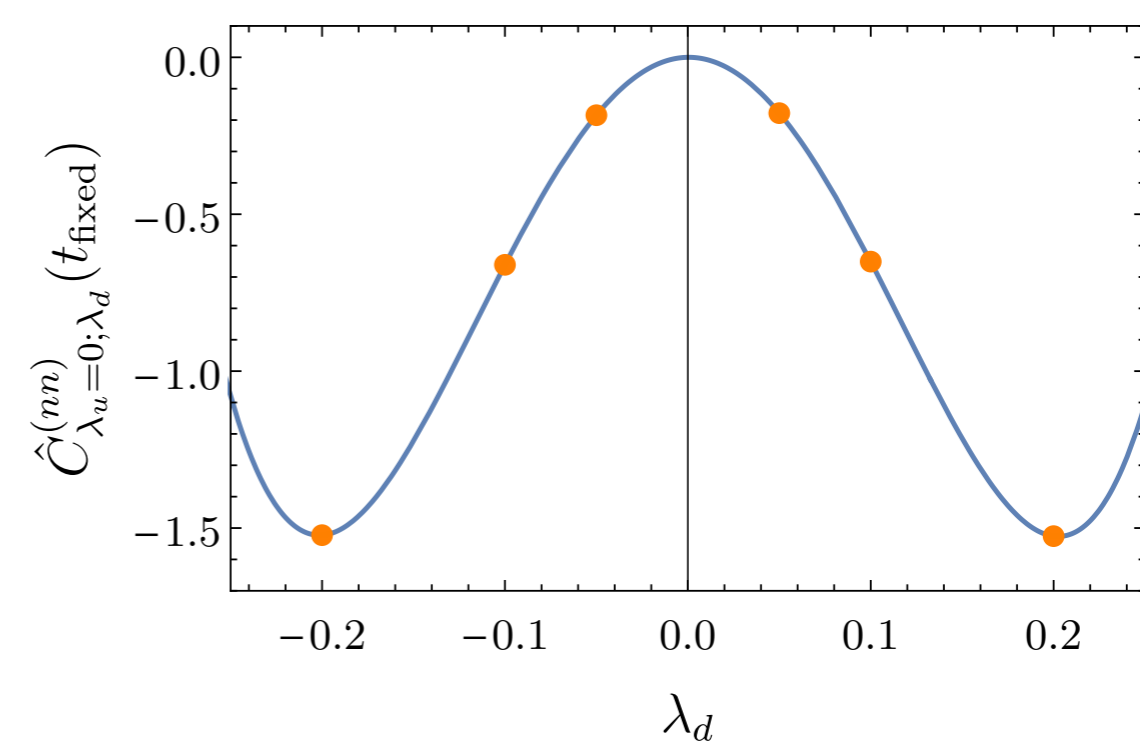
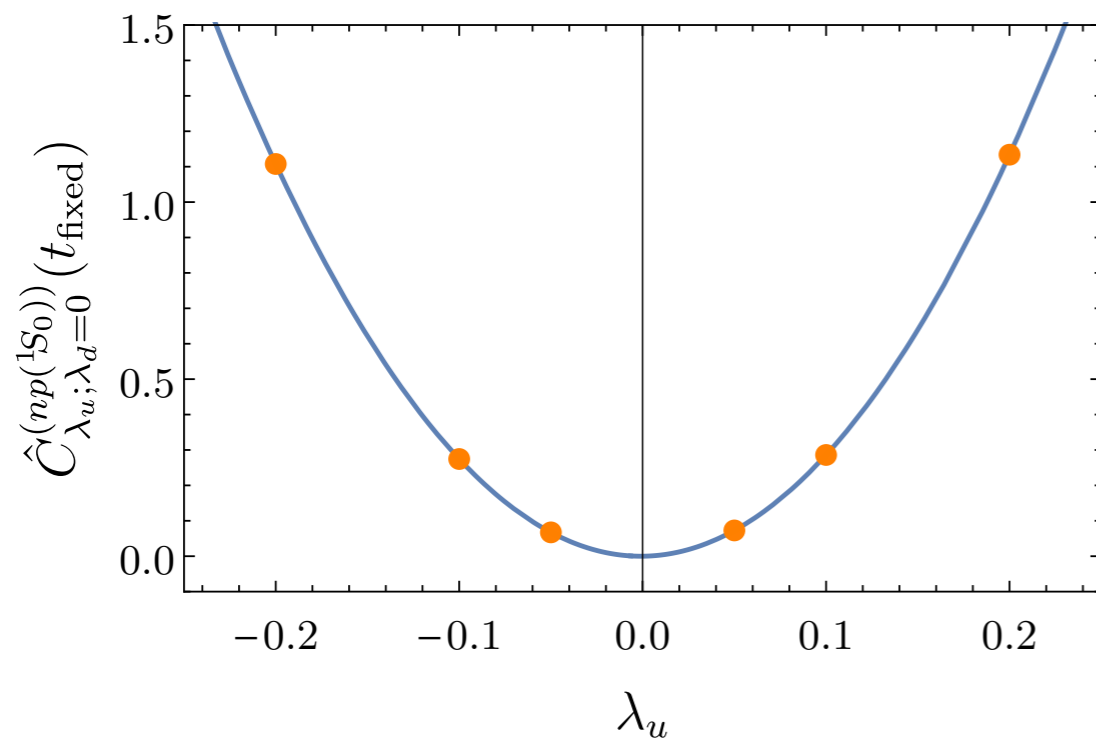
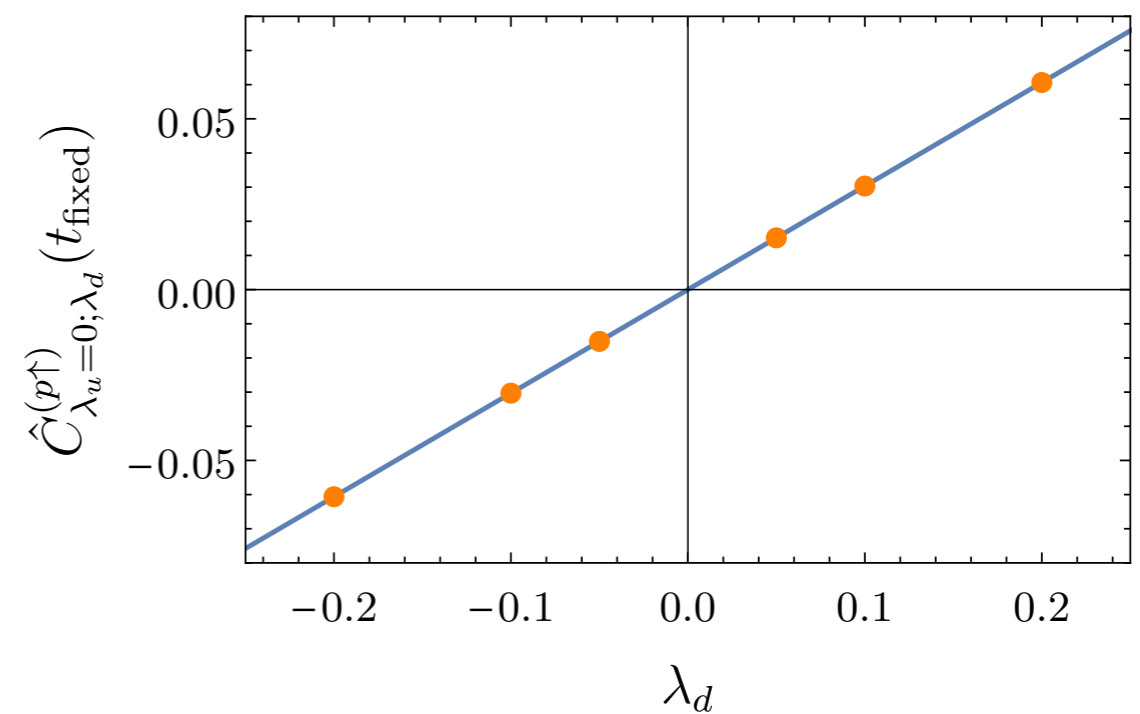
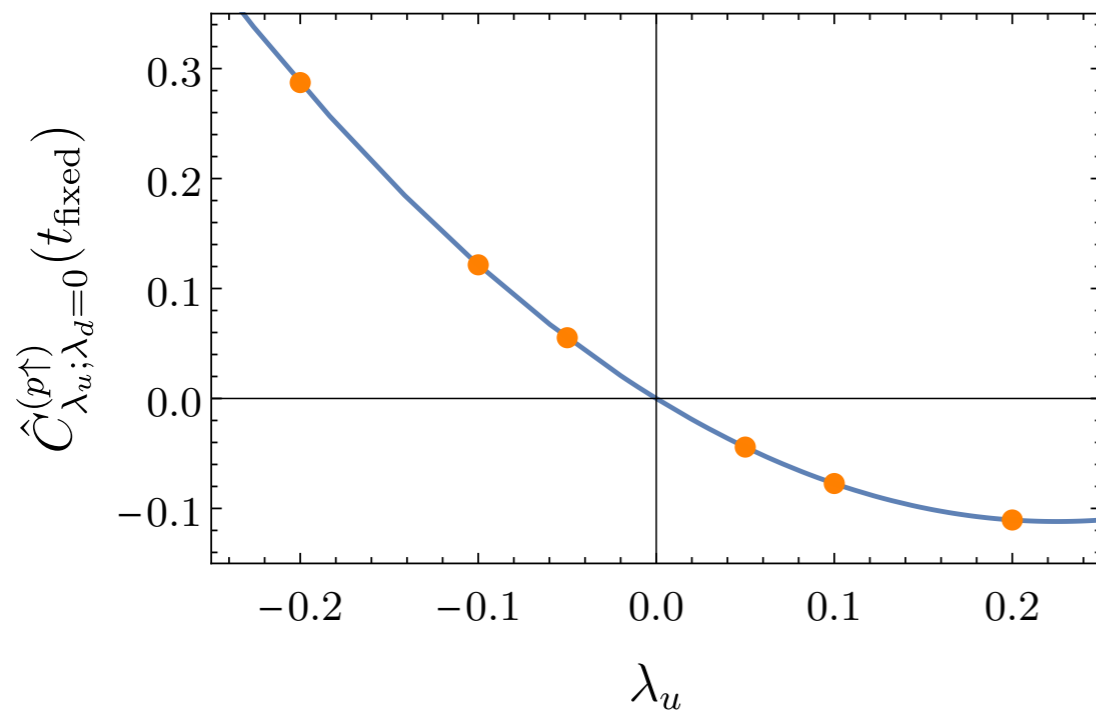
All possibilities $\longrightarrow + \lambda^2 \sum_{\tau_0=0}^T \sum_{\tau'_0=0}^T \sum_z \sum_{z'}$



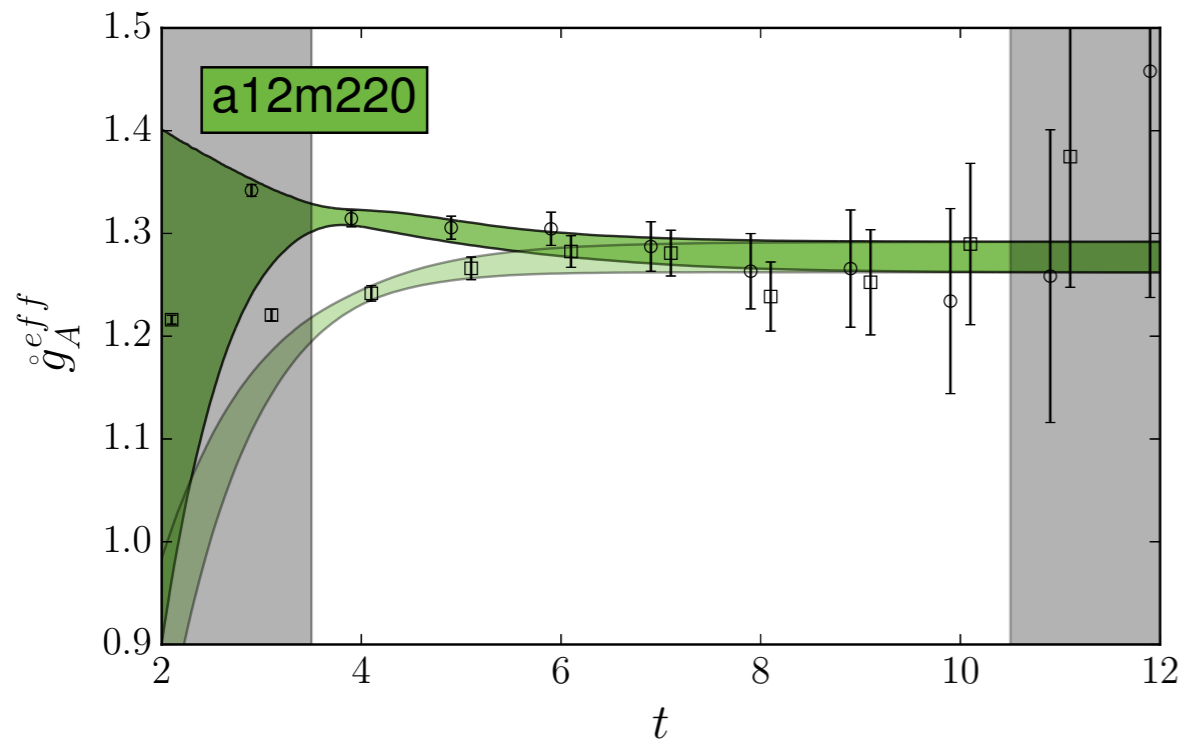
Double-current MEs are exact for isotensor quantities.

+ ...

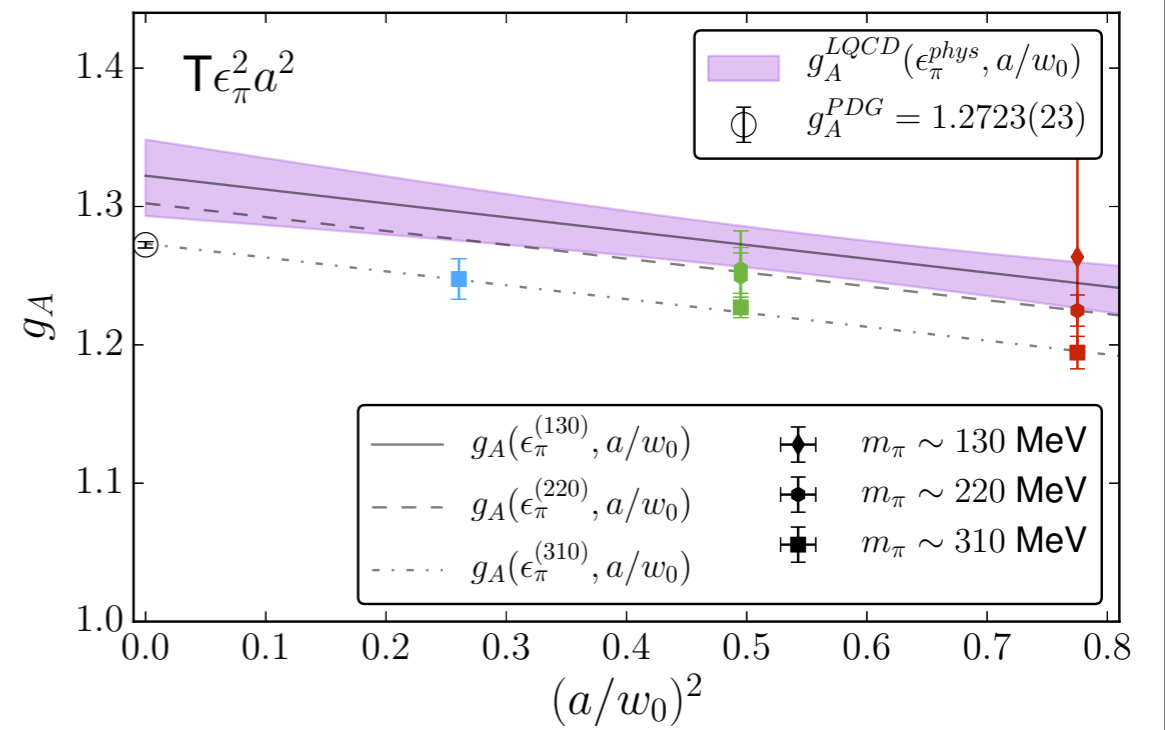
Matrix elements from a compound propagator/background field



Example of a work using the method:
Axial charge of the nucleon



Chang et al (CALLATT), Nature volume 558, 91–94 (2018).



Let's enumerate a some of the methods that give access to structure quantities in general:

Three(four)-point functions

For e.g., form factors, moments of structure functions, Compton amplitude, transition amplitudes

Background-field methods

For e.g., EM moments and polarizabilities, charge radius, form factors and transition amplitudes.

Feynman-Hellmann inspired methods

Similar to background fields. For e.g., axial charge, form factors, EM moments, transition amplitudes

We did not discuss many other interesting directions in the field, e.g.,

Moments of structure functions

Hadron tensor through inverse transform methods

Quasi-PDFs and pseudo-PDFs

GPDs, TMDs, gluonic observables, etc.

LECTURE III: NUCLEAR STRUCTURE, CHALLENGES AND PROGRESS



**LECTURE III:
TOWARDS NUCLEAR STRUCTURE FROM LATTICE QCD**



Three features make lattice QCD calculations of nuclei hard:

i) The complexity of systems grows rapidly with the number of quarks.

Detmold and Orginos, Phys. Rev. D 87, 114512 (2013).

**See also: Detmold and Savage, Phys.Rev.D82 014511 (2010).
Doi and Endres, Comput. Phys. Commun. 184 (2013) 117.**

ii) Excitation energies of nuclei are much smaller than the QCD scale.

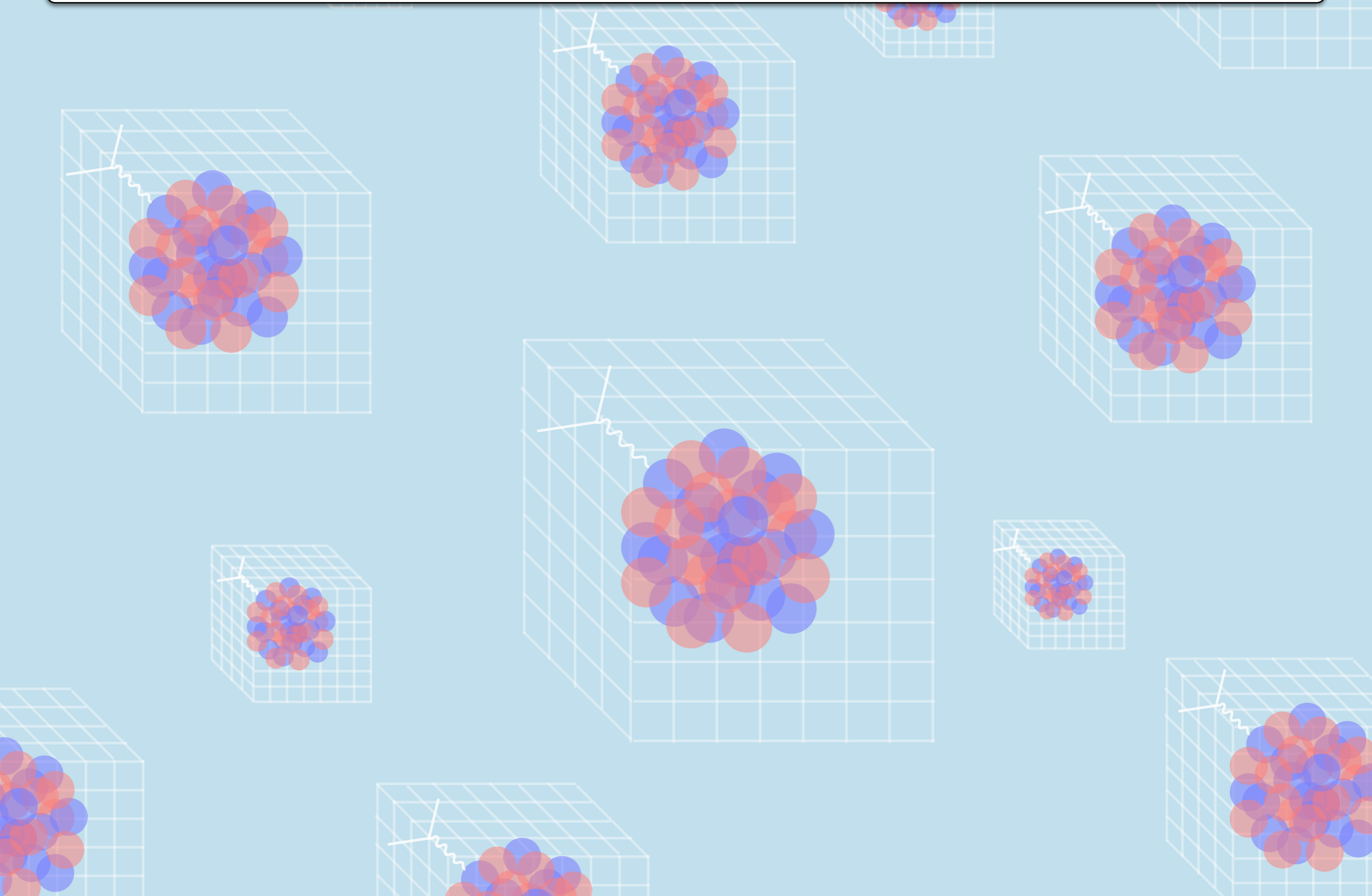
**Beane et al (NPLQCD), Phys.Rev.D79 114502 (2009).
Beane, Detmold, Orginos, Savage, Prog. Part. Nucl. Phys. 66 (2011).
Junnakar and Walker-Loud, Phys.Rev. D87 (2013) 114510.
Briceno, Dudek and Young, Rev. Mod. Phys. 90 025001.**

iii) There is a severe signal-to-noise degradation.

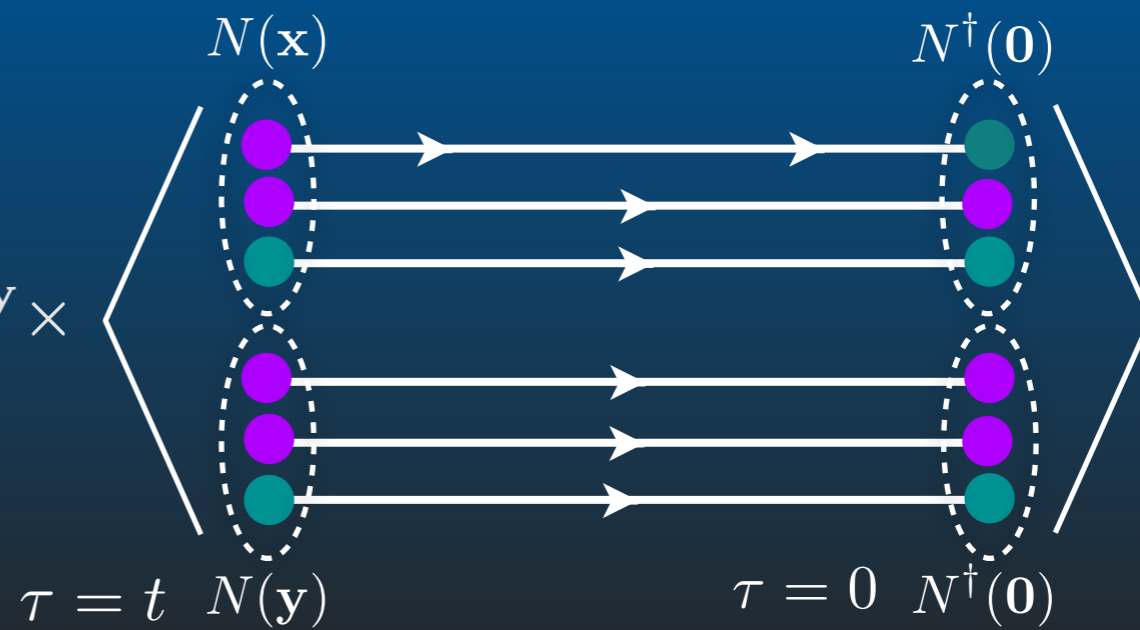
Paris (1984) and Lepage (1989).

**Wagman and Savage, Phys. Rev. D 96, 114508 (2017).
Wagman and Savage, arXiv:1704.07356 [hep-lat].**

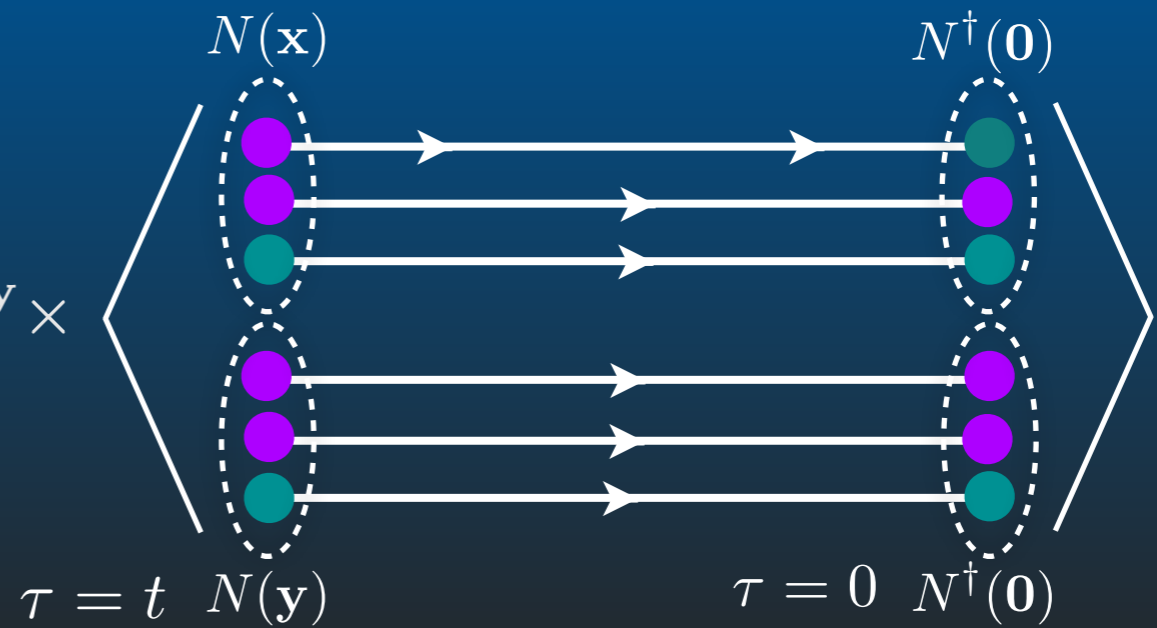
i) The complexity of systems grows rapidly with the number of quarks.



$$C(\mathbf{P}; t, t_0) = \sum_{\mathbf{p}_1 + \mathbf{p}_2 = \mathbf{P}} \sum_{\mathbf{x}, \mathbf{y}, \mathbf{z}} e^{i\mathbf{p}_1 \cdot \mathbf{x} + i\mathbf{p}_2 \cdot \mathbf{y}} \times$$



$$C(\mathbf{P}; t, t_0) = \sum_{\mathbf{p}_1 + \mathbf{p}_2 = \mathbf{P}} \sum_{\mathbf{x}, \mathbf{y}, \mathbf{z}} e^{i\mathbf{p}_1 \cdot \mathbf{x} + i\mathbf{p}_2 \cdot \mathbf{y}} \times$$



COMPLEXITIES OF
QUARK-LEVEL
INTERPOLATING FIELDS

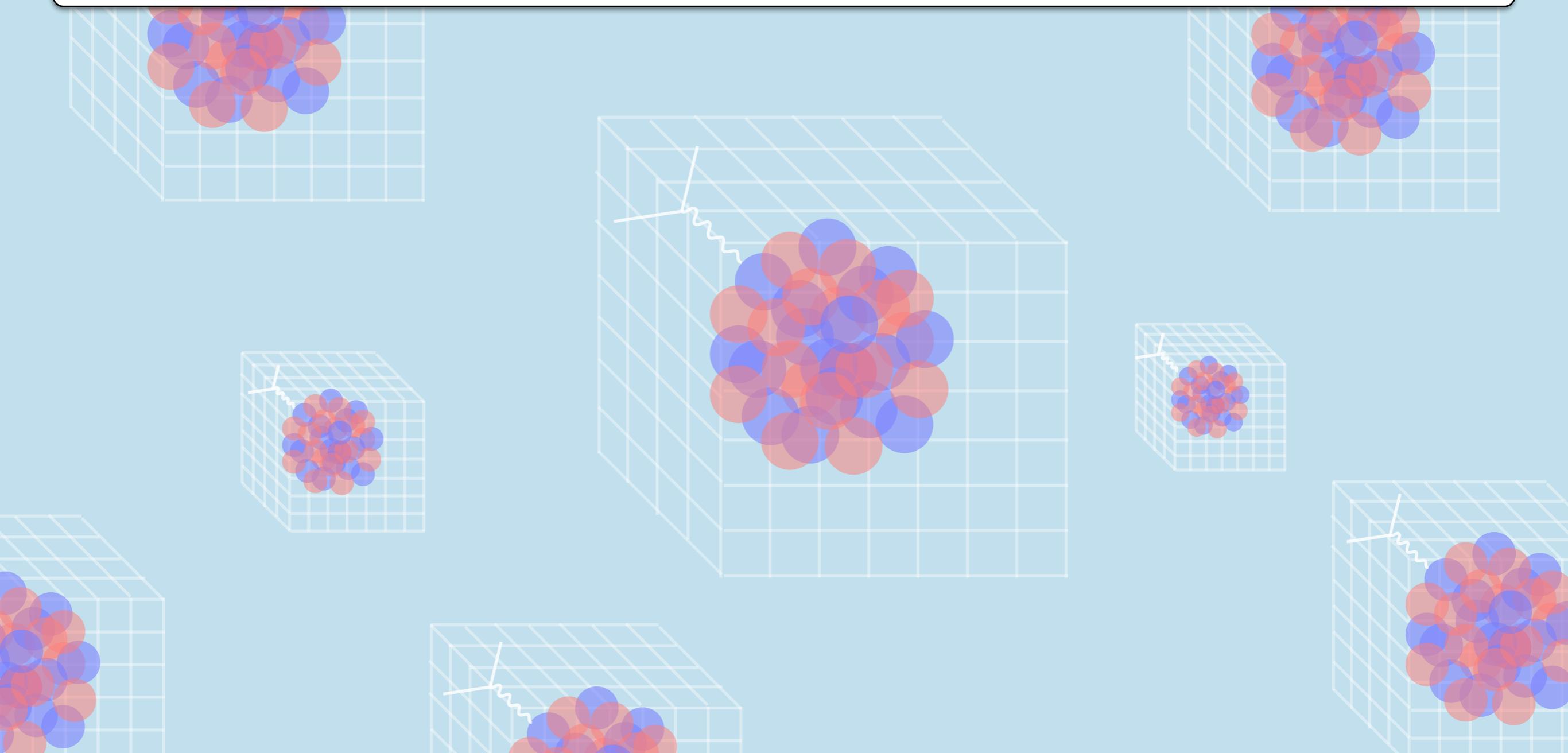
COMPLEXITIES
OF QUARK
CONTRACTIONS

Naively the number of quark contractions for a nucleus goes as:

$$(2N_p + N_n)! (N_p + 2N_n)!$$

How bad is this?

Example: Consider radium-226 isotope.
the number of contractions required is $\sim 10^{1425}$



Naively the number of quark contractions for a nucleus goes as:

$$(2N_p + N_n)! (N_p + 2N_n)!$$

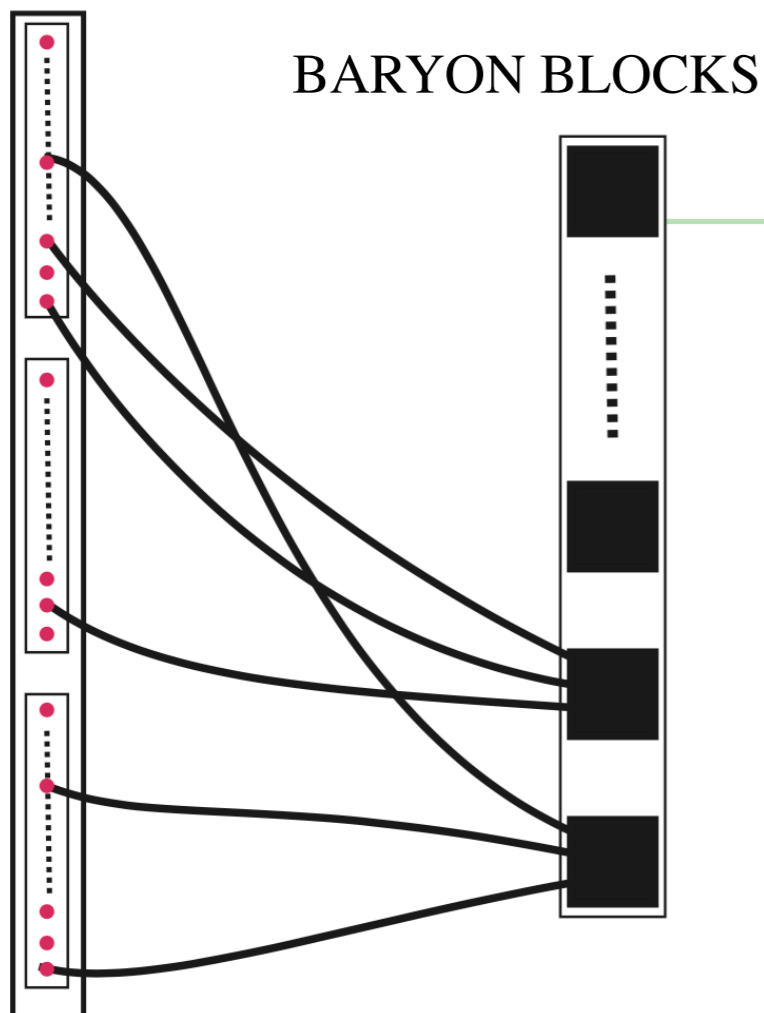
How bad is this?

Example: Consider radium-226 isotope.

the number of contractions required is $\sim 10^{1425}$



An example of a more efficient algorithm:



$$\mathcal{B}_b^{a_1, a_2, a_3}(\mathbf{p}, t; x_0) = \sum_{\mathbf{x}} e^{i\mathbf{p} \cdot \mathbf{x}} \sum_{k=1}^{N_B(b)} \tilde{w}_b^{(c_1, c_2, c_3), k} \sum_{\mathbf{i}} \epsilon^{i_1, i_2, i_3} S(c_{i_1}, x; a_1, x_0) S(c_{i_2}, x; a_2, x_0) S(c_{i_3}, x; a_3, x_0)$$

Can also start propagators at different locations.

Naively the number of quark contractions for a nucleus goes as:

$$(2N_p + N_n)! (N_p + 2N_n)!$$

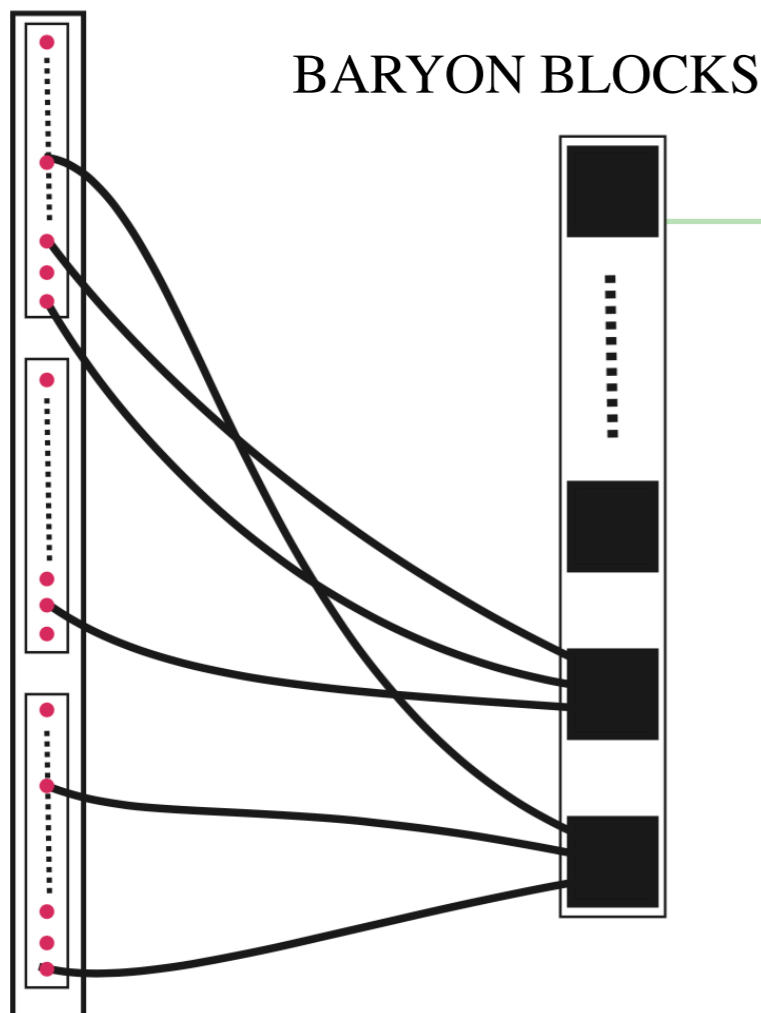
How bad is this?

Example: Consider radium-226 isotope.

the number of contractions required is $\sim 10^{1425}$



An example of a more efficient algorithm:



$$\mathcal{B}_b^{a_1, a_2, a_3}(\mathbf{p}, t; x_0) = \sum_{\mathbf{x}} e^{i\mathbf{p} \cdot \mathbf{x}} \sum_{k=1}^{N_B(b)} \tilde{w}_b^{(c_1, c_2, c_3), k} \sum_i \epsilon^{i_1, i_2, i_3} S(c_{i_1}, x; a_1, x_0) S(c_{i_2}, x; a_2, x_0) S(c_{i_3}, x; a_3, x_0)$$

Can also start propagators at different locations.

The new scaling is:

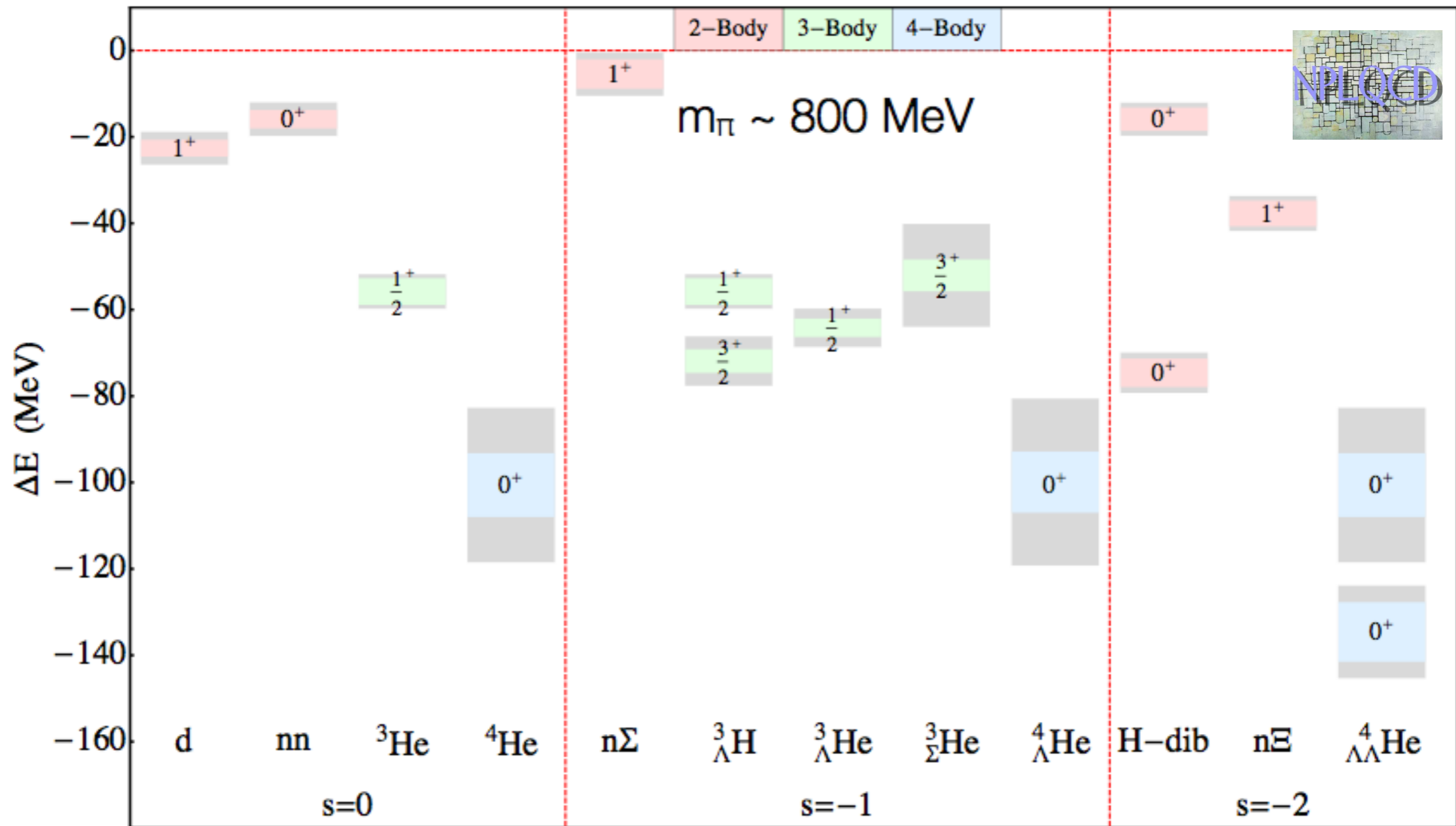
$$M_w \cdot N_w \cdot \frac{(3A)!}{(3!)^A}$$

Number of terms
in the sink

Number of terms
in the source

Nuclei obtained from such an approach (at a heavier quark masses)

$N_f = 3$, $m_\pi = 0.806$ GeV, $a = 0.145(2)$ fm

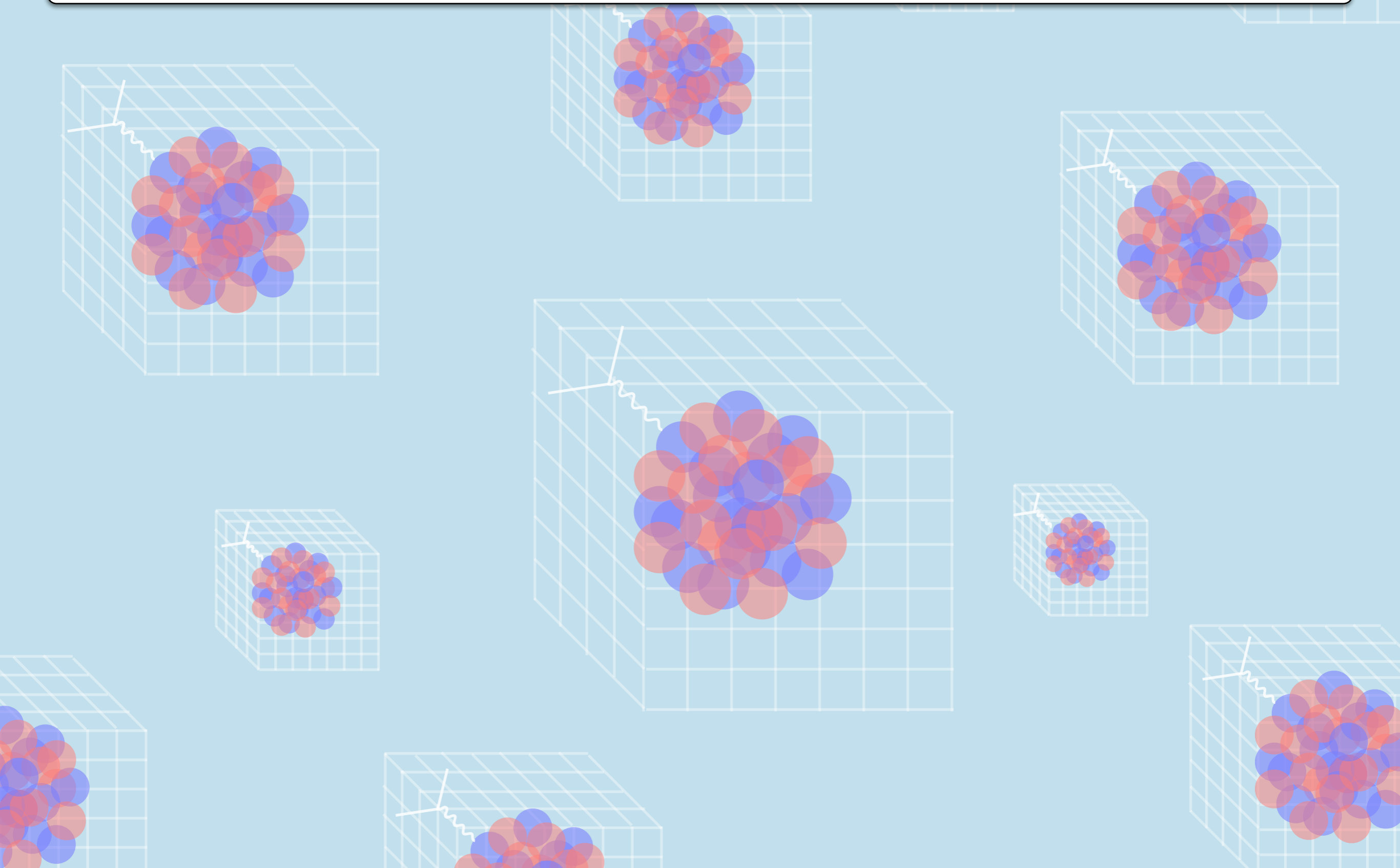


EXERCISE 6

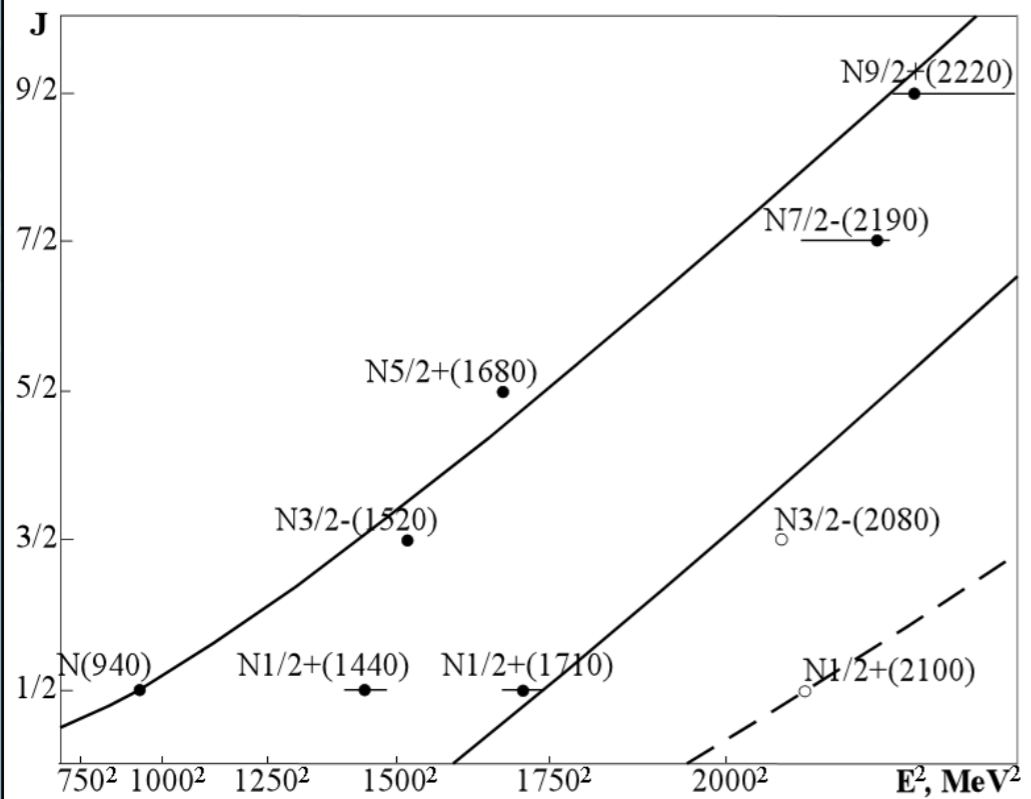


According to the naive counting, how many contractions are required for a nucleus at the source and sink with atomic numbers $A = 4, 8, 12, 16$? How many contractions are there with the use of the efficient algorithm described?

ii) Excitation energies of nuclei are much smaller than the QCD scale.

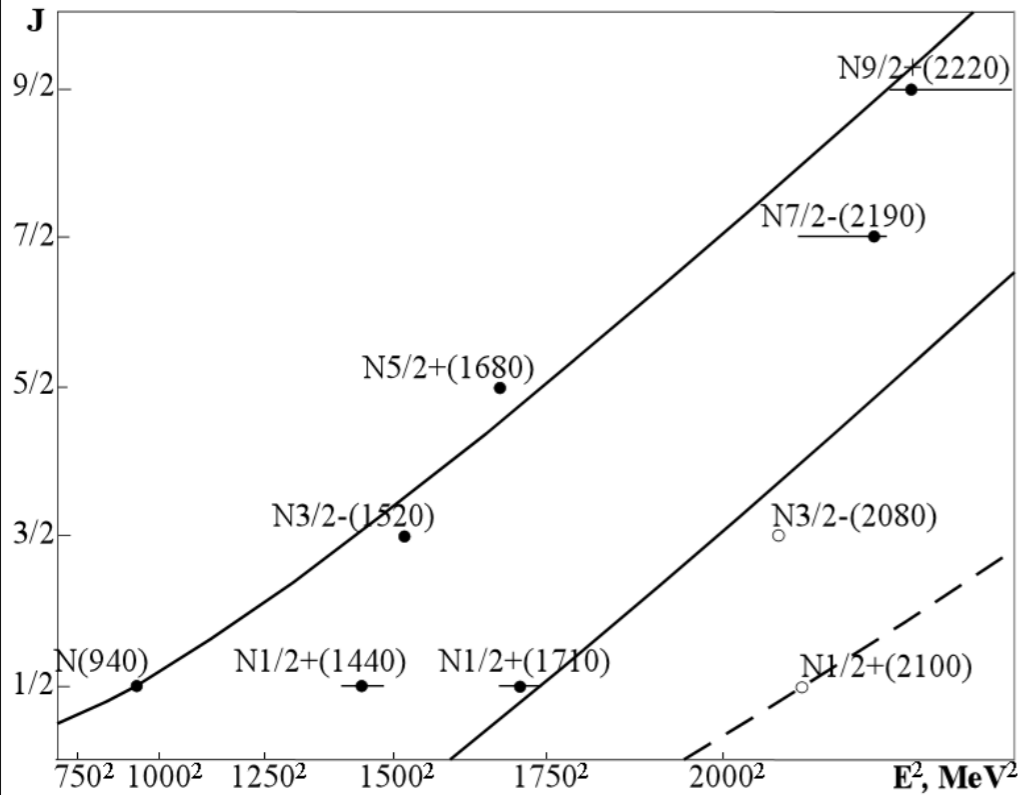


Nucleon excitations



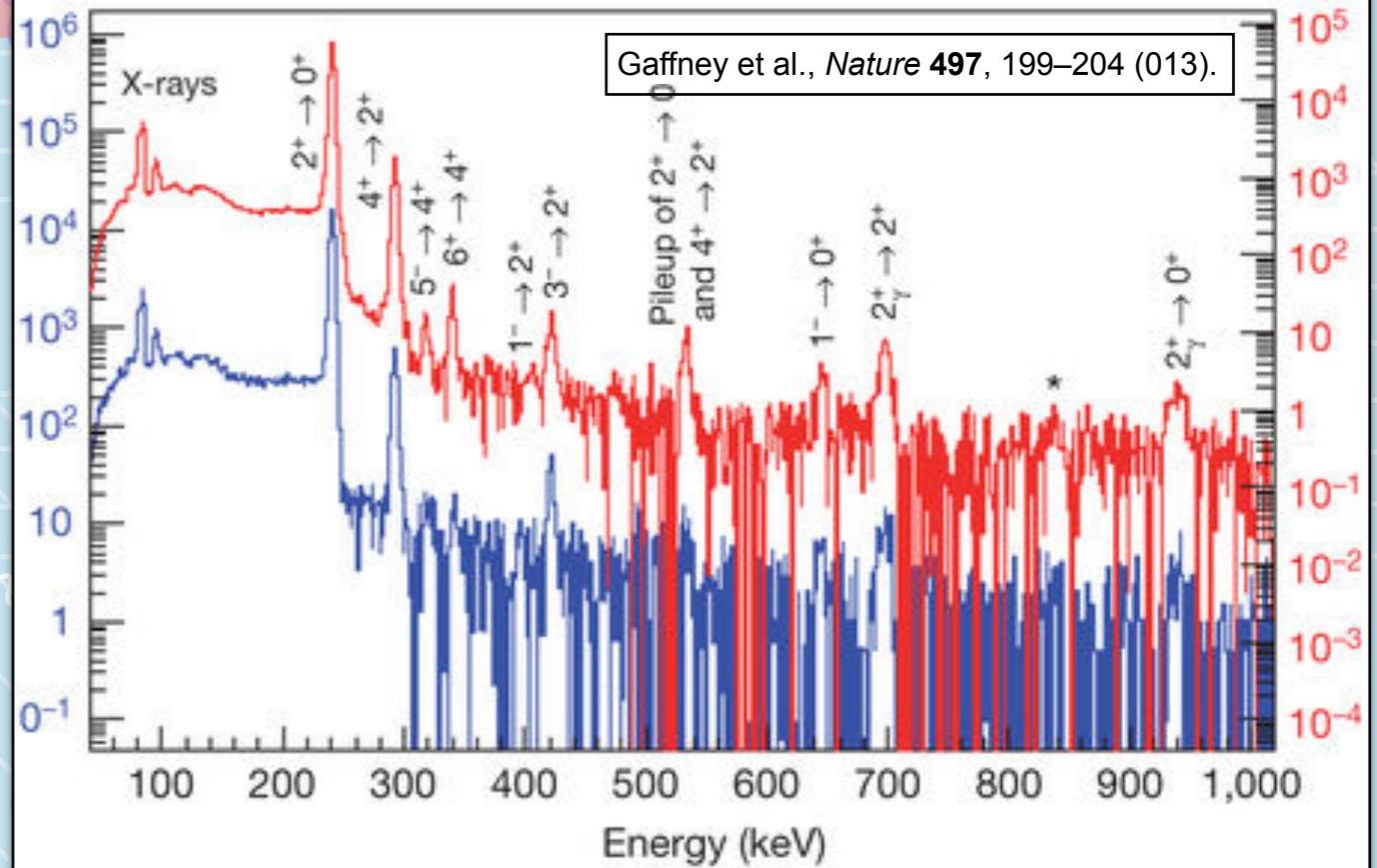
Kulikov, Dmitry A. et al., Central Eur.J.Phys. 11 (2013) .

Nucleon excitations



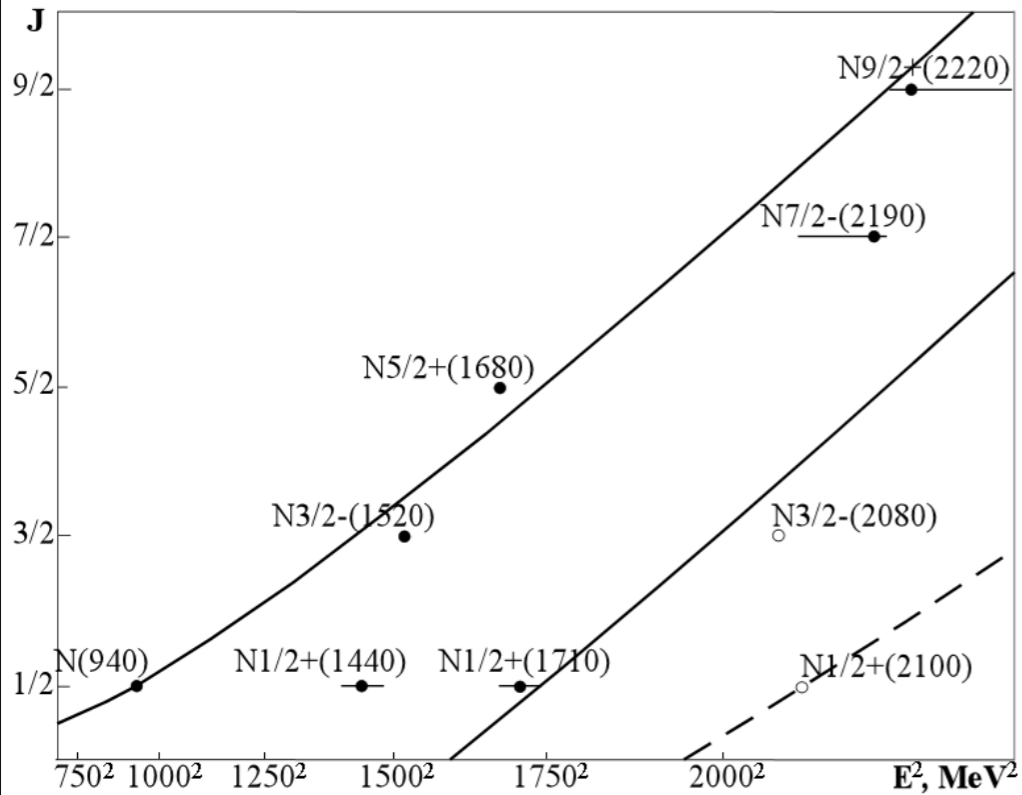
Kulikov, Dmitry A. et al., *Central Eur.J.Phys.* 11 (2013) .

Nuclear excitations of two pear-shaped nuclei (radium and radon)



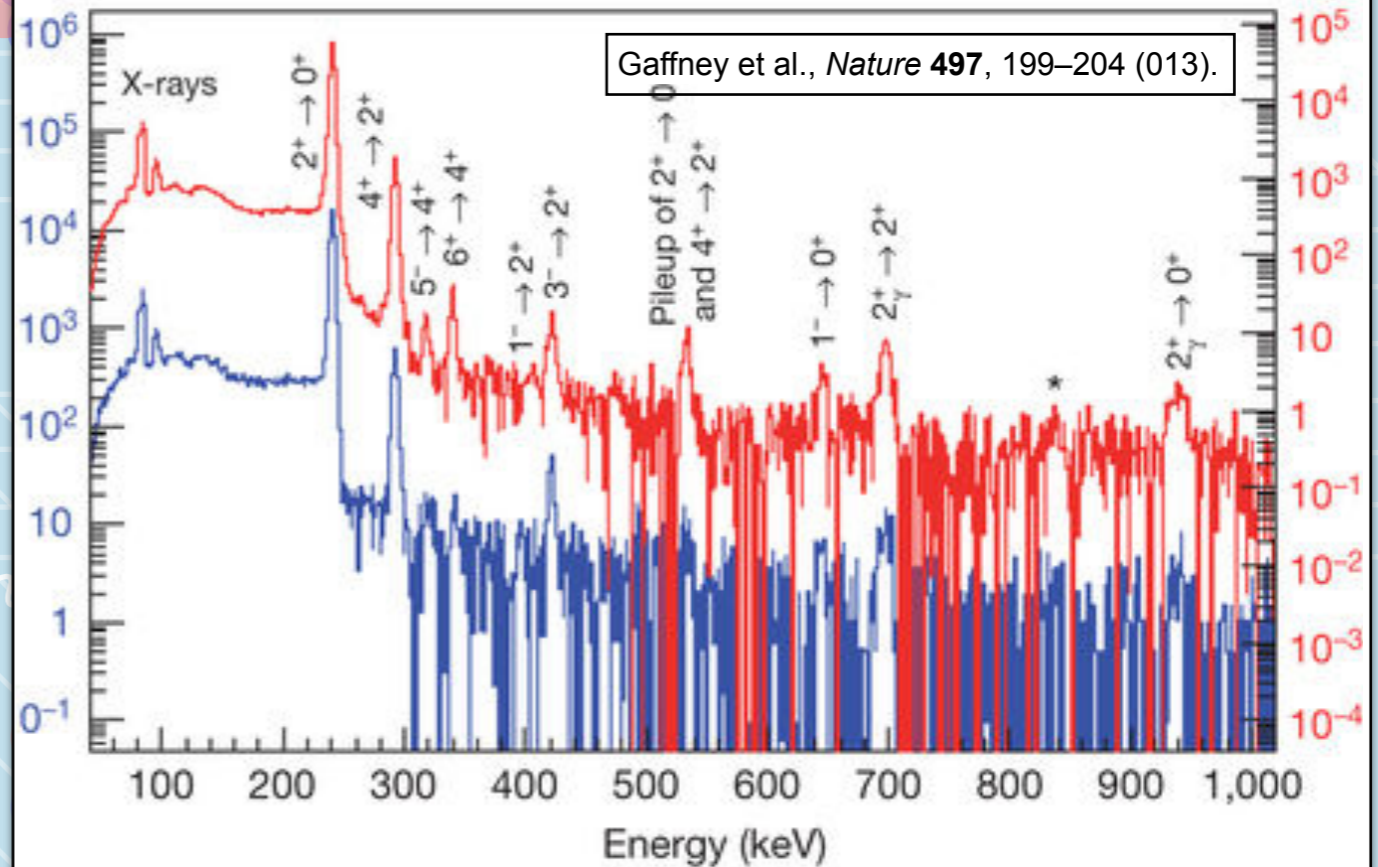
Gaffney et al., *Nature* **497**, 199–204 (013).

Nucleon excitations



Kulikov, Dmitry A. et al., Central Eur.J.Phys. 11 (2013) .

Nuclear excitations of two pear-shaped nuclei (radium and radon)



Getting radium directly from QCD will remain challenging for a long time! One should first compute $A = 2, 3, 4$ systems well. This is till not that easy: $B_d = 2$ MeV!

EXERCISE 7



With a given amount of computational resources, you have achieved a 1% statistical uncertainty on the extracted mass of the nucleon from your lattice QCD calculation. By what factor should you increase your computing resources (your statistics) to also achieve a 1% statistical uncertainty on the binding energy of the deuteron?

So what to do?

- With the most naive operators with similar overlaps to all states, unreasonably large times are needed to resolve nuclear energy gaps.
- The key to success of this program is in the use of good interpolating operators for nuclei. Since nuclei are bound states, interpolating operators with good overlap to compact states in a volume are desired.
- Ideally need to use a large set of operators for a **variational analysis**, but this has remained too costly in nuclear calculations, and only recently possible.

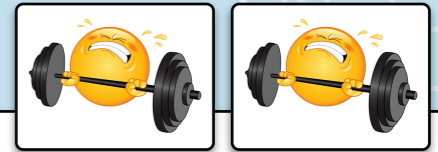
Applications in mesonic sector: Briceno, Dudek, and Young, Rev. Mod. Phys. 90 025001.

- Methods such as **matrix Prony** that eliminate the excited states in linear combinations of interpolators or correlations functions have shown to be useful.

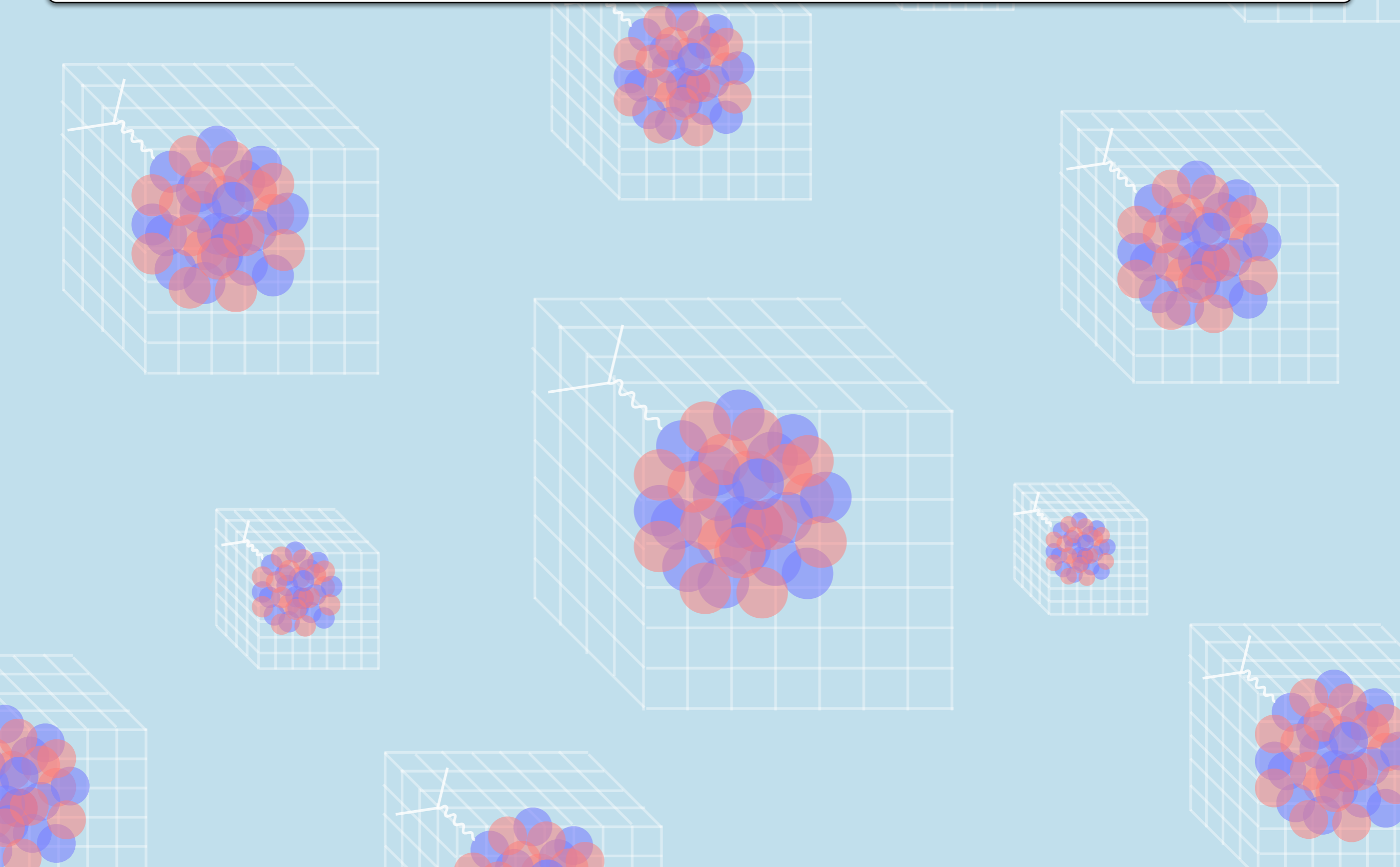
A good review: Beane, Detmold, Orginos, Savage, Prog. Part. Nucl. Phys. 66 (2011).

EXERCISE 8

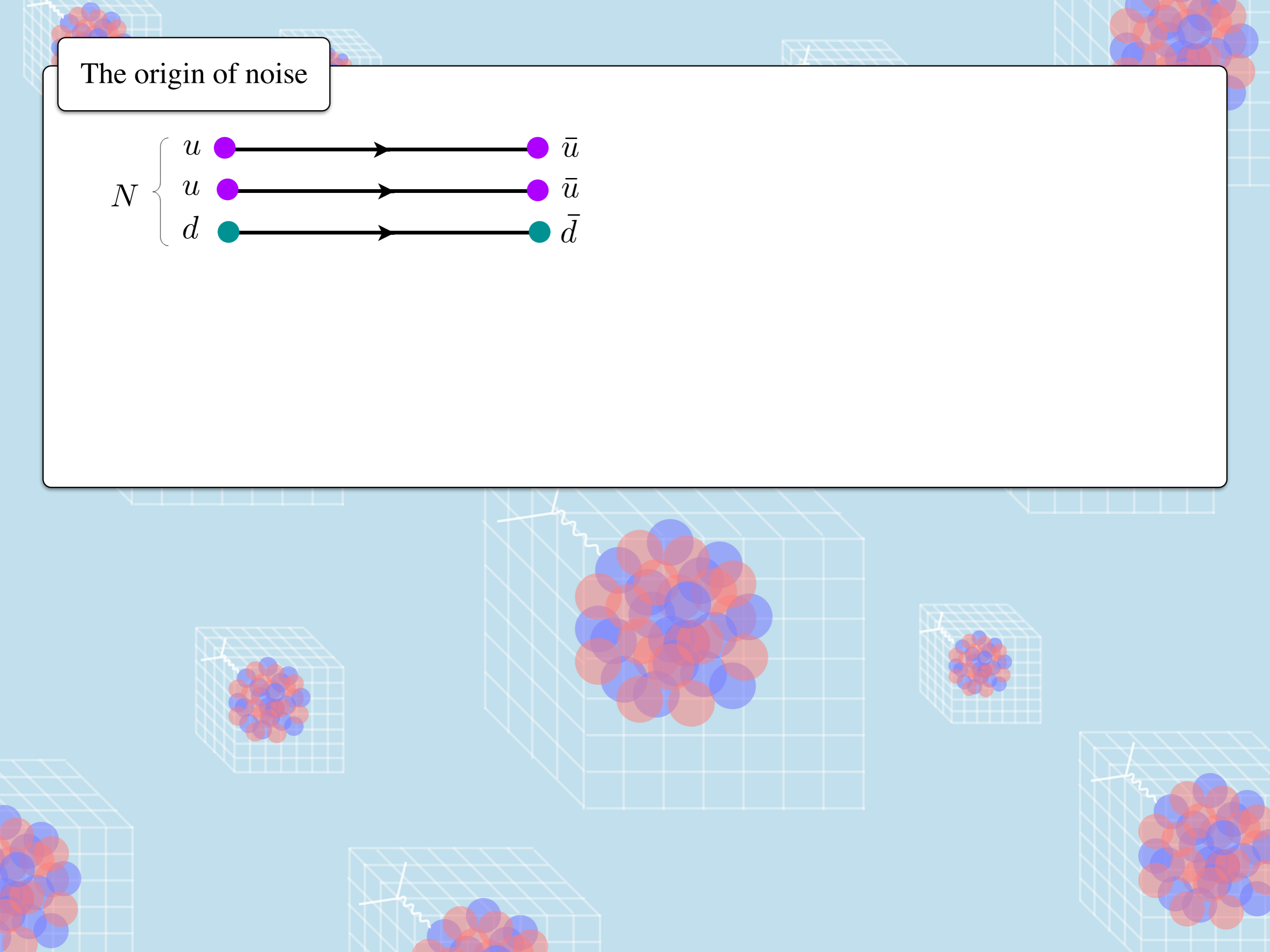
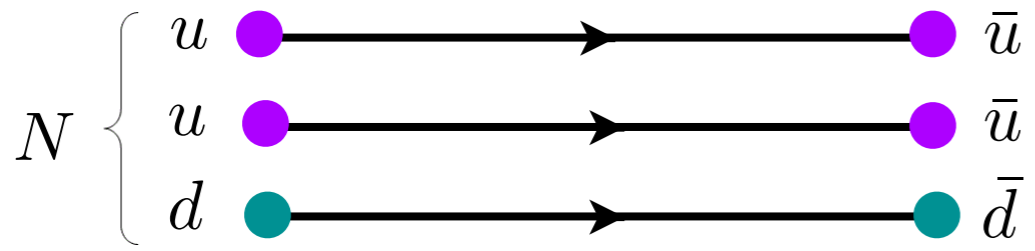
Consider a simple two-state model in the spectral decomposition of a Euclidean two-point function. Demonstrate that the time scale to reach the ground state of the model with a finite statistical precision can depend highly on the corresponding overlap factor for the state. It is sufficient to show this numerically and for a set of chosen energies and overlap factors.



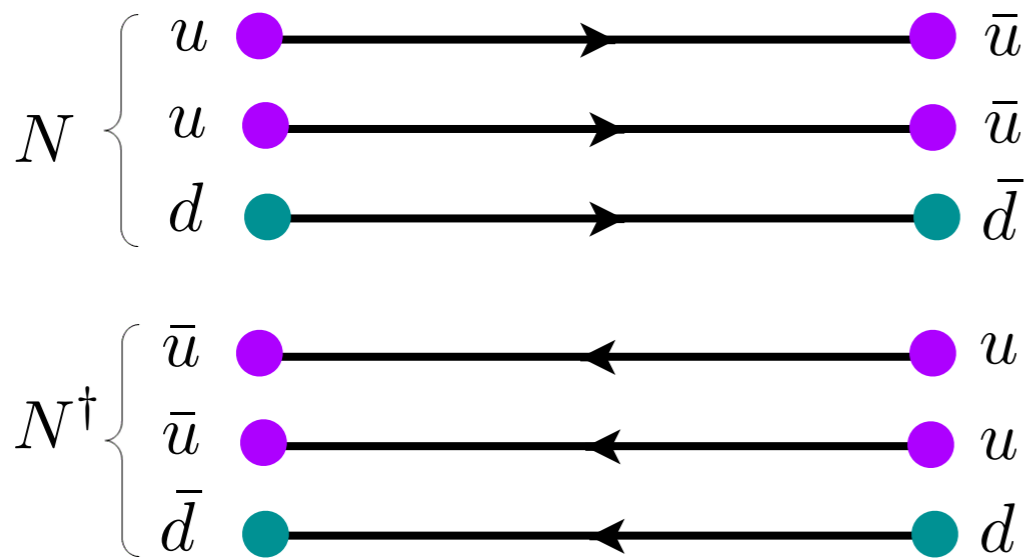
iii) There is a severe signal-to-noise degradation.



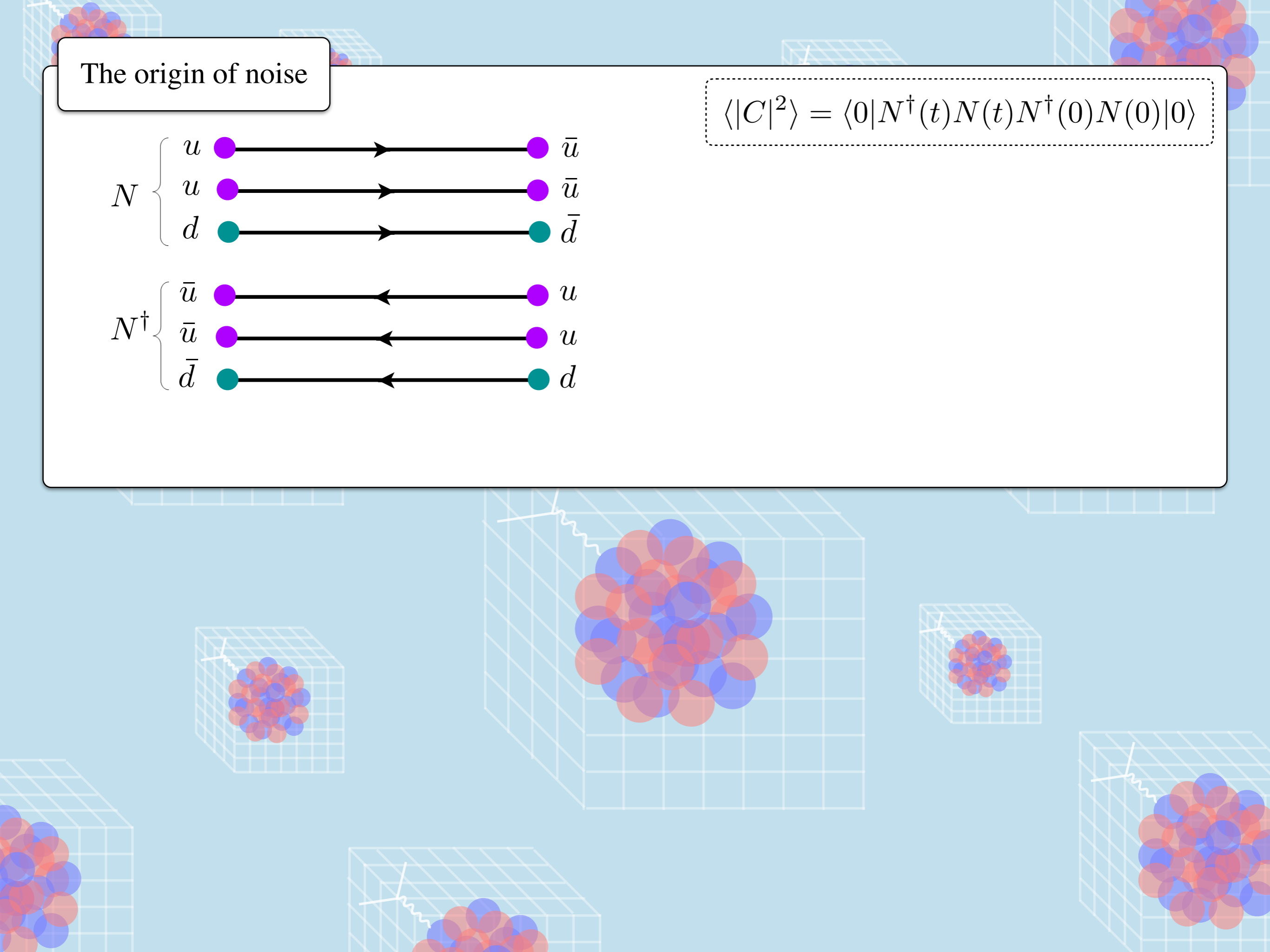
The origin of noise



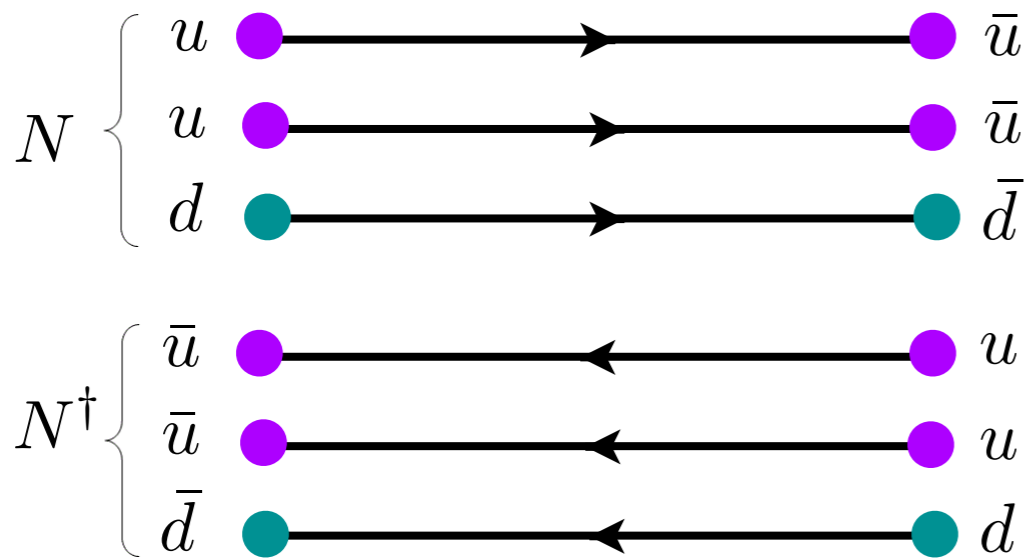
The origin of noise



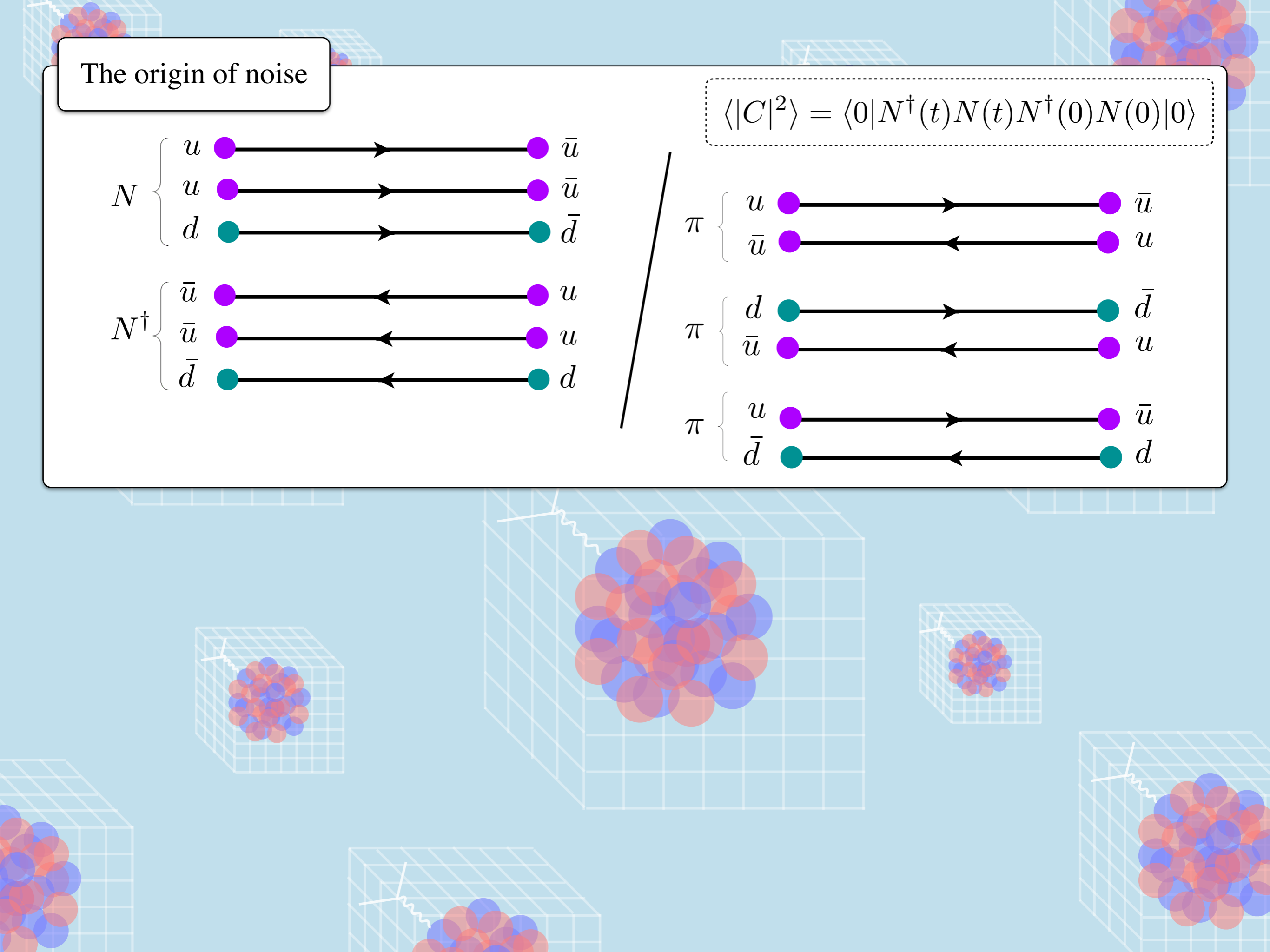
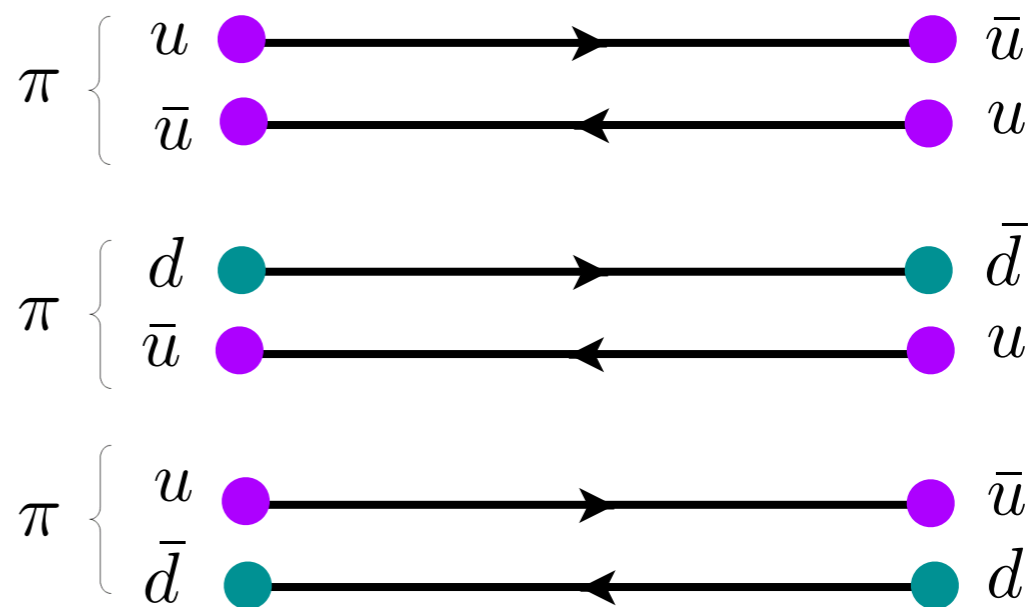
$$\langle |C|^2 \rangle = \langle 0 | N^\dagger(t) N(t) N^\dagger(0) N(0) | 0 \rangle$$



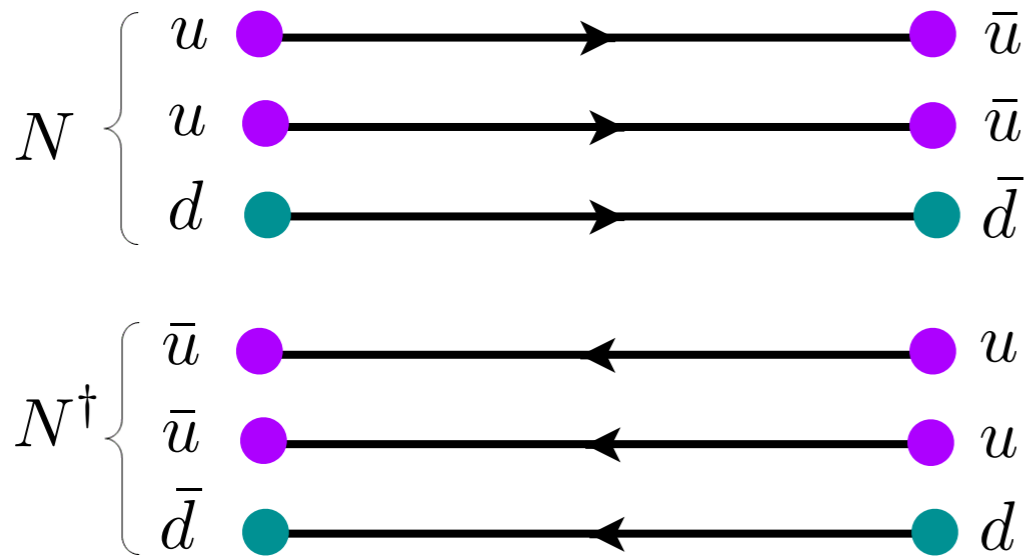
The origin of noise



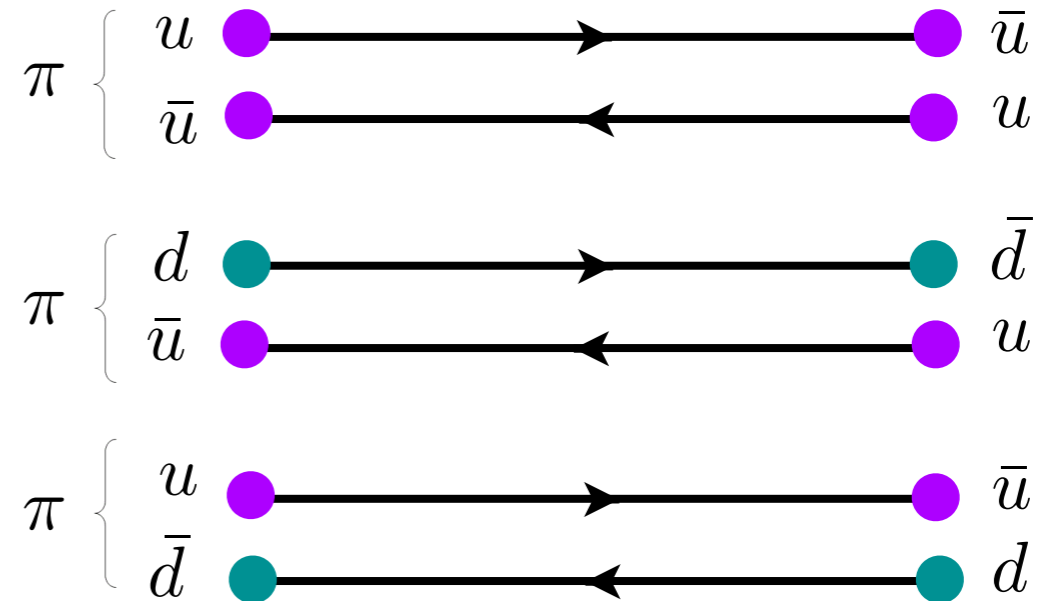
$$\langle |C|^2 \rangle = \langle 0 | N^\dagger(t) N(t) N^\dagger(0) N(0) | 0 \rangle$$



The origin of noise



$$\langle |C|^2 \rangle = \langle 0 | N^\dagger(t) N(t) N^\dagger(0) N(0) | 0 \rangle$$

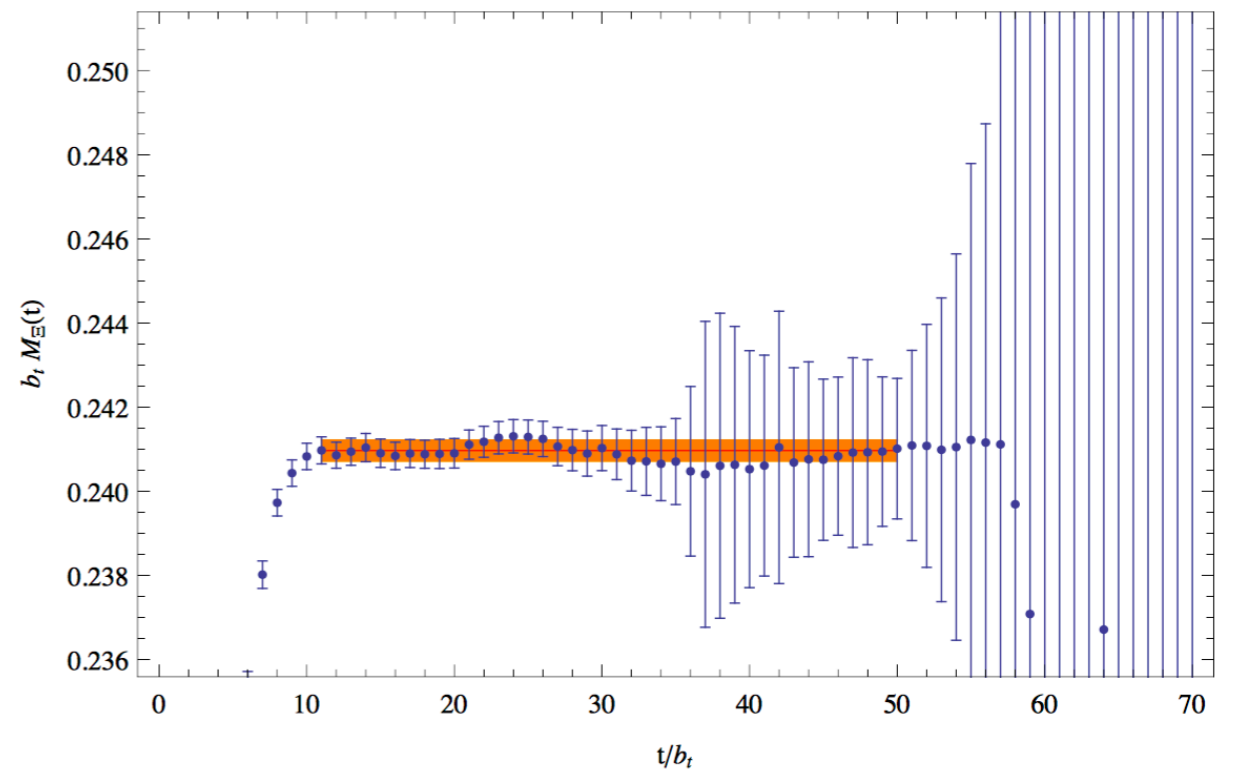


The ground-state of the variance correlator is three pions and not two nucleons:

$$\text{StN}(C_i) \sim \frac{\langle C_i \rangle}{\sqrt{\langle |C_i|^2 \rangle}} \sim e^{-(M_N - \frac{3}{2}m_\pi)t}$$

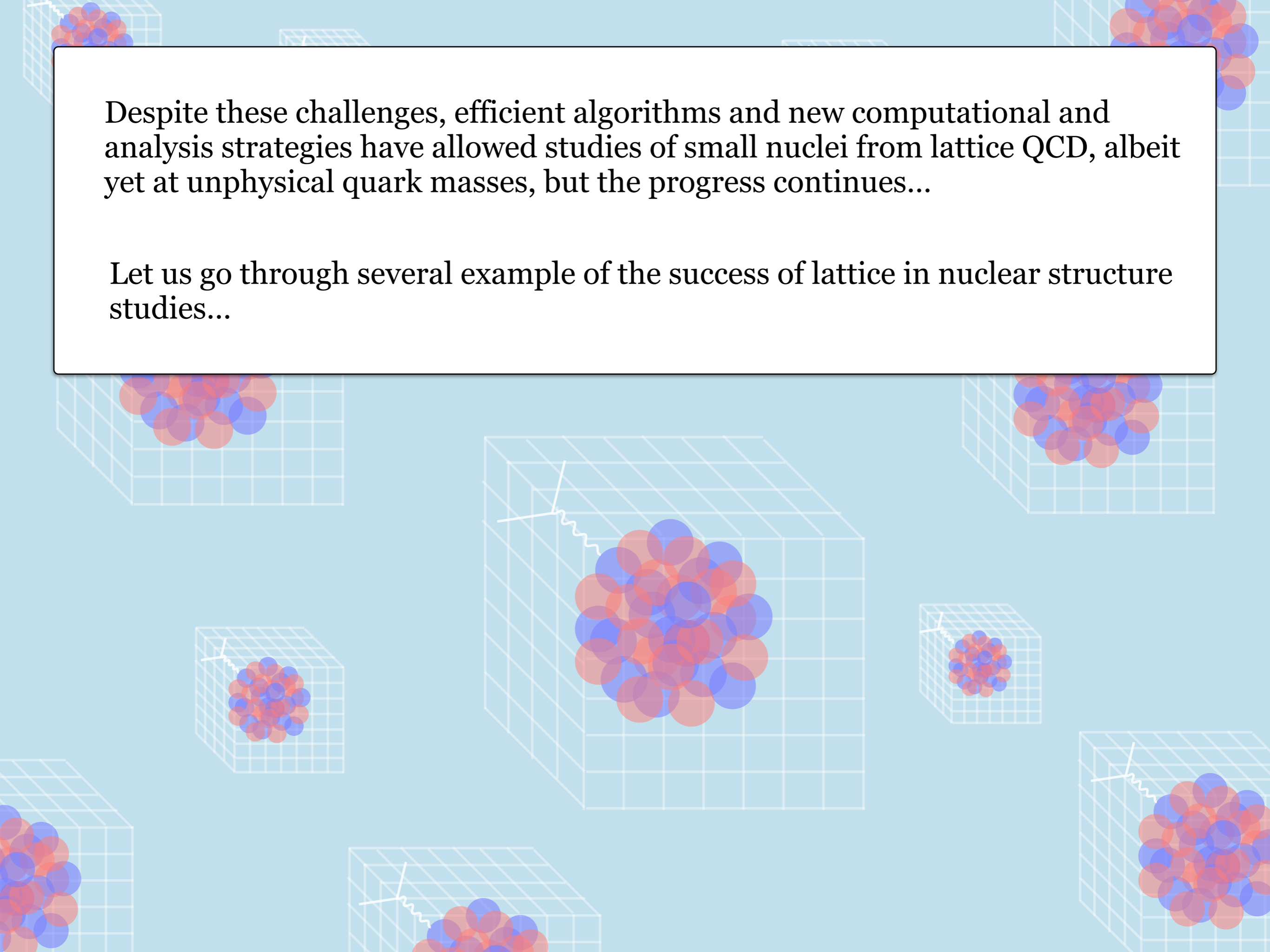
Parisi (1984) and Lepage (1989).

Wagman and Savage (2016, 2017).



Despite these challenges, efficient algorithms and new computational and analysis strategies have allowed studies of small nuclei from lattice QCD, albeit yet at unphysical quark masses, but the progress continues...

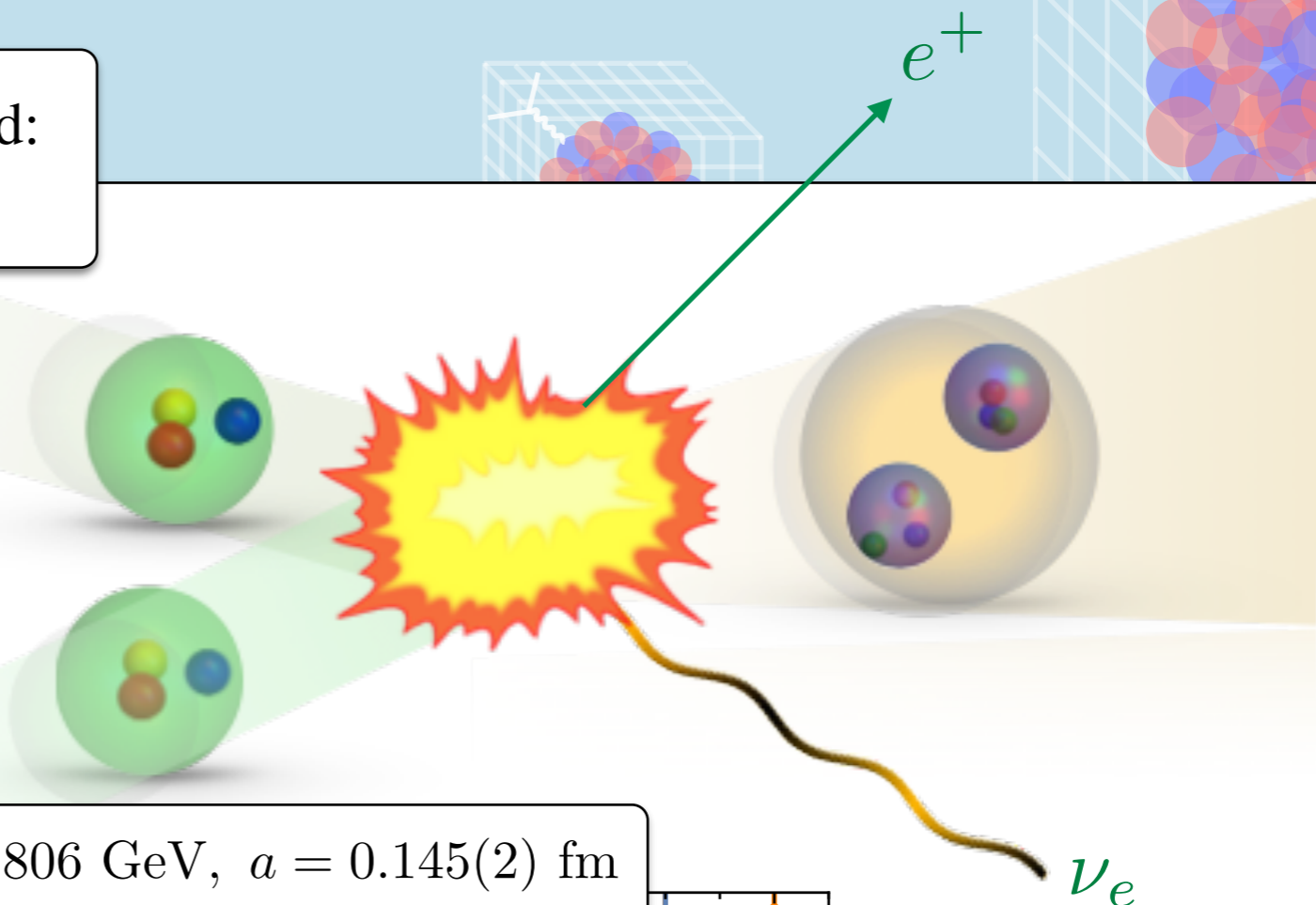
Let us go through several example of the success of lattice in nuclear structure studies...



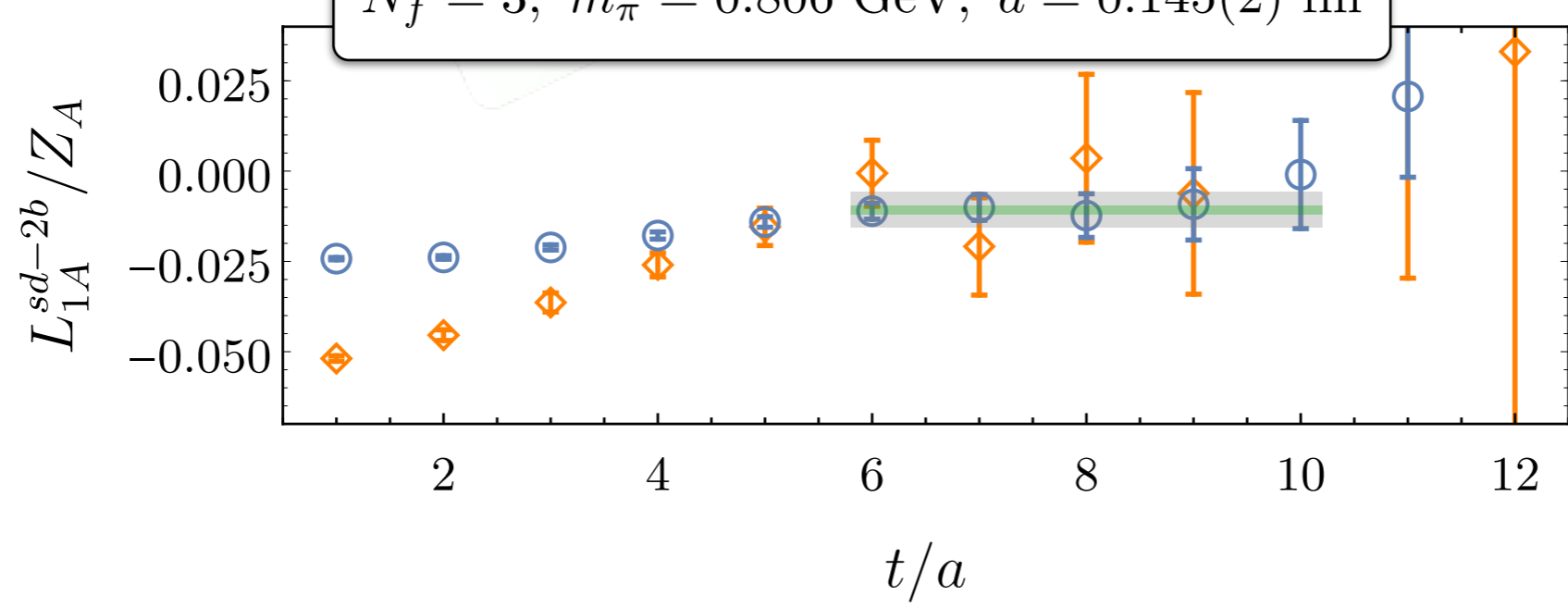
Application of Feynman-Hellmann method:

pp fusion $p + p \rightarrow d + e^+ + \nu_e$

Savage et al (NPLQCD), Phys. Rev. Lett. 119, 062002 (2017).



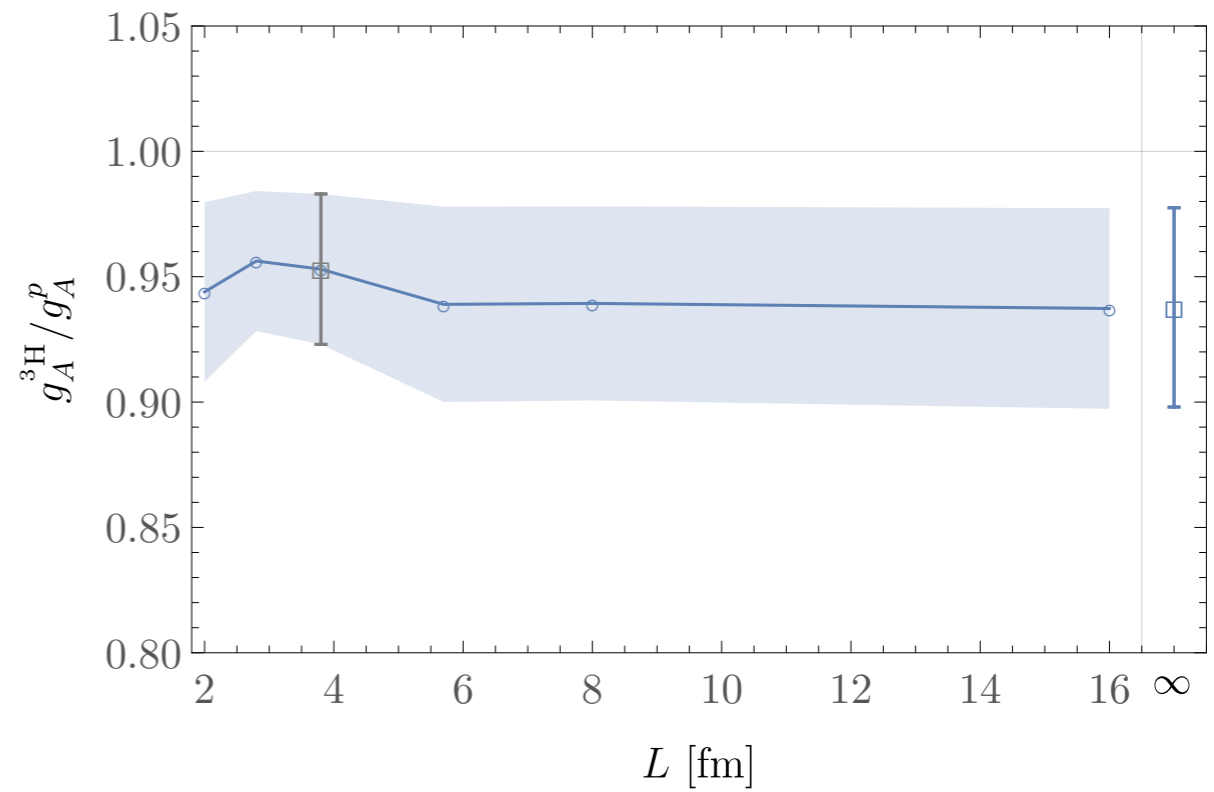
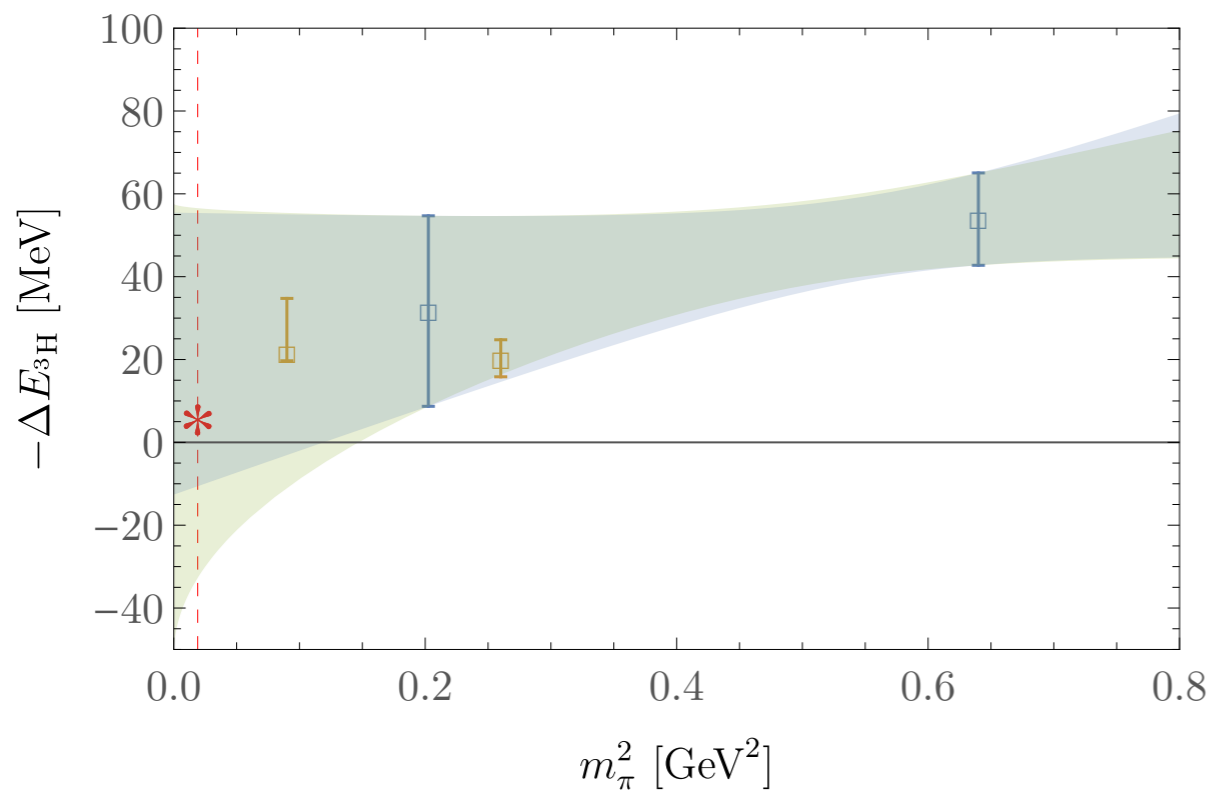
$N_f = 3, m_\pi = 0.806 \text{ GeV}, a = 0.145(2) \text{ fm}$



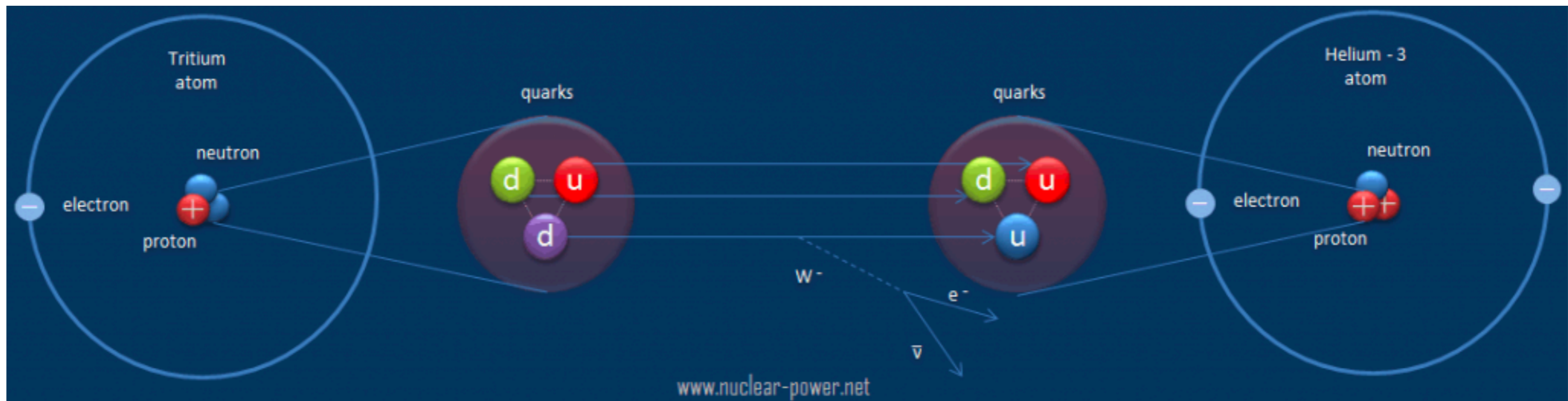
$L_{1,A} \approx 3.9(0.2)(1.0)(0.4)(0.9) \text{ fm}^3 @ \mu = m_\pi^{\text{phys.}} = 140 \text{ MeV}$

Application of Feynman-Hellmann method: Tritium beta decay!

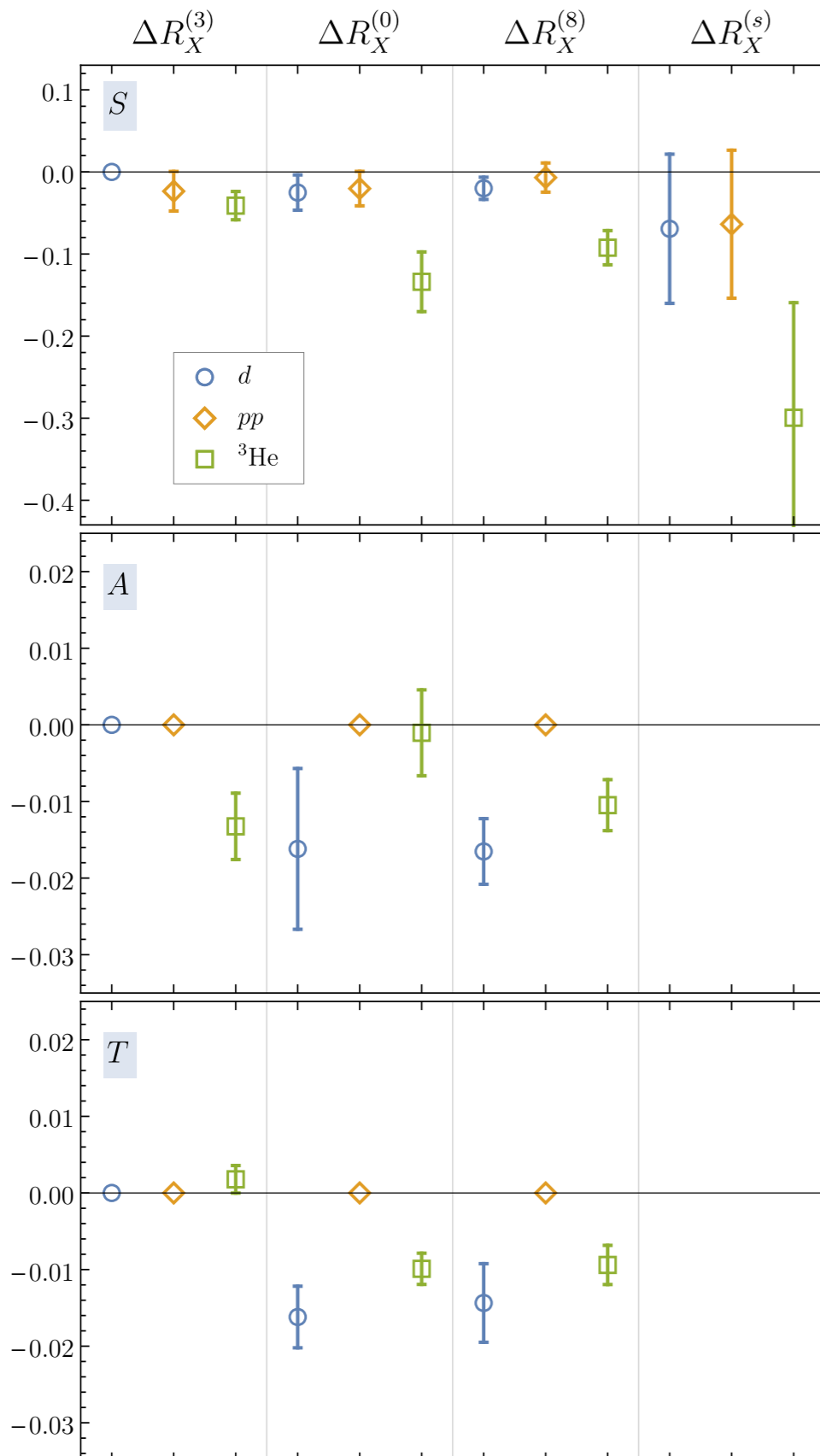
$N_f = 3, m_\pi = 0.806 \text{ GeV}, a = 0.145(2) \text{ fm}$



Parreno et al (NPLQCD), Phys. Rev. D 103, 074511 (2021),
Savage et al (NPLQCD), Phys. Rev. Lett. 119,062002(2017).



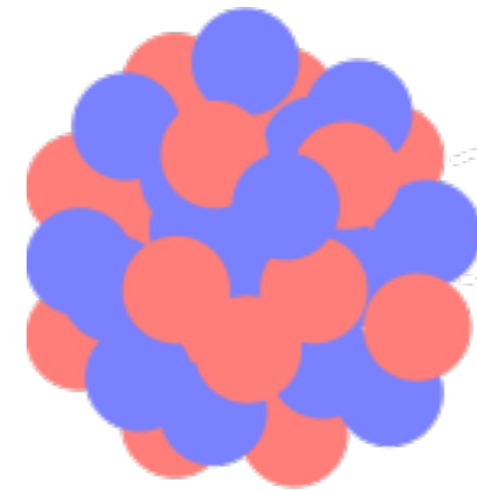
$N_f = 3, m_\pi = 0.806 \text{ GeV}, a = 0.145(2) \text{ fm}$



EMC effect from QCD?

How does the distributions of quarks in a nucleon change if bound to a nucleus?

CHANG et al. (NPLQCD), Phys.Rev.Lett. 120 (2018) 15, 152002.

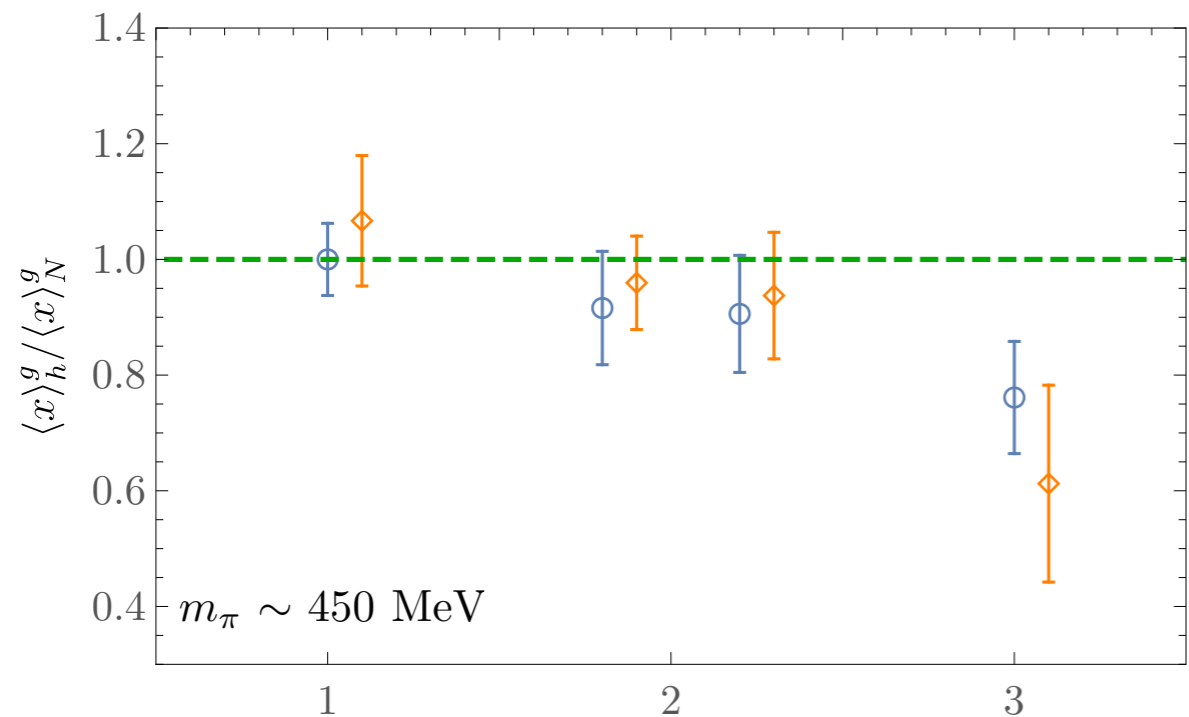
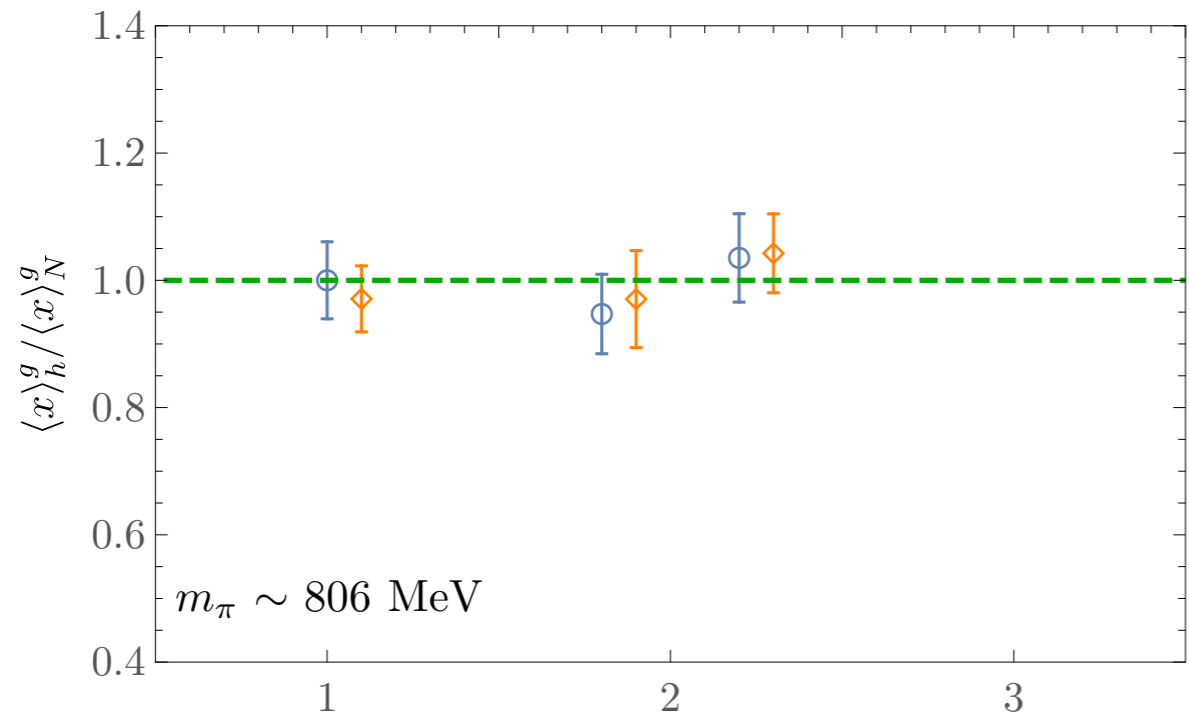


$$= \sum \text{red sphere, blue sphere ?}$$

$$g_X^{(f)}(A) = \langle A | \bar{q}_f \Gamma_X q_f | A \rangle$$

$$R_X^{(f)}(A) = g_X^{(f)}(A) / g_X^{(f)}(p)$$

$$N_f = 2 + 1, m_\pi \approx 450 \text{ MeV}, a \approx 0.12 \text{ fm}$$



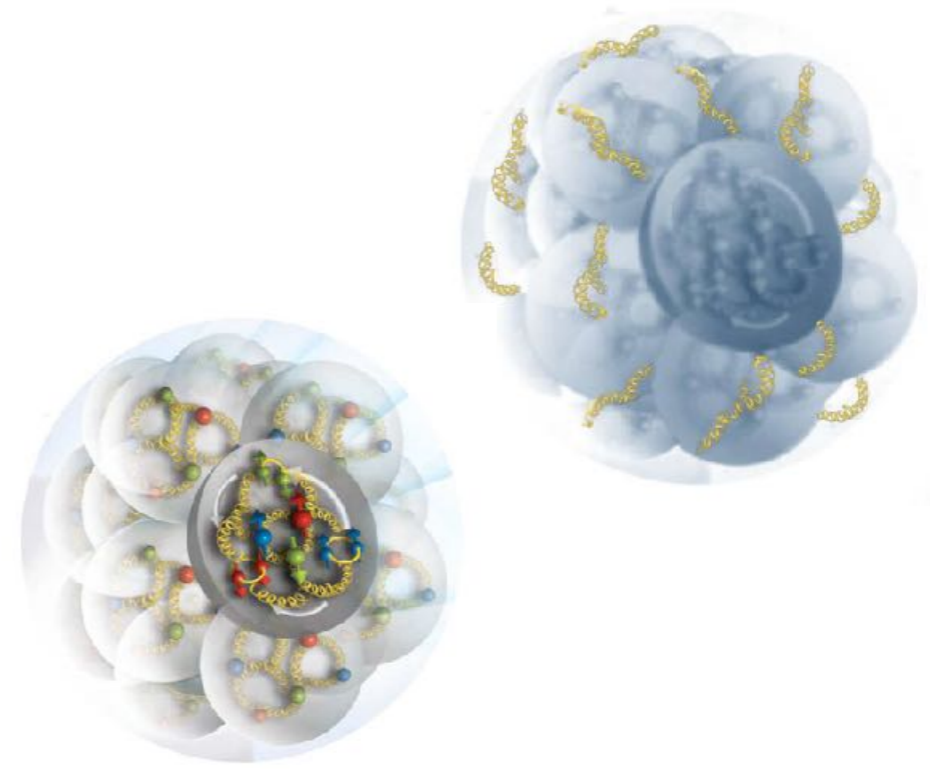
A

$$\overline{\mathcal{O}}_{\mu_1 \dots \mu_n}(\mu) = S \left[G_{\mu_1 \alpha} i \overleftrightarrow{D}_{\mu_3} \dots i \overleftrightarrow{D}_{\mu_n} G_{\mu_2}^\alpha \right]$$

A gluonic EMC effect?

How does the distributions of gluons in a nucleon change if bound to a nucleus?

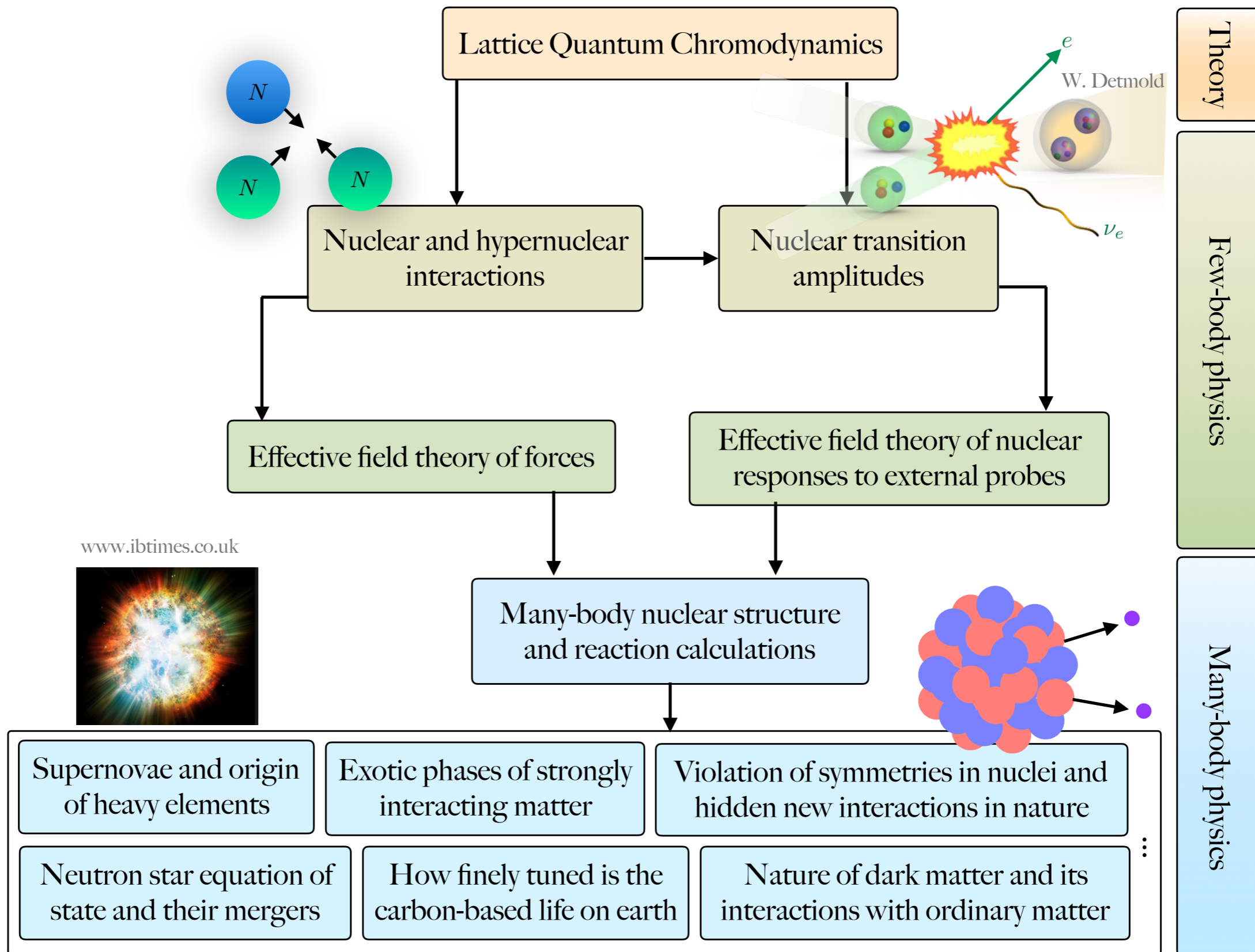
Winter et al. (NPLQCD), Phys.Rev. D96 (2017) 9, 094512



Graphic: EIC white paper (left), P. Shanahan (right)

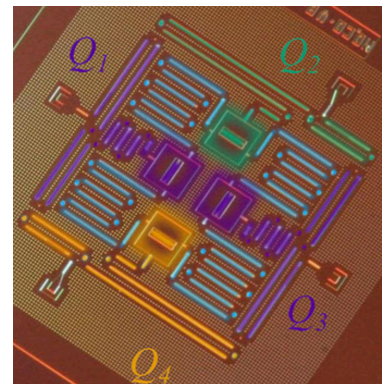
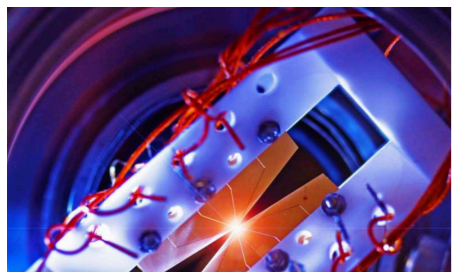
ROADMAP FOR NUCLEAR PHYSICS FROM LATTICE QCD

ROADMAP FOR NUCLEAR PHYSICS FROM LATTICE QCD

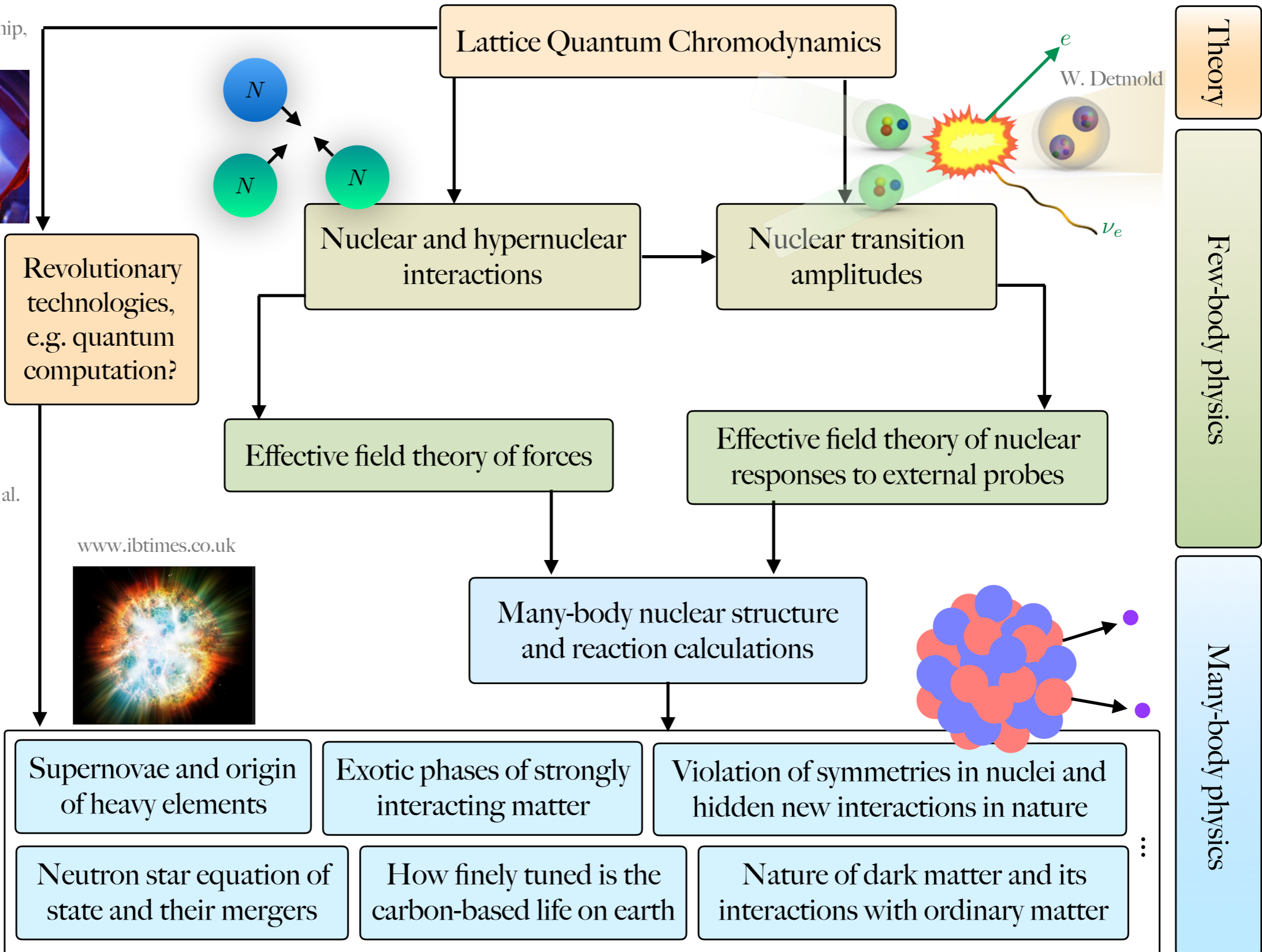


ROADMAP FOR NUCLEAR PHYSICS FROM LATTICE QCD

UMD's ion trap quantum chip, Image by E. Edwards



IBM superconductor quantum chip, Córcoles et al.



Revolutionary technologies, e.g. quantum computation?

www.ibtimes.co.uk

Dana Berry, Skyworks Digital, Inc.

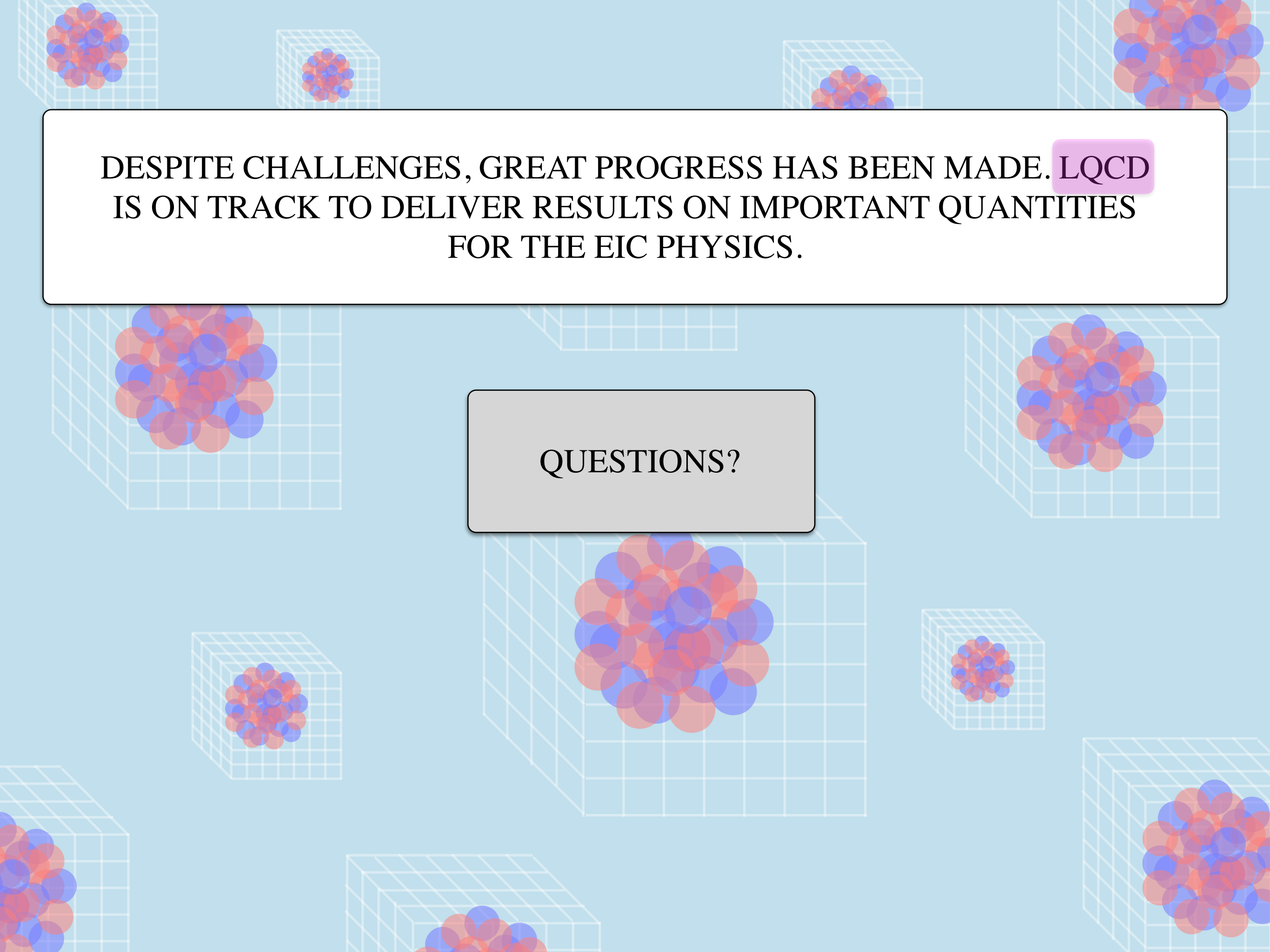


Theory

Few-body physics

Many-body physics

This program



DESPITE CHALLENGES, GREAT PROGRESS HAS BEEN MADE. LQCD
IS ON TRACK TO DELIVER RESULTS ON IMPORTANT QUANTITIES
FOR THE EIC PHYSICS.

QUESTIONS?